University of Stavanger

Faculty of Science and Technology

MASTER'S THESIS

Study program/ Specialization: Master of Science in Environmental Technology/ Offshore Environmental Engineering	Spring semester, 2014 Open / Restricted access
Writer: **Elena Bakrachevska**	…… (Writer's signature)
Faculty supervisor: **Torfinn Havn** External supervisor(s):	
Thesis title: **Analysis of Corrosion Resistance Property of Cold Bended 316L and 6Mo Stainless Steel Pipes**	
Credits (ECTS): 30	
Key words: Cold Bend, Corrosion, Pitting, Crevice, 316L, 6Mo, Potential, Current Density, Hardness	Pages: 66 + enclosure: 19 (Appendix) + CD Stavanger, 16 June, 2014 Date/year

Abstract

The variation in mechanical properties after cold deformation (bending) of pipes is one of the interesting subjects in material science. One major quality the material should possess is high corrosion resistance after cold deformation. The study deals with the observation of pitting corrosion resistant property of cold deformed (bended) tubes of 316 type and 6Mo stainless steel. ASTM G48 and ASTM G61 test methods are followed as experimental procedure for the completion of this project. The Scanning Electron Microscope (SEM) is used for the examination of pitting corrosion after G48 Test. Similarly, the cyclic polarization graph is used for measuring the pitting and repassivation potential after G61 Test. The cold deformed and the straight parts of both 316SS and 6Mo were seen to be holding a similar corrosion resistant property. The weight loss per unit area was found to be similar after G48 test and the pitting and repassivation potential values were in a similar range. The hardness of bended parts for both 316SS and 6Mo are measured higher than the straight parts.

Acknowledgement

I would like to express my sincere gratitude to my supervisor **Prof. Torfinn Havn** for his inspiration, proper guidance and supervision throughout this project. I would also like to thank **Ms. Ingunn Cecile Oddsen** for proving technical support in obtaining images from SEM and for providing suggestion for carrying out experimental activities.

I would like to appreciate the help from **HiTec Products** which provided the specimens to investigate and carry out the experimental work

I would like to thank **Mr. Vegard Øien** for his voluntary support for conducting ASTM G61 Test. My sincere acknowledgement to **Mr. Utsav Raj Dotel** for providing me motivation, and being co-operative and supportive throughout this project.

I am indebted to my parents, family members and friends in Norway and in Macedonia for their support and inspiration during my stay at University of Stavanger.

TABLE OF CONTENTS

LIST OF FIGURES

LIST OF TABLES

APPENDICES

1. INTRODUCTION

Cold Bending of pipes is not a new topic in material science. It is one of the easiest and cheap methods for making a curvature of straight pipes which could be fitted in a desired system. Different qualification test results are considered before their practical implication. Mechanical properties, corrosion properties, cracks observation, dimension tolerance are needed to be studied along with their compliance with codes/requirements[1]. 316 type stainless steel and 6Mo stainless steel are among different materials which are particularly considered for cold work. However, still some leading companies are reluctant to use the cold bended pipes though they qualify these tests done by third parties. Literature have been found to be limited in terms of study of corrosion properties of these materials and this might be one of the reasons for not having clear ideas about the difference in properties due to cold bending.

This study is aimed to visualize the difference in pitting corrosion behaviour of bended tubes of outer diameter 0.935 cm and inner diameter 0.5 cm. The pipes were R=2.5ND and R=5ND bended and were provided by HiTec Products. The testing method in accordance with American Standard for Testing and Materials (ASTM) are followed i.e., ASTM G48 and ASTM G61. ASTM G48 method deals with exposing the specimens at acidic ferric chloride solution which is very acidic and observing the pitting corrosion behaviour of the specimens. Straight and bended parts were tested simultaneously at the same environment for comparing the corrosion resistant behaviour. ASTM G61 method is potentiodynamic polarization scan obtained by varying the potential of the specimen. Plot of Potential vs current density is obtained and the pitting potential and repassivation potential values are measured and analysed. The hardness of the specimens was also measured to compare the straight and bend part.

Chapter 2 of this report is about the literature background. Most of the topics that were studied for this project are included. It gives an idea about the subject matters that are dealt within this study. Chapter 3 provides details about the materials and methods designed for the experimental activities. The calculations done and procedures for standard test methods are described along with the modification done. Chapter 4 presents all the results obtained in tabulated, graphical form. The results are analysed partly in this chapter and are described and interpreted in Chapter 5, Discussion.

Chapter 6 presents the conclusion obtained from the results and discussion. Some recommendations are provided for carrying out further studies in this subject matter in the future.

2. LITERATURE BACKGROUND

2.1 Corrosion

Corrosion is one of the major issues for the increment of service life and reliability of metallic materials, and detailed knowledge and understanding of its mechanism is vital to solve the existing and future corrosion problem[2]. It can simply be defined as the electrochemical reaction on the metal's surface which causes the degradation[3]. It is a natural process and is the result of the tendency of the metal to reach to the lowest energy state. To reach to that level, for example iron and steel combine with oxygen and water to form hydrated iron oxide (rust) which is similar to that of iron ore[4]. This phenomenon is described in Figure 1.

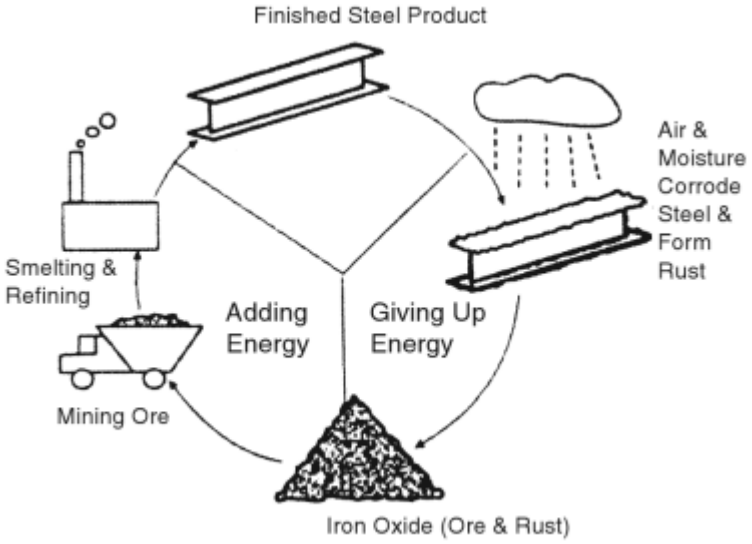

Figure 1: Life Cycle of Steel

Corrosion is restricted mostly to metals and non-metals are not subjected to corrosion. For instance, plastic can swell or crack, wood may split or decay, cement can leach away, etcetera. Thus, corrosion is not a deterioration by physical causes but only due to chemical or electrochemical reaction with the environment[5].

There are several primary and secondary factors essential for the corrosion to occur. Primary factors include Anode, Cathode, and Medium for metal dissolution, metal ions, and electrons[6]. At anode, electrons are generated that move towards cathode through an electronic path, and reduces the positively charged ion. Positively charged ions move from anode to cathode through ionic current path. The electrical circuit is thus completed with

the flow of current from anode to cathode by ionic current path, and cathode to anode by electronic path. These anode and cathode reactions occur at the same rate (which is corrosion rate) and is defined by *American Society For Testing and Material* as material loss per unit area and unit time[4, 6].

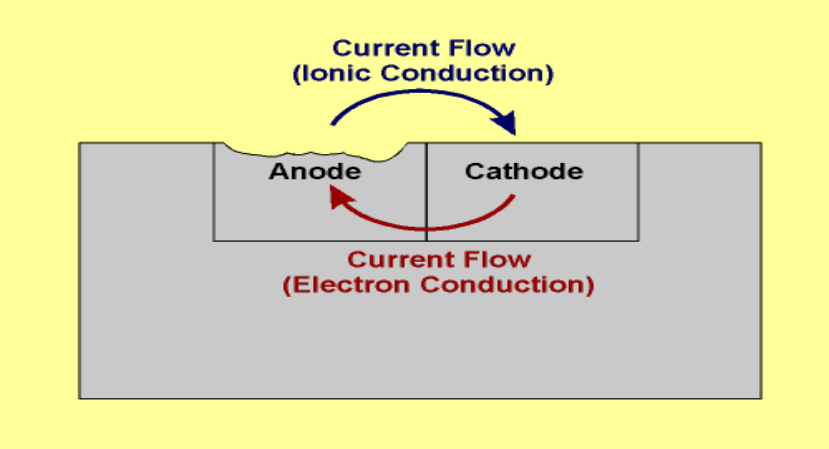

Figure 2: Simple schematic representation of current flow in a simple corrosion cell

Let's describe this process with a suitable example of iron placed in hydrochloric acid. The chemical reaction and a simplified description is mentioned below[7]:

$$Fe + 2HCl \longrightarrow FeCl_2 + H_2$$

This reaction is followed by the gradual decrement of solid iron and the formation of hydrogen bubbles rising to surface. Also electrons are being exchanged.

$$Fe + 2H^+ + Cl^{2-} \longrightarrow Fe^{2+} + Cl^{2-} + H_2$$

The iron gives two electrons and form iron ion. Electrons are captured by hydrogen ion and reduced to hydrogen gas. The reaction takes place at the surface and the anode is distinguished as the part where electrons are donated. Similarly, cathode is where the electrons are absorbed. There is the difference in an electrical potential and electrical circuit is developed. Electrons flow from anode to cathode and hydrogen ions that are positively charged move towards cathode, and the circuit is completed. The dissolution of metal is the corrosion; and its rate depends on the rate of current flow[7].

2.2 Passive films and Passivity

For most of the metals we can say that they have " an inheretant tendency to corrode"[8]. In most realistic condition, metals upon exposure to the atmosphere form a protective oxide film called passive film, and the process of its formation is known as passivation. Passive film presents diffusion barrier layer of reaction produced on the surface of the metals, mostly metal oxides or other components. If the film stays stable and undamaged, it will protect metal from further corrosion.

For proper understanding of this phenomenon, an experiment was performed with an iron submerged into a container with concentrated nitric acid (HNO_3). Iron in concentrated acid was not attacked (corroded) just because thin layer of oxide was formed on its surface and causes loss of reactivity. If in an aqueous solution, there are metal ions, oxides and hydroxides will form. Chemical reactions are as following [30]:

$Fe^{3+}(aq) + 3OH^{-}(aq) \rightarrow Fe(OH)_3(s)$

Later, the hydroxide undergo a reaction where oxide and water are produced:

$2Fe(OH)_3 \rightarrow Fe_2O_3 + 3H_2O,$

or if there is no metal ion in solution, film is formed by chemical reaction with adsorbed oxygen [30]:

$2Fe(s) + 3/2O_2(ads) \rightarrow Fe_2O_3(s)$

These oxide films are very stable, and they represent strong barrier between metal and the environment. Many conditions will determine the stability of this film. On one hand there are physical and chemical nature properties of the passive film and on other the environmental condition in which metal is. For instance: temperature, pH and anion content of the solution[9]. Passivity is the major reason for the effectiveness of all corrosion resistant alloys. There are two generally accepted definitions for passivity[10]:

Thick film passivity: It means that the metal can resist corrosion even if it is in the environment where there is a large thermodynamic force for its oxidation.

Thin film passivity: It occurs if the rate of dissolution in metal decreases though its potential is increased to more positive values.

2.3 Polarization

Polarization can simply be defined as the difference between the real potential and the equilibrium potential. Polarization is a very important corrosion parameter by which we can make statements about corrosion rates [11]. Corrosion rates are of important role when comes to selection of materials for specific environment[12]. There are many techniques for measurement and assessment of corrosion rate. Because corrosion process is electrochemical in nature thus monitoring technique are mostly electrochemical techniques like: corrosion potential measurement, linear polarization resistance, electrochemical impedance spectroscopy, electrochemical noise analysis and many others[13].

Mixed potential theory

When process of corrosion is taking place on a metal, there are several electrochemical reactions occurring simultaneously on the metal-solution interface. For better dealing with this reaction and better understanding, Evans diagram was developed. In this diagram, corrosion potential is a mixed potential and lies between anodic reaction on one side and hydrogen evolution on another side. In Evans diagram electrode potential in volts is plotted against corrosion current in ampere per unit area[14].

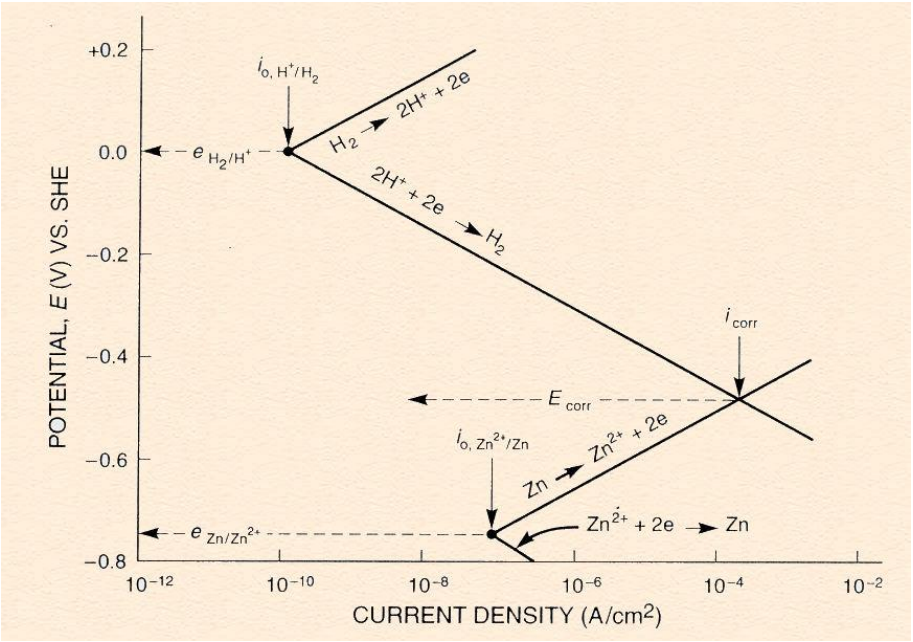

Figure 3: Graph representing Mixed Potential Theory (Evans Diagram)[11]

Figure 3 represents an Evans Diagram. In this diagram, there are four very important parameters: corrosion potential $E_{corr,}$ current $I_{corr,}$ anodic $ß_a$ and cathodic $ß_c$ Tafel constants could be determined.

If the E_{corr} potential is changed by the value of $+\Delta E=E-E_{Ccorr,}$ a straight line is obtained:

$$Ɔ_A = ß_A \log \left(\frac{i\ app}{icorr}\right)$$

Where $Ɔ_A = E - E_{corr}$

If the E_{corr} potential is changed by the value of $-\Delta E$ following equation is obtained:

$$Ɔ_c = ß_c \log \left(\frac{i\ cpp}{icorr}\right)$$

Ɔ is designated as a polarization or over potential.

This method is a common method used for determination of corrosion rates in metal, where by polarizing the sample, we can measure change in corrosion current[14]. By plotting the measurement, polarization curve can be obtained[11].

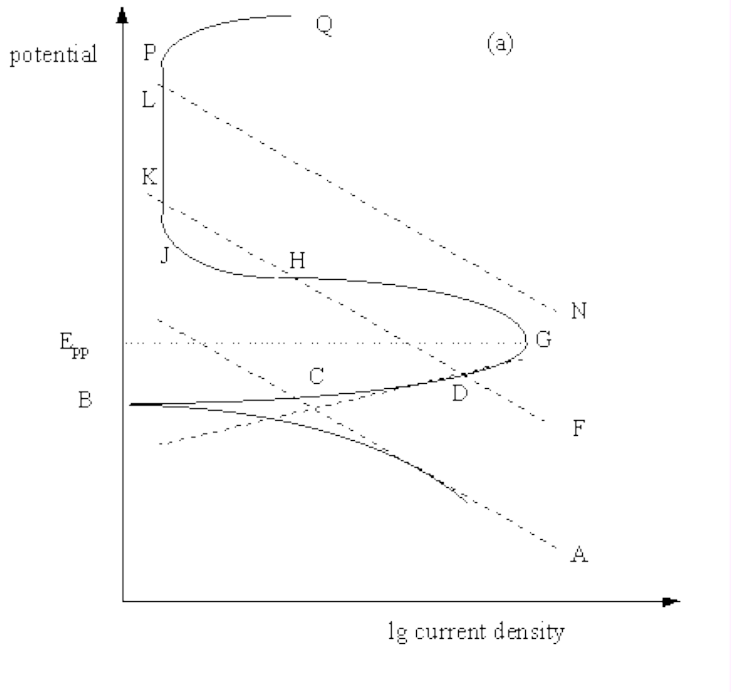

Figure 4: Polarization curve[11]

Mostly, study of anodic polarization behavior is used for the understanding of alloy system in a different environment. Equipment for this anodic polarization test is very simple, and results are ready in a short time. This is helpful in understanding active-passive behavior that many materials exhibit[12].

2.4 Types of Corrosion

There is not any unique and specific classification of corrosion, however below are some types of corrosion based upon the nature of the surface affected.

2.4.1 General Corrosion

General corrosion, also known as uniform corrosion, is a type of corrosion where the entire metal surface exposed to the environment (liquid electrolyte, gas electrolyte, and hybrid electrolyte) is corroded. When talking about general corrosion we talk about corrosion dominated by uniform thinning of exposed surface without noticeable localized attack[15].This type of corrosion can be easily recognized by roughness of the metal surface and by evidence of corrosion products on the metal surface. However, this form of attack is slow, can be easily measured and predicted and therefore major failure of the material can be prevented. Prevention from uniform corrosion can be achieved by usage of coating and painting of the surface, cathodic protection or other methods that prevent corrosion to occur.

Some types of General Corrosion are mentioned below[16]:

- Atmospheric Corrosion
- Galvanic Corrosion
- High Temperature Corrosion
- Liquid Metal Corrosion
- Molten Salt Corrosion
- Biological Corrosion

2.4.2 Localized Corrosion

In this type of corrosion, the specific part of the exposed surface is corroded. Localized corrosion is directly connected with the breakdown of passivity on specific parts on the material surface. In this type of corrosion discrete parts of the surface are being attacked and they start to corrode actively, while the rest of the surface remain passive. Penetration rates in these isolated regions can be of the order of 10 mpy or more, leading to rapid

perforation of the material[10]. Those high rates of metal penetration at specific sites, and the fact that the attack can be under surface and therefore very difficult for eye detection, makes this localised corrosion more difficult to deal with. Additionally, this form of attack is very important economically and as a threat of premature failure of the material, or failure of a structure. Types of localized corrosion are mentioned below[16]:

- Pitting Corrosion
- Crevice Corrosion
- Filiform Corrosion
- Oral Corrosion
- Biological Corrosion
- Selective Leaching Corrosion

The focus of this literature review has been given to pitting corrosion as it is the main topic of this thesis.

2.5 Pitting Corrosion

Pitting Corrosion is a type of localized corrosion which selectively attacks the specific part of metal that has surface scratch or mechanically induced break, an emerging dislocation or slip step, heterogeneous structure in terms of composition like inclusion or precipitate[3]. This form of corrosion manifest itself as holes on a metal surface, and at the beginning of the formation it is very difficult to detect pits due to the small size, and extend time is necessary for the pits to be visually noticeable[16]. It is usually associated with active-passive-type and occurs under condition specific to each alloy and environment[13]. Very small, narrow pit with insignificant overall metal loss can cause an entire system failure. Once initiated, pit continues to grow inward in the direction of the gravity. This advocate that bottom of pits are rich in metal ions (M^{+z} ions) because of anodic reaction occurring there [16]. Pitting corrosion is the most dominant type of localized corrosion and can have various shapes. It can produce pits having semi-permeable membrane of corrosion products[17].

Types of Pitting Corrosion[17]:

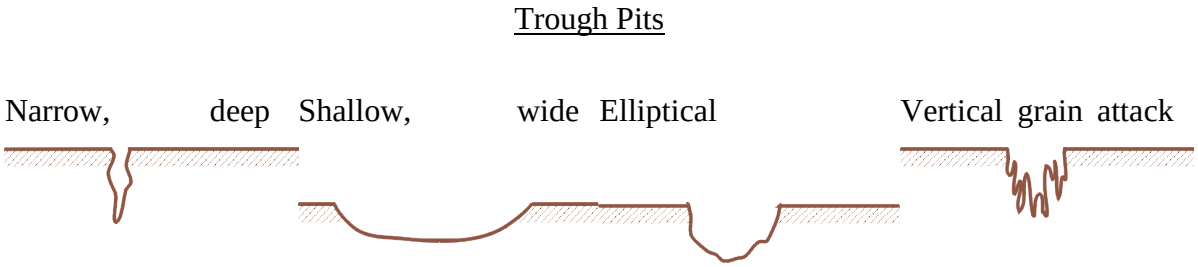

Mechanism of pitting corrosion

The breakdown of passive layer is the reason for the initiation of pitting corrosion[18]. After breakdown, electrolytic cell is formed, and it is assumed that many anodic and cathodic reactions take place at localized sites[16, 19].

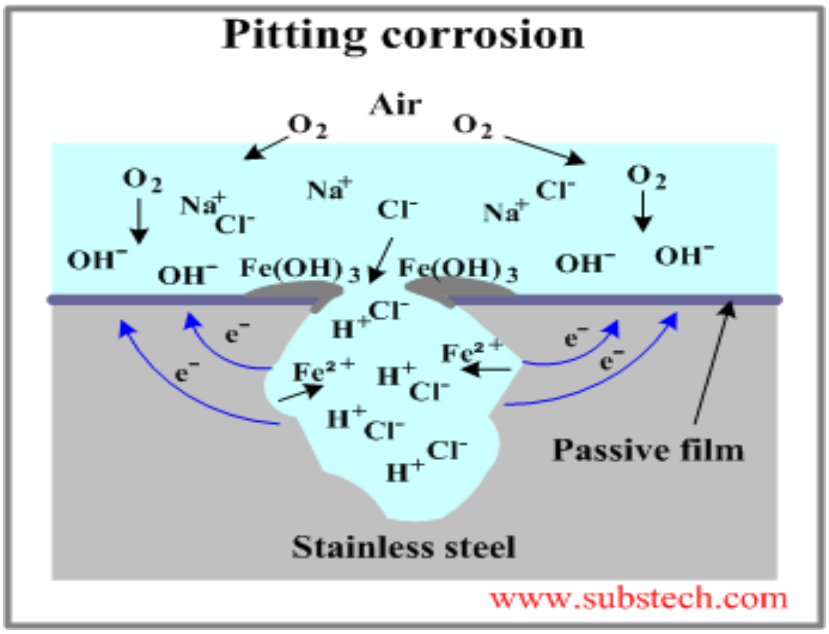

Figure 5: Pitting mechanism[20]

After formation of pits, corrosion processes within a pit govern its propagation. Those processes are illustrated in Figure 5.

Pitting process begin with a dissolution of metal. When metal is found in environment that is electrolyte and contains chlorine ion Cl^- and molecules of oxygen (O_2), the following reaction happens [16, 19] :

Reaction for metal dissolution on the bottom of the pit (anodic reaction),

$$M \rightarrow M^{n+} + ne$$

is balanced by reaction on the nearby surface:

$$O_2 + 2H_2O + 4e \rightarrow 4OH^-$$

As the result of this reactions, there is an increase of concentration of Mn^+ inside the pits, and for neutrality to be maintained chloride ions Cl^- migrate into the pit. That is how metal chloride (M^+Cl^-) is formed. Further, metal chloride is hydrolyzed by water:

$$M^+Cl^- + H_2O \rightarrow MOH + H^+Cl^-$$

From this equation it can be seen that product of this reaction if free acid that lowers the pH values in the pit. In the pit pH values are around 1.5 to 1.0, while pH values is neutral in the bulk solution.

Metal hydroxide that is formed is also not stable, and it reacts with oxygen and water to form the final corrosion product:

$$2M(OH)_2 + ½\ O_2 + H_2O \rightarrow 2M(OH)_3$$

2.6 Crevice corrosion

Crevice corrosion is a localized corrosion and it may rise when there is existence of narrow opening or gap between metal and metal/non-metal components. Non-metallic components that can cause crevice corrosion are rubber, glass, wood plastic and even living organism[9]. Crevice corrosion can also occur where unintentional crevices exist for instance crack, metallurgical defects and other[21]. Crevice corrosion usually occurs where local differences of oxygen concentration exist[9]. When there is a crevice, oxygen within the crevice electrolyte is consumed where the rest of the metal surface has ready access to oxygen. In that case metal surface becomes cathodic relative to crevice area[21]. The larger the ratio between cathode and anode area will give increment of corrosion

rate[22]. Crevice corrosion mechanism is similar to mechanism of pitting corrosion. Crevice corrosion of steel in presence of chloride ion in the solution is illustrated in the Figure 6:

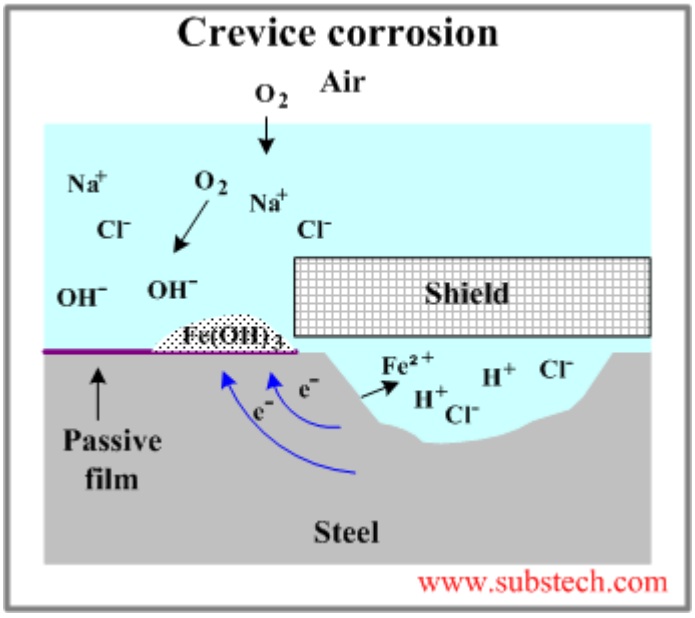

Figure 6: Crevice corrosion mechanism[22]

2.7 Steel and Stainless Steel

Steel is an alloy of carbon combined with other elements, and the most common combination in steel is between iron and carbon. Different composition of these elements gives different properties to steel [23]. Besides carbon all modern steel contains other elements such as manganese (Mn), some impurity atoms as sulphur (S) and phosphorus (P). Due to this steel can be presented as Fe+C+X, where Fe and C are symbols for iron and carbon, and X is third element addition or impurities [24] . It is customary to divide steel into two categories: plain carbon steel and alloy steels. X in plain carbon steel is represented only by manganese, sulphur and phosphorus, whereas in alloy steels X is one or more additional element added to the steel chemical composition.[24]

Steel alloy with a minimum of a 12% chromium content by mass is called stainless steel[12].

Categories of Stainless Steels

When talking about stainless steel we do not talk only about one material, but about the family of alloys. Each of this family has their properties like mechanical, physical and corrosion-resistant properties [25]. Stainless steel can be categorized in different ways but

the best and most accurate way is by the metallurgical phases presented in their structure[17].

- Ferrititic
- Martensitic
- Austenitic
- Duplex steel, consisting of mixture of ferrite and austenite

2.8 Austenitic Stainless steel

Austenitic steel is the most produced stainless steel per year, and it represents the largest group within the stainless steel family[26]. They are alloys that contains nickel and chromium and by adding these elements, stabilization of austenite at room temperature is achieved [25]. Austenitic stainless steel has a single phase face centred cubic structure that shows stability over a wide range of temperatures. Typical composition of austenitic stainless steel is: iron-chromium-nickel alloys and iron-chromium-manganese-nickel alloys. Typical content of each material in this composition are chromium (16-26 %), nickel (6-12 %) and manganese (<15%). The main purpose for developing these materials was their application in different types of environment, from mild to very corrosive. Another characteristic of these materials is that they are nonmagnetic and can find their place of use in application where magnetic material should not be used [27].

Austenitic stainless steel is divided into standard SAS grades and nonstandard grades. Most of the nonstandard grades have been given UNS designation. The standard grades are further subdivided into 200-series and 300- series of stainless steel. The nonstandard grades of austenitic stainless steel comprise revised version of the 200-series and 300-series standard series and highly alloyed austenitic. For the high corrosive environmental condition where 300-series couldn't withstand the corrosive environment, high alloy stainless steel were developed[27].

Super-austenitic stainless steel are highly alloy austenitic stainless steel containing 6% Mo and 0.15 to 0.3 % N [23]. In 1969 year, first super austenitic steel was produced and had very high commercial success. The name of this material was Al-6X (NO8360). But later was replaced with nitrogen bearing Al-6XN (N08367). Nitrogen was added as it is austenitic stabilizer, also it enhance strength and improve resistance to pitting and crevice corrosion. 254 SMO (S31254), 654 SMO (S32654), 20Mo-6 (NO8026) and 1925 HMo(NO8925) present other examples of this super austenitic grades, and they all show

great material properties that allowed them to be used in the wide variety of application. They are mostly used in sea water application, in the process and other industries because they have resistance to most acids like phosphoric, sulphuric, nitric acid, etc. [27].

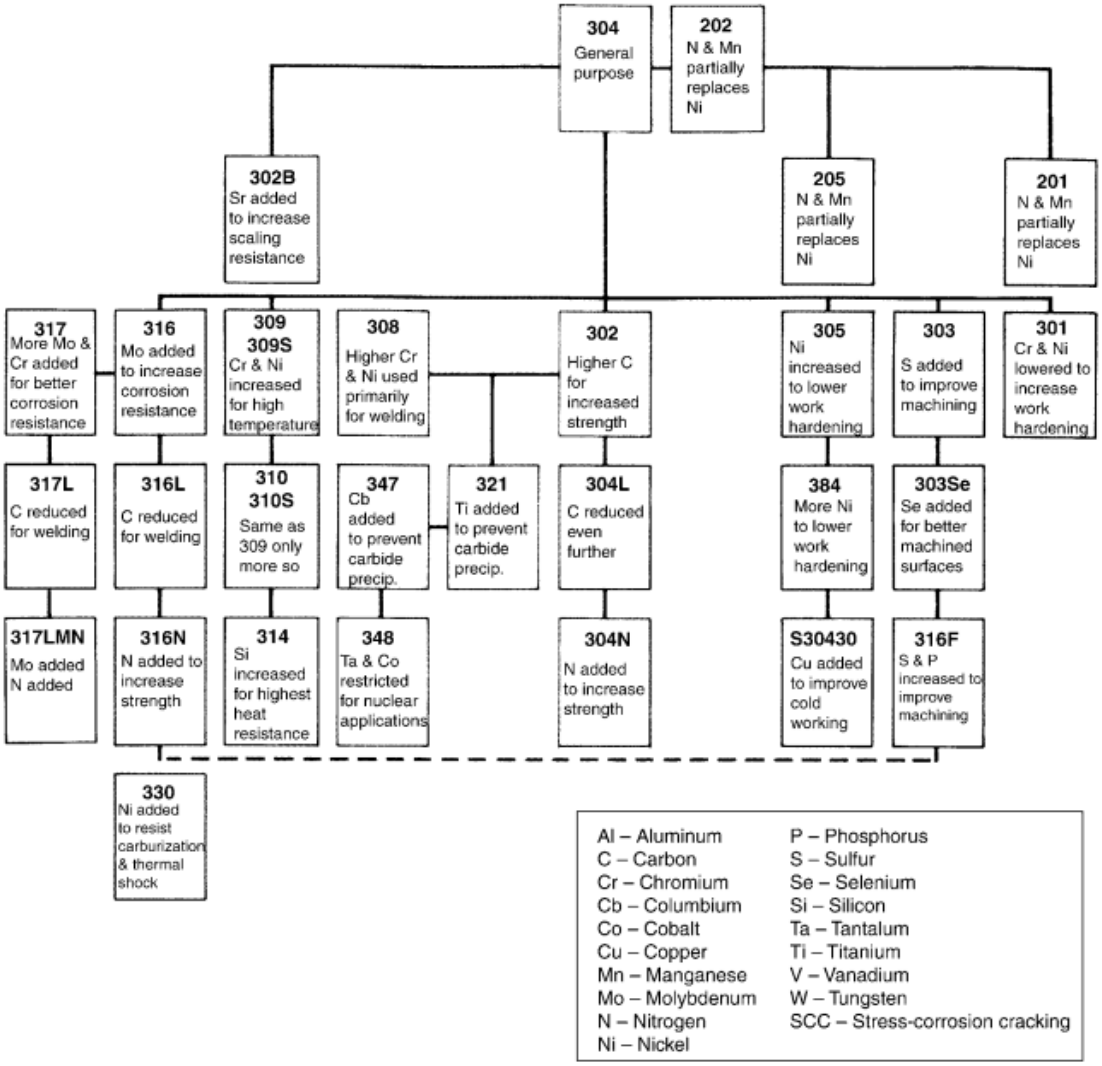

Figure 7: Austenitic Stainless Steel family[28]

2.9 Austenitic stainless steel UNS S31603 (316 L)

It is the one of the most widely used low-carbon stainless steels [29]. The typical chemical composition of UNS S31603 is presented in Table 1[30].

Table 1: Chemical Composition of UNS S31603

C	Mn	Si	Cr	Ni	P	S	Mo
0.030	2.00	1.00	16.00- 18.00	10.00- 14.00	0.045	0.030	2.00-3.00

The molybdenum in this chemical composition has a role to increase PREN value up to 26 for 316L. This austenitic stainless steel is tough over a wide range of temperatures, and because of not showing any transitional behaviour, it is considered that this material has useful cryogenic properties[29]. Mechanical properties for 316 L are presented in Table 2[31].

Table 2: Mechanical properties for 316 L

Grade	Tensile Strength ksi (min)	Yield Strength 0.2% ksi (min)	Elongation %	Hardness (Brinell) MAX
316 L	70	25	40	217

Physical properties for 316 are presented in Table 3[31]:

Table 3: Physical properties for 316 L

Density lbm/in3	Thermal Conductivity (BTU/h ft. °F)	Electrical Resistivity (in x 10-6)	Modulus of Elasticity (psi x 106	Coefficient of Thermal Expansion (in/in)/°F x 10-6	Specific Heat (BTU/lb/°F)	Melting Range (°F)
0.29 at 68°F	100.8 at 68 212°F	29.1 at 68°F	29	8.9 at 32-212°F	0.108 at 68°F	2500 to 2550
				9.7 at 32 – 1000°F	0.116 at 200°F	

316L stainless steel finds its application wherever there is existence of aggressive corrosion environment, and where risk of pitting attack of chloride environment is high. Great success is seen in application offshore oil and gas platforms modules for external cladding and significant decrement in cost for maintenance and repainting has been achieved[29].

2.10 Super Austenitic stainless steel UNS S31254 (6Mo)

Super Austenitic stainless steel is significantly highly alloy steel that comprised of chromium to more than 20 % and molybdenum up to 6 %. The typical chemical composition is presented in Table 4[29].

Table 4: Chemical Composition of UNS S31254

UNS S31254	C	Mn	Si	S	P	Cr	Ni	Mo	Cu	N
Weight %	<0.02	1	0.5	<0.01	<0.02	20 to24	18 to25	6.05	~1	0.22

High Molybdenum content has a tendency to destabilize austenitic structure and to reduce corrosion resistance, but with raising nitrogen to 0.2 %, this effect is solved. Nitrogen factor of 16 gives PREN number in a range of 43 to 45. This stainless steel finds its application in aggressive environments where corrosion of any type like general, crevice, and pitting and stress corrosion are frequent. They are mostly used in applications in oil and gas industry: tanks, piping system, valves, and tanks. They are a good choice for the environment containing sea water and hydrogen sulphide contaminations[29].

Mechanical and physical properties of the UNS S31254 (6Mo) are given in Table 5 and Table 6[32]

Table 5: Physical properties at room temperature for UNS S31254 (6Mo)

Density (Kg.m-3)	8000
Magnetic Permeability	<1.05
Young's Modulus (N/mm2)	200 x 103
Specific Heat 20°C (J.Kg-1.°K-1)	500
Electrical resistance, 20°C (µ.O.m)	0.85
Thermal conductivity, 20°C (W.m-1.°K-1)	13.5

Table 6: Mechanical properties for UNS S31254 (6Mo)

0.2% Proof Stress (N/mm2)[ksi] minimum	300 [43.5]
Ultimate Tensile Strength (N/mm2) [ksi] minimum	650[94.2]
Elongation (%) minimum	35
Hardness (HBN)	270 max
Reduction of Area(%) minimum	50

2.11 Laboratory corrosion test techniques for assessment of pitting corrosion

Laboratory tests are very effective and efficient method for predicting the rate of corrosion. It also helps for the selection of material in a different environment; study the mechanism of corrosion and quality control of material. There are various kinds of test for studying typical forms of corrosion, and because corrosion is an electrochemical process electrochemical measurements are basic for these tests. These tests can vary from simple immersion test to test conducted in a specific environment to sophisticated electrochemical test. The existence of standardized test methods is useful as the results can be compared and discussed. Annual book of ASTM Standards (Vol. 03.02, Metal, Corrosion, Erosion, and Wear) contains such tests. Sometimes these tests can be and needed to be modified by investigator[10, 33].

There are two generic types of testing[10]. They are described in the section below.

2.11.1 Accelerated coupon testing

Many standard tests from ASTM fall in this category. These tests are developed for accelerated testing the material in highly aggressive environment and elevated temperature. These tests have proved successful in the ranking of the relative resistance of materials to localized corrosion[10]. One of these tests is Ferric Chloride Test.

Ferric Chloride Test

This test is described in ASTM G48[34]. This test is specially designed for testing stainless steels and related alloys (including Ni-base alloys containing a large amount of Cr). Test is for determining pitting (and crevice) corrosion resistance property. Material is exposed to a 6 % by weight $FeCl_3.6H_2O$ solution which is highly oxidizing, concentrated

metal chloride solution. Testing time is of 24 to 72 hours. Temperature for this test can be room temperature (22±2º C) or higher temperature (50º±2º C) [34].

Mechanism behind this test can be explained as: The ferric salt that forms Fe^{3+}/Fe^{2+} redox couple acts as a chemical potentiostat in this test. Potential of this couple is +0.45 V (SCE). Solution contains a high concentration of ferric ion. That is allowing the redox couple to provide a large current (approaching an ideally nonpolarizable electrode). Reduction reaction of ferric to ferrous ion occurs on exposed metal surface. This is cathodic reaction. Other parameters that accelerated aggressiveness of solution are high chloride concentration, high temperature, very low pH of a solution (approximately around 1.3). When high potential of solution exceeds the pitting potential of tested material, then pits start forming[10].

Ferric chloride test can be modified with changing temperature or exposure time. Test is an important tool in alloy development and in corrosion science.

Evaluation of pitting corrosion after Ferric Chloride Test

ASTM G46 provides assistance in examination of pits and evaluation of pitting corrosion. After the test is finished identification and examination of pits can start. Visual examination is the first step. In this step naked eye or low power microscope is used to inspect the material surface. Size, density and shape of the pits are determined and photographs are taken. Metallographic examination can be performed to determine whether the cavities are true pits or intergranular corrosion or dealloying. Also non-destructive inspection can be performed like radiographic, electromagnetic, ultrasonic and dye penetration inspection[35]. Extent of pitting can be evaluated by measuring the mass lost, or measurement of pit depth. Mass measurement is not always a good indicator for inspecting pitting especially when there is uniform corrosion or other kind of corrosion present. Then the contribution of mass loss due to pitting is very small. However, mass lost along with visual comparison of pitted surface may give enough information in ranking relative resistance of alloys in laboratory test. Pitt depth measurement is a better indicator for extend of pitting. These measurements can be made by using several methods: metallographic examination, use of micrometre or depth gage, and the microscopic method[35].

2.11.2 Electrochemical testing

There are several advantages of using electrochemical testing. It is an efficient method; corrosion can be studied in solution of interest rather than in less relevant environment and useful information can be collected for critical potential for initiation of pitting corrosion (or other localized corrosion). Furthermore, they can also be used in design decision [27].

Cyclic Potentiodynamic Polarization Test

Procedure for this test is described in ASTM G 61. Setup for this test is shown in the Figure 8. In test practice for performing this electrochemical test, a typical electrochemical cell is needed and an instrument for electrochemical polarization of the metal that is tested. This instrument is potentiostat. Electrochemical cell consists of tree electrodes placed in electrolyte solution. Three electrodes are[36]:

- Working electrode- that is metal of interest for the test
- Axillary electrode –that supplies the current to the working electrode
- Reference electrode- electrode with stable and well known potential

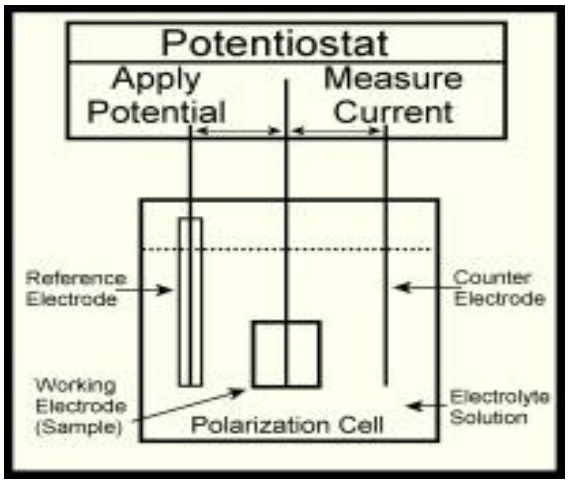

Figure 8: Electrochemical cell[36]

When test starts, electrochemical potential (voltage) is generated between electrodes. In cyclic potentiodynamic polarization, the potential that is applied on working electrode increases with time while current is measured. The result is shown in a graph where current is plotted versus the potential. The potential is increased till it reach a predetermined potential or current density, and the potential scan may be reversed but the current density continues to be measured. Typical cyclic polarization curve is presented in the Figure 9.

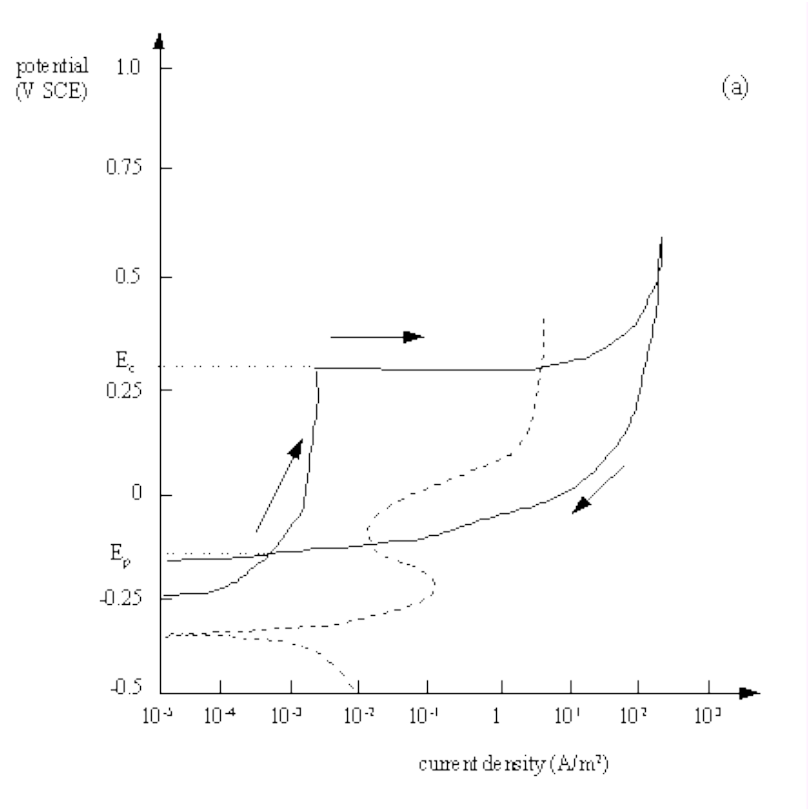

Figure 9: Cyclic potentiodynamic polarization curve[3]

When analysing the cyclic polarization curves attention is given on two features: the pitting (breakdown) potential E_{pitt} and protection (repasivation) potential E_p. Potential at which anodic current increase significantly is called pitting potential. Protection potential is the potential at which the hysteresis loop is completed when we perform reverse polarization scan. Overall, once initiated, pitting corrosion can propagate at some potential more positive than the protection potential. Thus, the more positive is protection potential the less likely is that localized corrosion will occur [35].

2.12 Pitting Resistance Equivalent Number (PREN)

The measure of performance of material in area of pitting corrosion is measured by critical pitting temperature (CPT), pitting potential and Pitting Resistant Equivalent number PREN[37]. It is also called pitting index [38]. PREN number is a theoretical way for knowing and comparing the resistance for pitting corrosion of different types of stainless steel, based on the chemical composition of an alloy[4]. It can be calculated from the following equation[38]:

PREN = %Cr + 3.3 % Mo, for ferritic alloys without nitrogen in solution

Or,

PREN = %Cr + 3.3 (%Mo + 0.5 % W) + 16 % N

According to formula PREN number is determined by chromium, molybdenum and nitrogen content. These alloying elements are added to the stainless steel because they have the highest impact on material when it comes to pitting corrosion resistance. Materials with higher PREN number have higher resistance to pitting corrosion[37]. As a rule, steel that has PREN number higher than 32 are considered resistant to seawater corrosion and steels with PREN numbers of 40 or above (like duplex steel) are used in hydrogen sulphide environments[4].

2.13 Cold Bending of Tubes

Cold bending of pipes are performed to minimize the cost of using connectors and also the cost for pipe installation. The expansion and contraction occur on the bended part of the tube. The outer wall of bend expands and inner wall contracts.

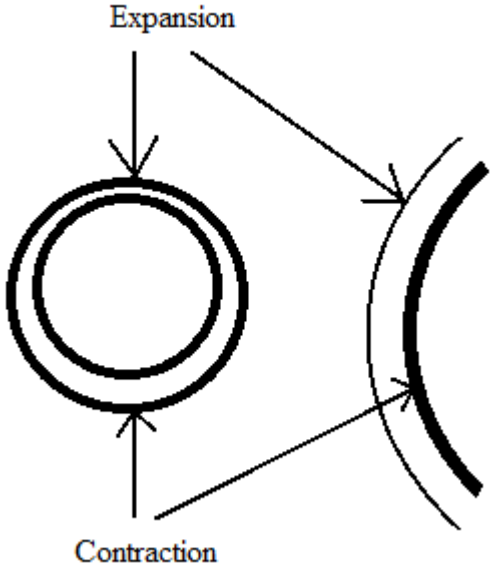

Figure 10: Change in pipe wall after bending

Wall factor and Degree of bend are the major factor to be considered for the bending of tubes.

Wall Factor= (Tube outside diameter)/(Tube wall thickness)

Degree of Bend= (Bend centreline radius)/(Tube outside diameter)

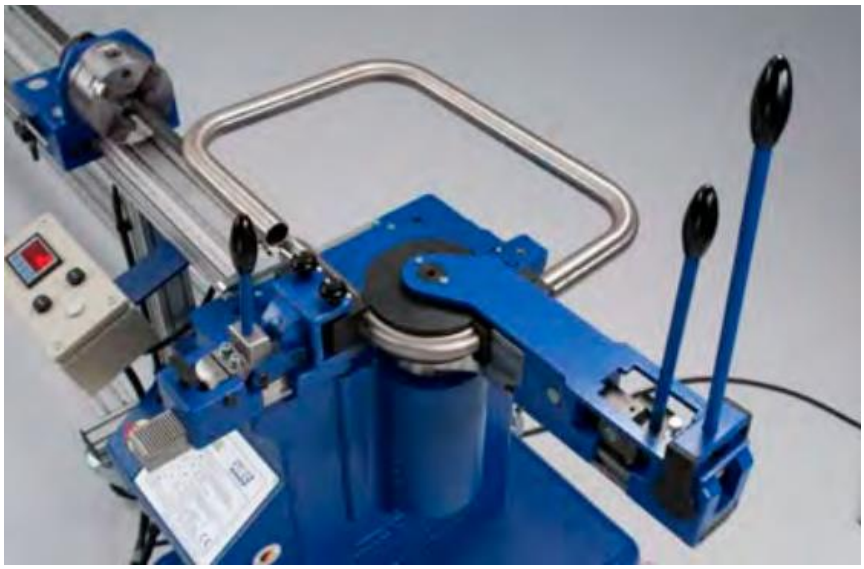

Figure 11: Modern Tube Bender[39]

There are some advantages of cold bending over mechanical or welded connection. There is requirement of preventing or removing of heat tint in welded joints. Removal of heat tint requires involvement of toxic and hazardous chemicals. Furthermore, only for outer surface it is possible to remove the heat tint. Similarly, there is minimal chance of crevice corrosion as there is less probability of trapping corrosive substance. The bended part is even and continuous[39].

2.14 Hardness

Strength of a metal can be tested by using hardness test. In hardness test, a hard material called indenter is forced into material surface with some fixed load. Indenter makes an indent on the metal surface. Indent is defined by some number which expresses the hardness of the metal[24]. Resistance of steel to indentation can be described as hardness of steel. Hardness measurement can be obtained using different methods[40]:

- The Brinell Test that uses 10 mm- diameter ball indenter under a load of 29.420 N.
- The Vickers Test where the shape of the indenter is a diamond pyramid. Load can be changed
- The Rockwell Test where the load is fixed -1471 N. Indenter is diamond cone.

There are some interrelationships between hardness and material. It is well known that hardness of metal alloys are higher than hardness of their individual components[41]

3. MATERIAL AND METHODS

According to oil and gas standards, materials used in industry should pass different mechanical qualifying test in order to be allowed to be used in industry. These tests determine the properties of the material and check if these properties are according to standards specifications. For testing, standard test methods should be used for the result obtained to be comparable.

For this project Norsok M-630 Material data sheets and Elements data sheets for piping was followed for the acceptance criteria for corrosion testing. In this standard there are two sheets of special interest concerning materials that are tested in this project[42]:

Material data sheet S01

The material data sheet contains specification for austenitic stainless steel, type 316 and its product like: wrought fittings, welded pipes, seamless and welded pipes, plates, forging, tubes, bars. There is not any requirement for corrosion test.

Material data sheet R18

This data sheet contains specification for Austenitic stainless steel, type 6Mo for product-pipes. Specification for corrosion is of interest for this project. According to the standard, corrosion test is required. Test should be performed according to ASTM G48, following method A. Test shall be performed at 50º C, and exposure time shall be 24 hours. Test specimen shall be prepared according to ASTM G48. All surfaces of test specimen shall be exposed to test solution. Also, specimen shall be pickled for 5 minutes at 60º C in a solution of 20% HNO_3 + 5% HF before being weighed and tested.

The acceptance criteria are:

- No pitting at 20 x magnification
- The weight loss shall be less than 4.0 g/m^2

Although Norsok standard M-630 has no requirement for corrosion testing for 316 austenitic stainless steel, corrosion test is performed according to ASTM G48 following the same procedure of the test as for austenitic stainless steel, type 6Mo. Because stainless steel 316 is known to be less resistant to pitting corrosion than type 6Mo, small modification for ASTM G48 was done. The aim of this project is to compare the corrosion resistance property of bend and straight part of a pipe made of those materials.

In addition to ASTM G48 test, pitting corrosion resistance of austenitic stainless steel type 316 and type 6Mo was tested based on ASTM G61. Hardness measurement was also performed. These selected tests are performed and described in details in the following subsection.

3.1 Materials

The materials used in this project were provided by HiTec Products, namely 316 SS (UNS S31603) and 6Mo (UNS S31254). Material specification can be found in appendix. They were received as finished cold bent tubes. Within each material group there were four specimens with R=5ND and four specimens with R=2.5ND i.e.16 bends in total. The corrosion test was done following ASTM G48 and ASTM G61. The hardness of the materials was measured. The steps and procedures carried out are described below.

3.1.1 Preparation of Specimen

The bend tubes obtained from the company are shown in Figure 12.

Figure 12: 316SS (Top two) and 6Mo (bottom two)

It was not possible to carry out the G48 and G61 test on received tubes. So it was decided to make them suitable for test by cutting the pipes and separating the straight and bend part. Since, comparison between the straight and bend part is the major objectives of this

project the straight and bend tubes are tested simultaneously. The materials were cut in different way for G48 and G61 test as shown in Figure 13.

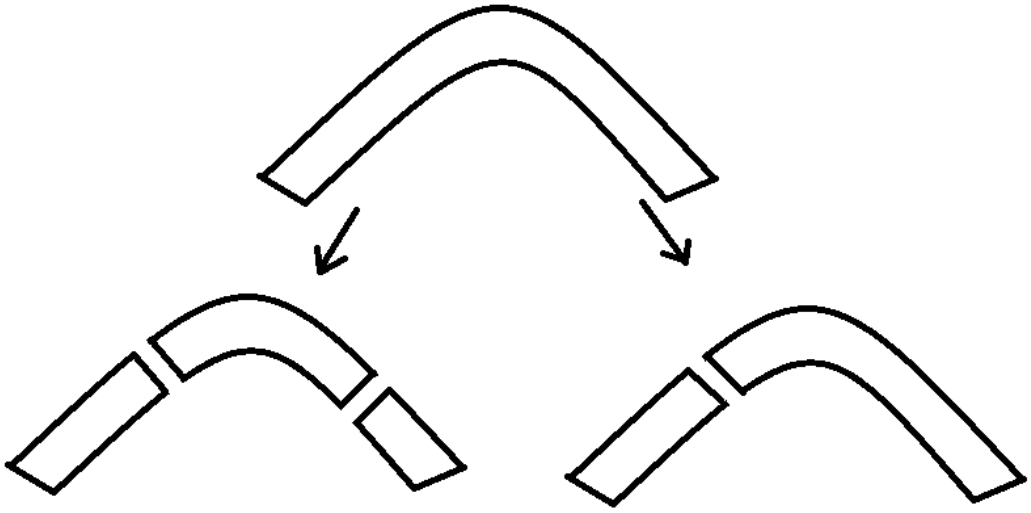

Figure 13: Cutting Method for G48 Test (Left) and G61 Test (Right)

Tubes that were used in G48 test were cut into three parts as shown in figure: two straight tubes and one bend part. Among straight parts, one straight part was larger than other and further in text we refer to a larger part as large straight and to other as small straight. Accordingly two different bends were obtained, one bend with R= 5ND further in text is called bigger bend and one with R=2.5 ND is called smaller bend. Tubes used in G61 test were cut in a way to separate one straight part from bend part. In further text straight part is called straight and bended part is called smaller bend for R=2.5ND and bigger bend for R=5ND. Received tubes were needed to be prepared before experiments. According to Norsok standard specimen should be pickled before testing, and that was done by the company that provide test specimen. Preparation beside pickling and cutting include grinding the cut edge and cleaning the tubes according to guidelines of standard test used. Mechanical saw was used for the cutting the specimen.

Figure 14: Mechanical saw used for cutting the specimens

The edge was found to be very rough after cutting. The cut edge was made smooth with the use of 120-grit abrasive paper. It was necessary to avoid the rough surface so that there would not be an initiation of corrosion from that site. The 120-grit abrasive paper and wet polishing was used for smoothing the surface.

Figure 15: 120- Grit sandpaper for removing the roughness on edge of specimens

After grinding specimen were left for a 24 hours for air passivation, as recommended in standard for G48 test. Furthermore, samples were cleaned with air jet and dipped in acetone to avoid a presence of unwanted material in the pipe. Specimens were air-dried. After cleaning the specimen was not touched with bare hands to avoid contamination of the surface. Prior testing, every specimen was weight to the nearest 0.001 g and the weight was noted as initial weight. Every specimen surface area was measured and calculated. For measurement of surface area Vernier calliper and measuring tape were used. Area of every test specimen was calculated according to formula:

For straight part:

$$\text{Area} = \frac{\pi}{2}(D^2 - d^2) + \pi L (D + d),$$

Where,

D is outer diameter of the pipe

d is inner diameter of the pipe

L is length of the pipe

For bend pipes:

$$\text{Area} = \frac{\pi}{2}(D^2 - d^2) + \pi \left(\frac{L+l}{2}\right)(D + d),$$

Where,

D is outer diameter of the pipe

d is inner diameter of the pipe

L is length of outer curvature of the pipe

l is length of inner curvature of the pipe

3.2 ASTM G48

ASTM G48 Test states, *"Standard Test Methods for Pitting and Crevice Corrosion Resistance of Stainless Steels and Related Alloys by Use of Ferric Chloride Solution".* Method A is Ferric Chloride pitting test and it is the one being followed.

Different types of measurements were performed to see the variation of pitting corrosion results on the specimen. Two different approaches were followed to accomplish G48 test for this project.

First approach

This approach is modified version of ASTM G48 test. Specimen's resistance to pitting corrosion were tested on different temperature of ferric chloride solution to examine their weight loss. Specimen had multiple exposures, with increasing the time of exposure. The set of the test is given in Table 7 and Table 8.

Table 7: First set of G48 experiment for 316SS

Duration of exposure (hours)	24 h.	48 h.	72 h.	96 h.
Temperature in ºC	7º	15º	22º	30º

Table 8: First set of G48 experiment for 6Mo

Duration of exposure (hours)	24 h.	48 h.	72 h.	96 h.
Temperature in ºC	22º	30º	40º	50º

Second approach

This approach follows exact guidelines of the ASTM G 48 test. Examination on weight loss of specimen against ferric chloride solution was done but only for the time of exposure of 24 hours and temperature of 22±2º for 316 Stainless Steel and 50±2º for 6Mo. The setup of the experiment is given in the Table 9.

Table 9: Second approach set up of G 48 experiment for 316 SS and 6 Mo

316 SS		**6Mo**	
Exposure hours	24 h.	Exposure hours	24 h.
Temperature in ºC	22±2º	Temperature in ºC	50±2º

Furthermore, 6Mo was also tested at 60º Celsius.

3.2.1 Apparatus required

- Beaker
- Plastic Rod for Supporting Specimen
- Water Bath
- Nylon Wire
- Thermometer
- pH meter
- plastic balls for preventing evaporation of the water bath
- plastic folia

3.2.2 Procedure

100 g of Reagent grade ferric chloride $FeCl_3.6H_2O$ was dissolved in 900 ml of distilled water (6% $FeCl_3$ by mass). Solution volume was ensured to be at least 5 ml/ cm^2 of surface area for specimen tested. The pH was made sure to be maintained all over the experimental period according to G48. For every new test, new solution was made. The water bath was filled with distilled water and was used for maintaining the desirable temperature. The surface of the water in water bath was covered with plastic balls to prevent evaporation of the water on high temperature. The solution was poured in the beaker and kept in a water bath to bring it to the desirable temperature. At the same time, samples were tied with a thin nylon and tied on plastic rods

Figure 16: Samples ready for G48 experiment

After the solution reached desired temperature, the samples were immersed in the solution. Figure 17 illustrate the immersion of sample in ferric chloride solution.

Figure 17: Samples in Ferric Chloride solution

In every beaker two test specimen of the same material were placed. In one beaker one bend part and one straight part were placed to ensure that both straight and bend part will be in exactly the same environment condition and comparison after test will be more accurate.

After placing the specimen in a beaker immersing them into ferric chloride solution, plastic cover was used to cover the beakers to prevent evaporation of the test solution. Finally, beakers were ready to be placed in a water bath. They were left there for 24 hours.

Figure 18: ASTM G48 Experiment

After the test time was over, specimens were rinsed with water and nylon brush was used for removing corrosion products. After cleaning they were dipped in acetone for 15 minutes and left for drying on a room temperature for 24 hours.

Dried specimens were first visually inspected for pits, than their weight loss was measured. At the end, scanning electron microscope was used for better examination of the specimen surface.

After measurement and examination of the specimens, test was repeated on the same specimen but on higher temperature. 24 hours was time for each temperature of the test. Initial temperature for 316 SS was 7º C and for 6Mo was 22 º C (for first approach). For second approach, temperature was 22±2º C for 316 SS and 50±2º C for 6Mo. Test was stopped after 24 hours.

Deviation from G48 Test

A glass cradle or hook was supposed to be used according to G48 Test. The trial was done by using a glass cradle and a thin nylon wire on a sample specimen of 316SS. The reason for this was to find a method that would cause the least crevice corrosion on the specimen. Between these tests, the amount of weight loss due to the use of glass cradle was found more than the use of nylon wire. Hence, the nylon wire was used. The crevice corrosion effect due to nylon wire at higher temperatures was neglected as the focus was on pitting corrosion of the material. In the first approach of the experiment besides recommended

temperature of 22±2º C and 50 ±2º C, other temperatures 30º C and 40º C were used. This was done for studying the resistance to pitting of the material tested on different temperature and exposure time. Although, ASTM G48 states that examination for pits should be done at low magnification microscope with 20x magnification, in this case was impossible to be performed because of the curvy surfaces of the pipes. With low magnification microscope only flat surfaces can be studied. Hence, the Scanning Electron Microscope was used.

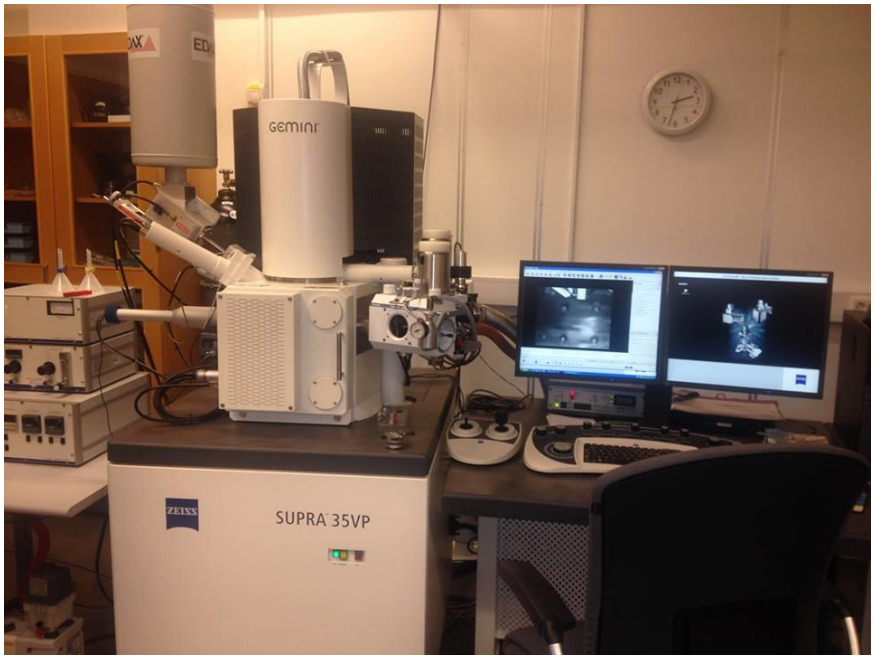

Figure 19: Scanning Electron Microscope (SEM)

The Scanning Electron Microscope (SEM) was used to detect any corrosion on the material and the pictures were taken at 40X and 100X magnification. SUPRA FE-SEM is used in this project. The straight and bend parts were closely studied after each test on electron microscope. The specimens where placed on a small metal disk and cleaned with air-jet before they were placed in a SEM.

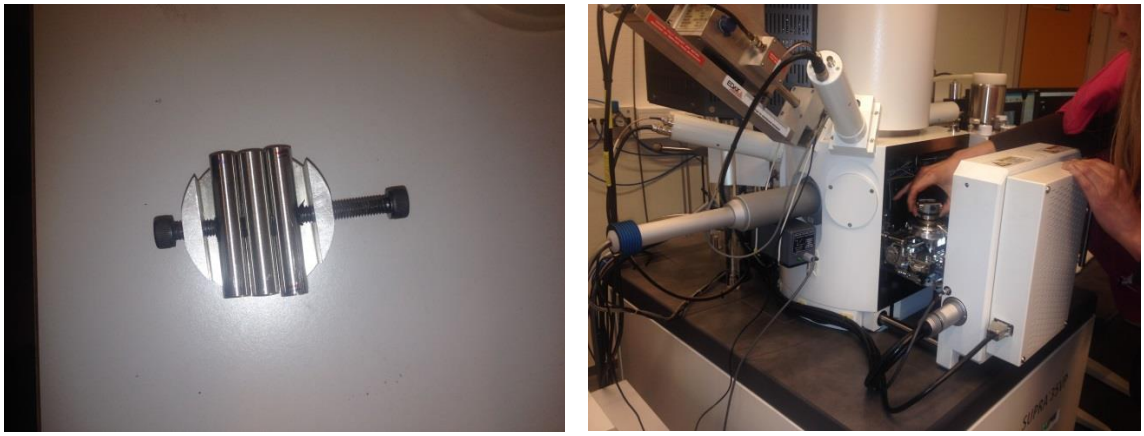

Figure 20: Samples ready for observation in SEM (Left) and placement in SEM (right)

The specimens were finally cut to wide open the tubes laterally to see any corrosion effect inside the tubes. The cutting was done after exposure at final designated temperature for every specimen. The results observed are discussed in Results and Discussion chapter and the images taken are presented in Appendix.

3.3 ASTM G61

ASTM G61 states, "Standard Test Method for Conducting Cyclic Potentiodynamic Polarization Measurements for Localized Corrosion Susceptibility of Iron-, Nickel-, or Cobalt-Based Alloys".

This standard test procedure was followed for finding the pitting potential of tested material and to study difference in pitting potential between straight and bend tubes. The result obtained by this test should be support for result obtained from ASTM G48 test.

3.3.1 Apparatus Required

- Beaker
- Gamry Potentiostat
- Working Electrode (Specimen)
- Reference Electrode (Saturated calomel electrode)
- Counter Electrode (platinum electrode)
- Electrode Holder
- Thermometer

3.3.2 Procedure

The procedure according to ASTM G61 was followed. 34 g of Sodium Chloride was dissolved in 920 ml of distilled water (3.56 % by weight). 900 ml of the solution was used

ensuring that the sample was immersed in the solution with desired part above a solution for connection to corresponding working electrode cable. Experiment was run on room temperature (22±2◦ C). Experiment setting is shown in Figure 21.

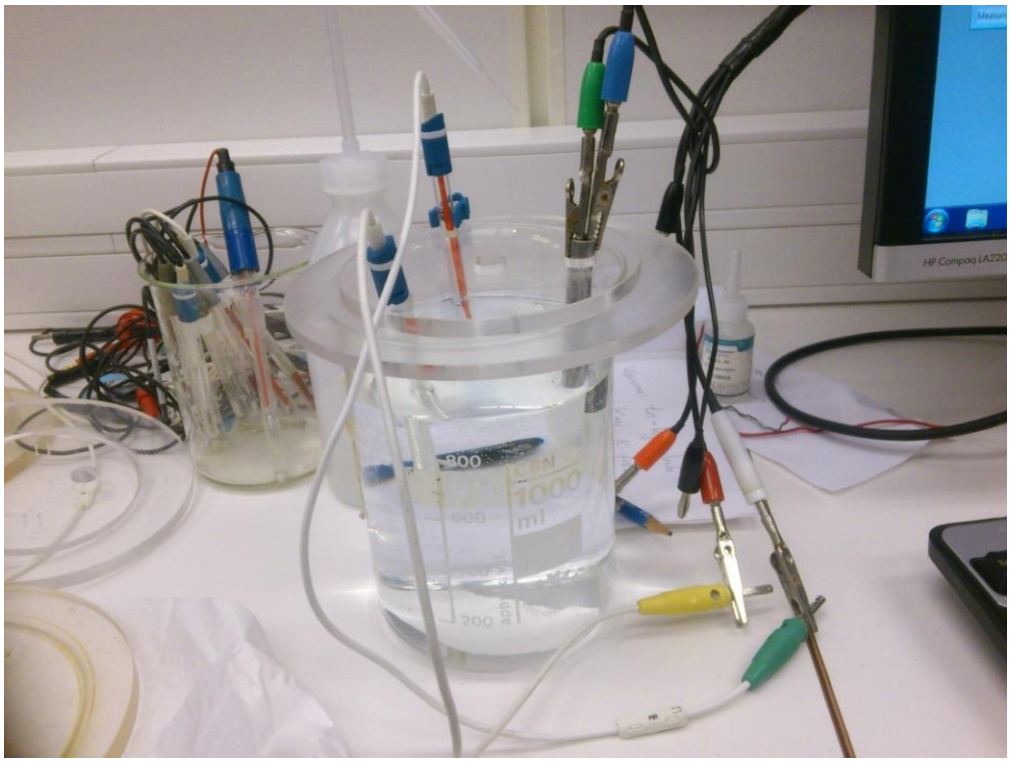

Figure 21: ASTM G61 Test

After the circuit was made ready, the open circuit potential (OCP) was allowed to run for an hour. The OCP was run under the setting shown in Figure 22.

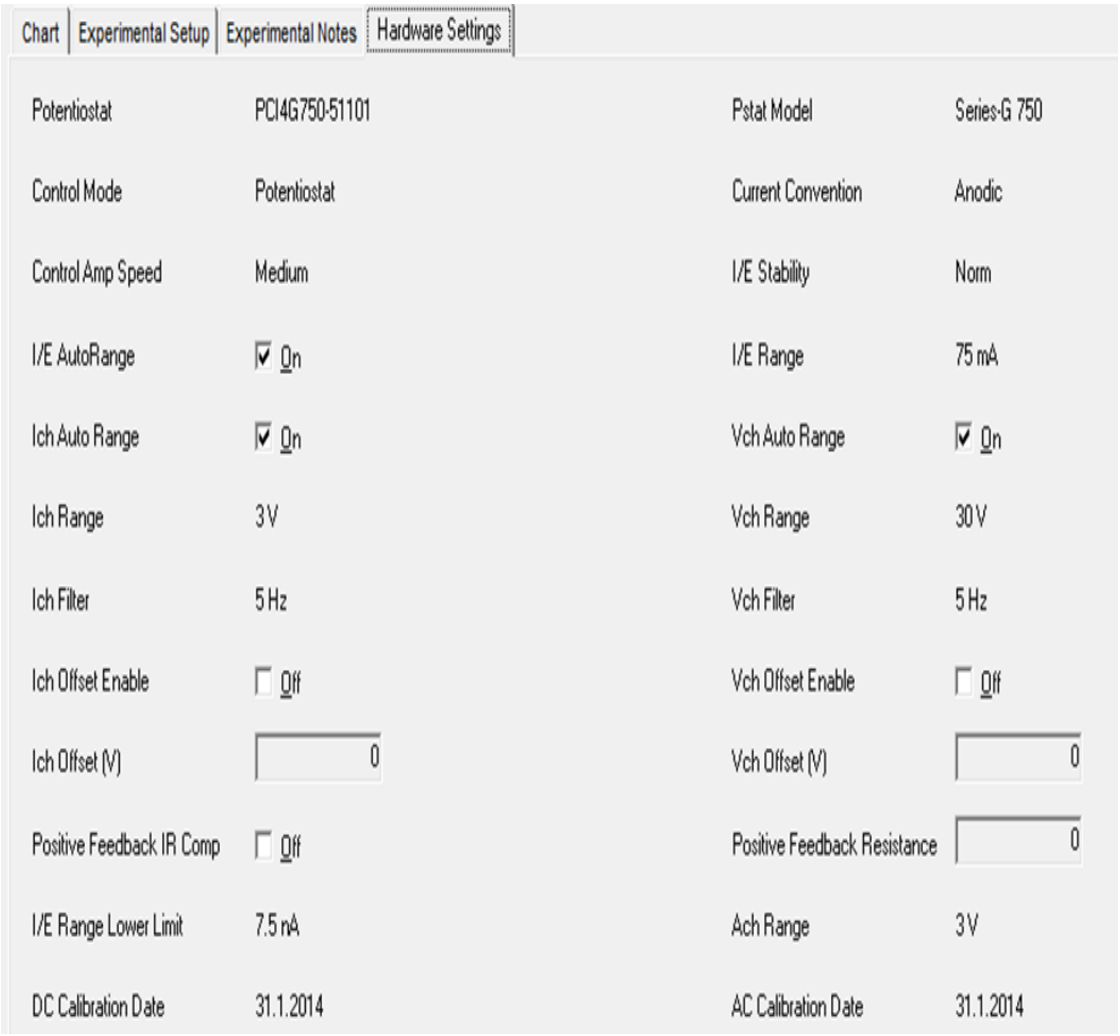

Figure 22: Hardware setting for OCP Run

After completing OCP run for an hour, cyclic polarization test was conducted. They were performed in a hardware setting shown in Figure 23.

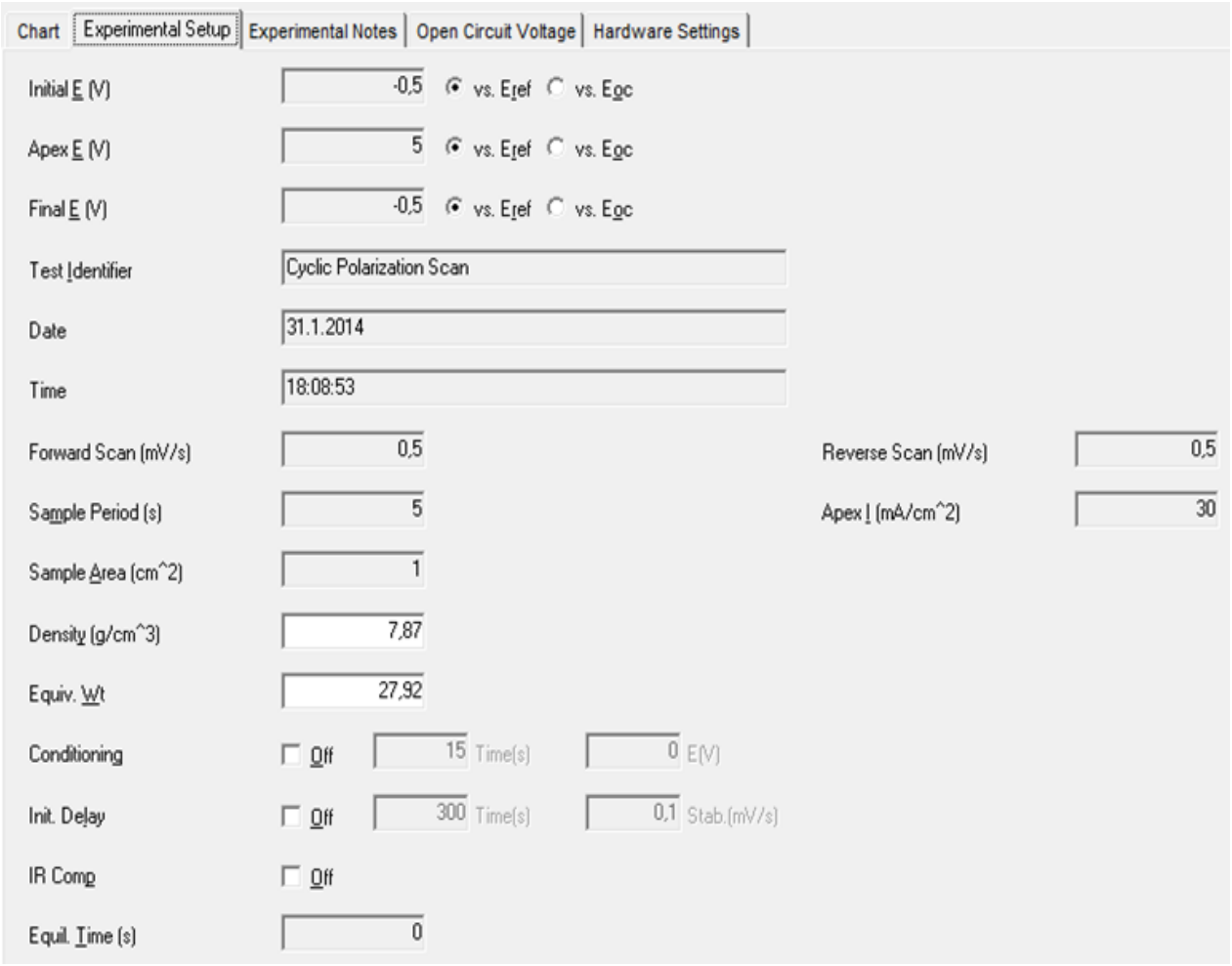

Figure 23: Hardware Setting for Cyclic Polarization

The area of the immersed portion of the specimen was measured for the calculation of current density. There was a mark left on the specimens after the test due to sodium chloride solution. After area calculation current density (A/cm^2) was calculated and plotted against potential. The area of 316SS and 6Mo specimens after ASTM G61 test are presented in the Table 10.

Table 10: Area calculation for 316 SS and 6Mo after G61 test

Material testet	Inner diameter	Outer diameter	Length	Area
316 Bigger bend	0.5	0.935	8.75	39.9368
316 Smaller bend	0.5	0.935	8.30	37.9081
316 Straight	0.5	0.935	1.16	5.7197
6Mo bigger bend	0.5	0.935	9.30	42.4163
6Mo Smaller band	0.5	0.935	8.55	39.0352
6Mo straight	0.5	0.935	1.47	7.1172

Before the experiment was started, Gamry Potentiostat was calibrated. The instrument was supposed to be calibrated in every six months or if the program has not been used for longer period. Calibration of instrument has been illustrated in Figure 24.

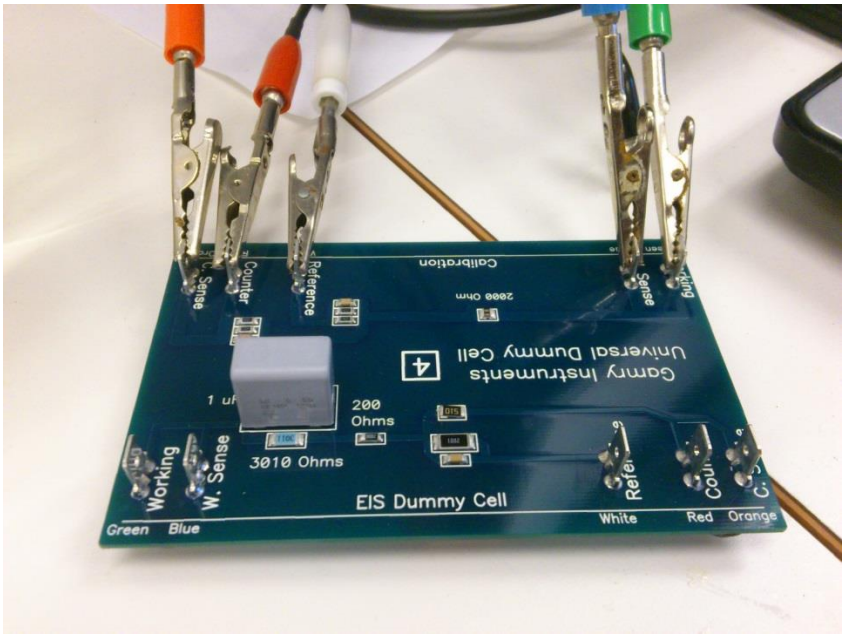

Figure 24: Calibration of Gamry Potentiostat

3.4 Hardness Measurement

The hardness of the material was measured at the straight and bend part to compare with the hardness provided earlier at specification. Hardness of material was measured before and after testing. Vickers method was used for the measurement of hardness of the material. HV10 or HV05 unit was used to express the hardness.

Figure 25: Hardness Measurement Instrument (Struers)

4. RESULTS

The results obtained in this project are divided into three parts. The first part presents the results obtained from ASTM G48 accompanied with the images obtained from scanning electron microscope (SEM). The results are presented in tabulated form and graph. The second part deals with the result obtained from ASTM G61 section where the cyclic polarization curves are plotted. It envisages the pitting potential and repassivation potential for the straight and bends part of the specimens. The final section shows the hardness measurement of the specimen before and after the G48 Test. It shows the susceptibility of the outer surface of the material to the acidic oxidizing environment.

4.1 ASTM G48

4.1.1 ASTM G48-316Stainless Steel

The results obtained from ASTM G48 for the first approach (refer method section for detail) are presented in this section. Table 11 presents the Area calculation for 316SS specimens. The diameters were measured by a Vernier calliper and length was measured by a measuring tape. Bigger Bend specimen was found to have the largest area with 68.2652 cm^2 and small straight has minimal surface area 17.7510 cm^2.

Table 11: Area Calculation for 316SS Specimens for First Approach

316 Stainless steel	Inner diameter (cm)	Outer Diameter (cm)	Length (cm)	Area (cm^2)
Bigger Curve	0.5	0.935	14.925	68.2652
Smaller Curve	0.5	0.935	13.775	63.0808
Straight large	0.5	0.935	4.92	23.1608
Straight small	0.5	0.935	3.72	17.751

The weights of the specimens were measured before and after exposure in ferric chloride solution. The initial weight and the final weight of specimen after testing at different temperature are shown in Table 12. The specimens were tested for 96 hours with increase in temperature after every 24 hours. The specimens were examined after exposure at each temperature.

Table 12: Weight of 316SS specimens for First Approach

316 Stainless steel	Initial Weight in g	Weight in g (24 h)	Weight in g (48 h)	Weight in g (72 h)	Weight in g (96 h)
Bigger Curve	57.5705	57.5705	57.5500	57.4827	56.8393
Smaller Curve	53.2482	53.2482	53.2264	53.2095	52.7875
Straight large	18.915	18.915	18.9031	18.7897	18.5145
Straight small	14.3178	14.3178	14.3151	14.2855	14.1517

After the measurement of weight of all specimens, the weight loss per unit area for each specimen was calculated. As it can be seen in Table 13, there was no weight loss in any specimen at 7°C. There was gradual increment in weight loss per unit area g/m^2 with increase in temperature. At the end of the experimental set, after multiple exposure of specimen to ferric chloride solution for total time of 96 h, the bigger bend was found to have 107.11 g/m^2 of weight loss whereas the large straight was also found to have weight loss of 172.92 g/m^2. Straight small and small bend were found to lose 93.5 and 73.03 g/m^2.

Table 13: Weight Loss per Unit Area for 316SS Specimens for First Approach

316 Stainless steel	Weight loss Per unit area in g/m2 at 7°C (for 24 h)	Weight loss Per unit area in g/m2 at 15°C (for 48 h)	Weight loss Per unit area in g/m2 at 22°C (for 72 h)	Weight loss Per unit area in g/m2 at 30°C (for 96 h)
Bigger Curve	0	3.002993949	12.86160335	107.1116671
Smaller Curve	0	3.45588559	6.134989557	73.03332529
Straight large	0	5.137990594	54.1000186	172.9214481
Straight small	0	1.521042594	18.19617621	93.57228696

Figure 26 compares the weight loss per unit area for different specimens of 316SS. It was expected that the cold bended part would lose significant weight compared to the straight part. There was not any relationship observed between the weight loss per unit area and straight/bend part. It can be noticed that weight loss per unit area of straight large was highest and of smaller curve was the lowest. However, the exposure temperature was seen

to have significant impact on weight loss of material. The weight loss was increased from 0 g/m^2 at 7°C to 73 g/m^2 for smaller curve and 172.9 g/m^2 for straight large at 30 °C.

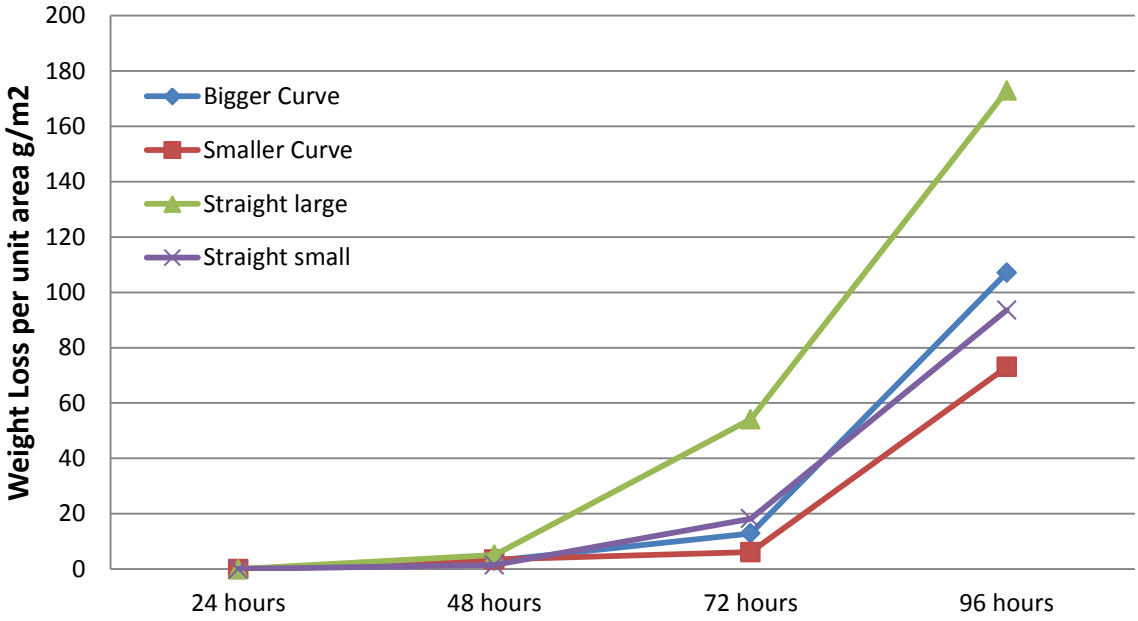

Figure 26: Comparison of weight loss per unit area for different specimens of 316SS

Figure 27 shows the images from Scanning Electron Microscope for 316SS Bigger Bend and Smaller Bend after ASTM G48 test at 7°C. As it can be seen that the surface was smooth and there was not any pitting or crevice corrosion.

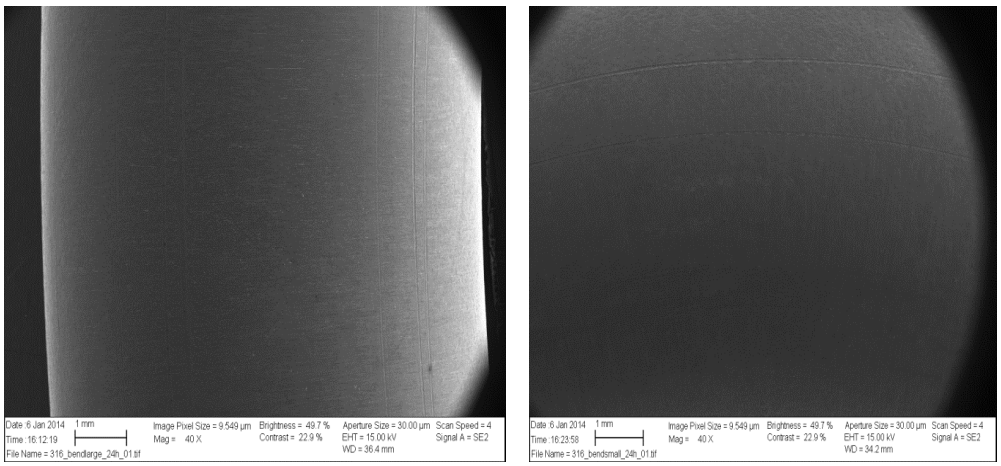

Figure 27: 316SS Bigger Bend (left) and Smaller Bend (right) after 24 h. exposure at 7°C

Figure 28 represents the images from SEM for 316 SS Large Straight and Small Straight after 24 hours exposure at 7°C in ferric chloride. There as well was not any corrosion seen on the surface.

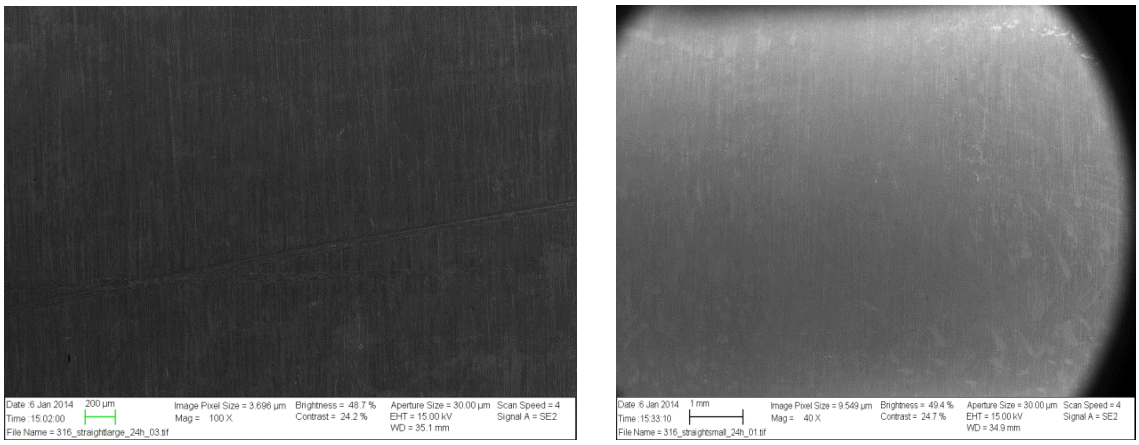

Figure 28: 316SS Large Straight (left) and Small Straight (right) after 24 h. exposure at 7°C

The images from SEM were taken after every G48 Test. They are presented in Appendix. The images show that there was no occurrence of pitting or crevice corrosion after testing at 15°C for both straight and bend part. The image of 316 SS Smaller Bend after exposure at 22°C is shown in Figure 29. After exposure at 22°C as well, there were not any pits seen at lower magnification. However, at 500X magnification, a pit of 37.56 µm was visible. It shows that the initiation for pit can be seen at 316SS after exposure at 22°C. However, the pit was observed not only in the bend part, but in straight as well. Figure 31 shows that the pit with diameter 44.35 µm was seen at large straight part. Thus, there was no significant differences noticed between the straight and bend part after G48 Test on 316SS specimens.

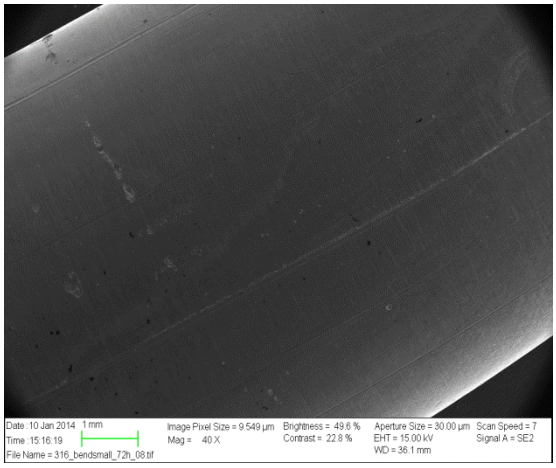

Figure 29: 316SS Smaller Bend after exposure at 22°C

Figure 30: 316SS Bigger Bend after exposure at 22°C

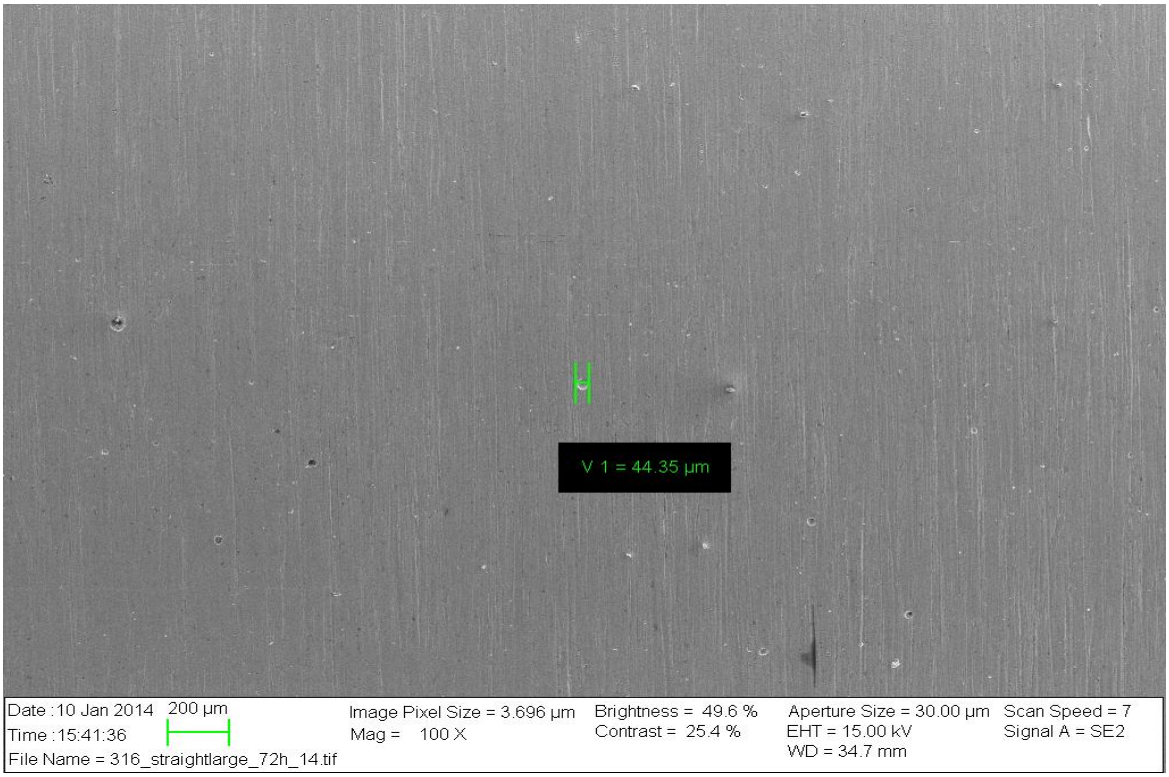

Figure 31: 316SS Large Straight after exposure at 22°C

These specimens were further tested at 30°C and the material was found to be heavily corroded. Lots of pits and crevice corrosion were visible. The pits were penetrating the surface of material making a depth of about 0.26 cm. However, the pattern was found to be similar for both straight and bend part. After testing at 30ºC, it was decided to cut the specimen laterally to observe its inner surface for presence of any pitting or crevice corrosion. Figure 32 shows the inner surface of the 316SS tubes.

Figure 32: Inner surface of 316SS straight part (left) and bended part (right)

4.1.2 ASTM G48-6Mo Stainless Steel

The area calculation for the specimens of 6Mo stainless steel for first approach test is shown in Table 14. Smaller bend specimen was found to have the largest surface area of 65.22 cm^2 whereas the straight small had least surface area of 18.044 cm^2.

Table 14: Area Calculation for 6Mo Specimens for First Approach

6Mo Stainless Steel	Inner diameter (cm)	Outer Diameter (cm)	Length (cm)	Area (cm^2)
Bigger Curve	0.5	0.935	14.125	64.6587
Smaller Curve	0.5	0.935	14.25	65.2222
Straight large	0.5	0.935	4.725	22.2817
Straight small	0.5	0.935	3.785	18.044

Like previously, the weight was measured before and after each ASTM G48 test. The weight was found to decrease with the increase in exposure temperature. Weight measured for each specimen at different exposure time is shown in Table 15.

Table 15: Weight of 6Mo Stainless Steel specimens for First Approach

6Mo Stainless steel	Initial Weight in g	Weight in g (24 h)	Weight in g (48 h)	Weight in g (72 h)	Weight in g (96 h)
Bigger Curve	55.3089	55.3089	55.3085	55.3084	55.3075
Smaller Curve	55.6121	55.6121	55.6119	55.6116	55.611
Straight large	18.4582	18.4582	18.4576	18.4478	18.4354
Straight small	14.7896	14.7896	14.7885	14.7821	14.7772

Weight loss per unit area was calculated after measuring the weight. Table 16 shows that the weight loss per unit area at 22°C is 0 g/m^2. There was not any effect on material at this temperature in acidic environment. With the increase in temperature, the weight loss was observed but it was found to be less than 1 g/m^2 at 30°C. At 40°C, straight large and small were measured to lose more than 4 g/m^2 whereas bended parts lose less than 1 g/m^2. When temperature further increased to 50°C, weight loss per unit area increased as expected, however bended parts were found to lose less weight than straight parts.

Table 16: Weight Loss per Unit Area for 6Mo Stainless Steel Specimens for First Approach

6Mo Stainless steel	Weight loss Per unit area in g/m^2 at 22°C (for 24 h)	Weight loss Per unit area in g/m^2 at 30°C (for 48 h)	Weight loss Per unit area in g/m^2 at 40°C (for 72 h)	Weight loss Per unit area in g/m^2 at 50°C (for 96 h)
Bigger Curve	0	0.061863332	0.077329166	0.216521664
Smaller Curve	0	0.030664415	0.076661037	0.168654282
Straight large	0	0.269279164	4.667505514	10.23260824
Straight small	0	0.609620444	4.156503027	6.872085005

Figure 33 illustrates the comparison of weight loss per unit area of different 6Mo specimens. Straight parts were seen as losing more weight per unit area compared to the bend parts.

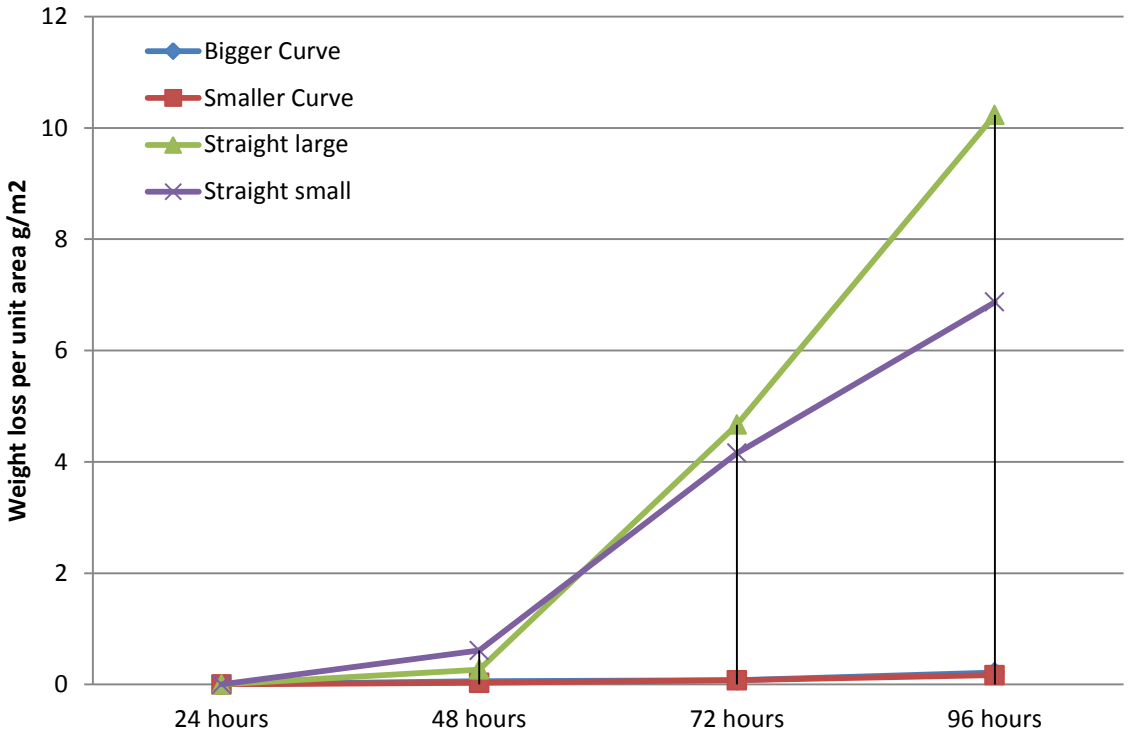

Figure 33: Comparison of weight loss per unit area for different specimens of 6Mo

Figure 34 and Figure 35 shows the images from SEM for 6Mo Bend parts and straight part respectively and after exposure at 22°C, and since the weight loss of 0 g/m^2, it can be seen that there is no effect on the smoothness of surface. On images of 6Mo Bigger Bend, a mark can be seen and it was due to the presence of dust on the surface.

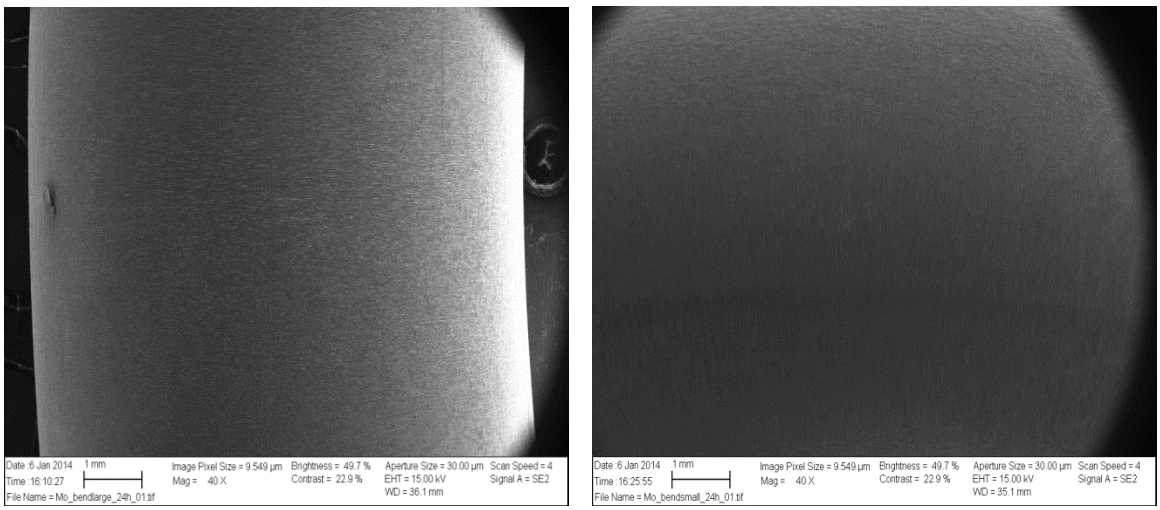

Figure 34: 6Mo Bigger Bend (left) and Smaller Bend (right) after exposure at 22°C

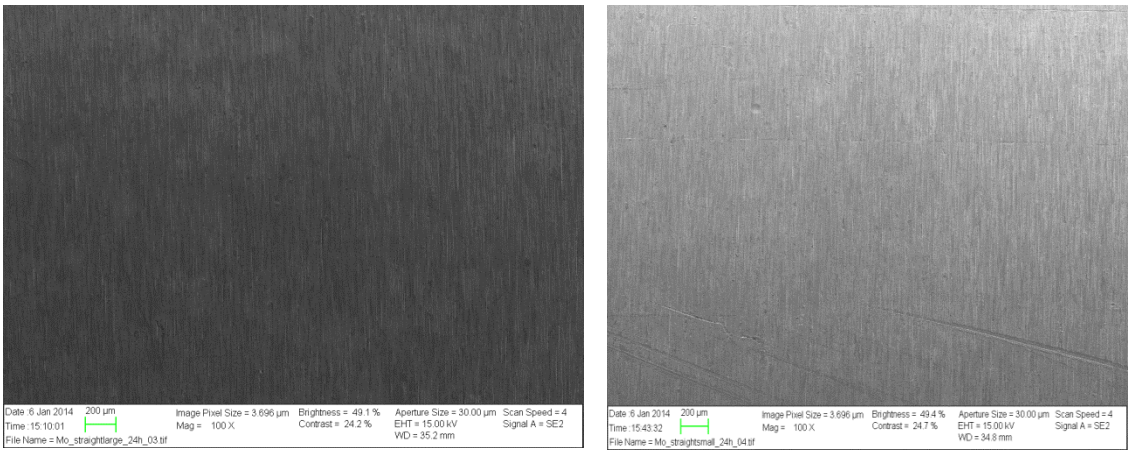

Figure 35: 6Mo Straight Large (left) and Straight Small (right) after exposure at 22°C

The images taken after testing at 30°C, 40°C and 50°C temperatures are presented in the Appendix. There was no observation of pitting corrosion on the specimens until 50°C. However, the crevice was seen due to the nylon wire at 50°C. The crevice was seen similar on straight and bend part. There was no significant difference between the straight and bend parts of 6Mo. At the end of the test, specimens were cut wide open for observation of pitting corrosion inside the pipes. The images also showed no sign of pitting corrosion inside of pipes.

Figure 36: Outer (left) and Inner surface (right) of 6Mo specimens after G48 Test at 50°C

After the completion of first approach testing, the second approach was initiated. The area was calculated for 316SS specimens for the initiation of second approach. Table 17 presents the dimension of specimen with the area calculated.

Table 17: Area Calculation for 316SS Specimens for Second Approach

316 Stainless steel	Inner diameter (cm)	Outer Diameter (cm)	Length (cm)	Area (cm^2)
Bigger Curve	0.5	0.935	12.4	56.88204
Smaller Curve	0.5	0.935	13.025	59.69965
Straight large	0.5	0.935	4.135	19.62188
Straight small	0.5	0.935	3.22	15.49689

The weight loss per unit area was calculated for 316SS specimens after G48 test at 22° Celsius. The weight losses per unit area for every specimen are presented in Table 18. It can be seen that the straight parts were found to lose more weight per unit area compared to bend parts.

Table 18: Weight Loss per unit area of 316SS specimens at 22°C for Second Approach

316 Stainless steel	Initial Weight (g)	Weight (after 24 hours in g)	Weight Loss (g/m^2) (at 22°C)
Bigger Curve	47.6852	47.5727	19.77777297
Smaller Curve	50.2658	50.2373	4.773897134
Straight large	15.993	15.9455	24.20767099
Straight small	12.3996	12.3407	38.00762796

There was no observation of visible pits on the specimens; however the crevice corrosion was caused due to the nylon wire. The weight loss was due to the crevice corrosion attack at the connection site between tube and wire. However, there was not any difference seen between the crevices seen on straight and bend parts.

The second approach for ASTM G48 for 6Mo stainless steel initiated with the measurement of dimension and calculation of area. Table 19 shows the area calculation of the specimen for 6Mo stainless steel for second approach.

Table 19: Area Calculation for 6Mo Stainless Steel Specimens for Second Approach

6Mo Stainless Steel	Inner diameter (cm)	Outer Diameter (cm)	Length (cm)	Area (cm^2)
Bigger Curve	0.5	0.935	12.7	58.23449
Smaller Curve	0.5	0.935	10.925	50.23246
Straight large	0.5	0.935	5.2	24.4231
Straight small	0.5	0.935	4.3	20.36573

The weight was measured before the experiment and after the test final weight was measured and the weight per unit area in g/m^2 was calculated. The experiment was done at 50°C and the results obtained are shown in Table 20. Results showed that 6Mo was much more resistant to corrosion. The weight loss per unit area was found to be nearly equal to 0 g/m^2. There was not any sign of pitting or crevice corrosion. There was not any difference found between straight and bend parts of 6Mo stainless steel after G48 test at 50° Celsius.

Table 20: Weight Loss per unit area of 6Mo stainless steel specimens at 50°C for Second Approach

6Mo Stainless Steel	Initial Weight (g)	Weight in g (after 24 hours)	Weight Loss(g/m^2) (at 50° Celsius)
Bigger Curve	49.7518	49.7516	0.034343907
Smaller Curve	42.6702	42.6702	0
Straight large	20.5227	20.5226	0.040944848
Straight small	17.0547	17.0547	0

Further, 6Mo Stainless Steel specimens where tested for 24 h. on 60˚ C. Figure 37 presents image of specimens after test.

Figure 37: Specimens of 6Mo Stainless Steel after exposure to ferric chloride solution on 60º C

It can be seen the failure of the material after this temperature. Big pits are formed and huge mass loss was measured. Calculation for weight loss in gram per meter square is presented in Table 21.

Table 21: Weight loss measurement for 6Mo Stainless Steel after exposure to ferric chloride solution on 60º C

6Mo Stainless Steel	Area (cm2)	Initial Weight (g)	Weight in g (after 24 hours)	Weight Loss(g/m2) (at 60° Celsius)
Bigger Curve	58.23449	49.7518	48.9644	135.212
Smaller Curve	50.23246	42.6702	42.0772	118.0512
Straight large	24.4231	20.5227	20.0373	198.7463
Straight small	20.36573	17.0547	16.6767	185.6059

4.2 ASTM G61-316

The potentiodynamic polarization scan was performed for straight and bend parts of 316 Stainless Steel. An open circuit potential (OCP) was run before starting a cyclic polarization. Different plots were obtained after the completion of scan and were analysed. Results obtained from open circuit potential are presented in Table 22. Graphs obtained from OCP are shown in Appendix.

Table 22: Open circuit potential for 316 SS and 6Mo Stainless steel

Specimens	316 stainless steel	6Mo stainless steel
Bigger bend	-10 mV	-110 mV
Smaller bend	0.5 mV	0 mV
Straight part	-28 mV	-50 mV

4.2.1 ASTM G61-316 Stainless Steel Stainless Steel

Figure 38 shows the cyclic polarization of straight part 316 Stainless Steel. As it can be seen, the corrosion potential is about -0.15 V. The plot of potential against current density is shown in appendix. Since there was not any visible breakpoint on plot to distinguish the corrosion potential, the current density of 10^{-5} A/cm^2 was considered and pitting potential of 0.25 V was observed. The hysteresis was seen and it shows that the material is less resistant to pitting and crevice corrosion. The repassivation potential was found to be at 0.1 V.

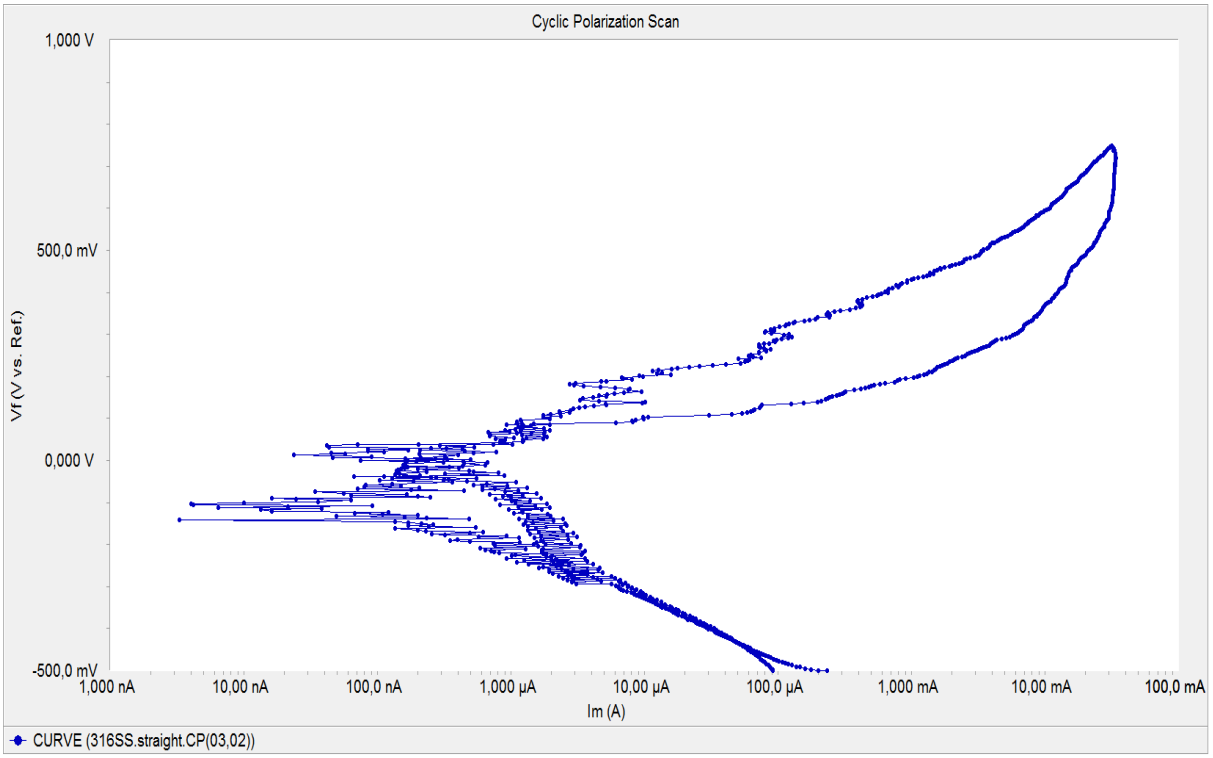

Figure 38: Cyclic Polarization for 316SS Straight Part

Figure 39 presents the cyclic polarization of bigger bend 316 Stainless Steel. The corrosion potential was found to be about 0 V. The current density of 10^{-5} A/cm^2 was considered in this case as well and the pitting potential of 0.52 V was observed. The hysteresis was seen in this plot as well. The repassivation potential was found to be about 0.15 V.

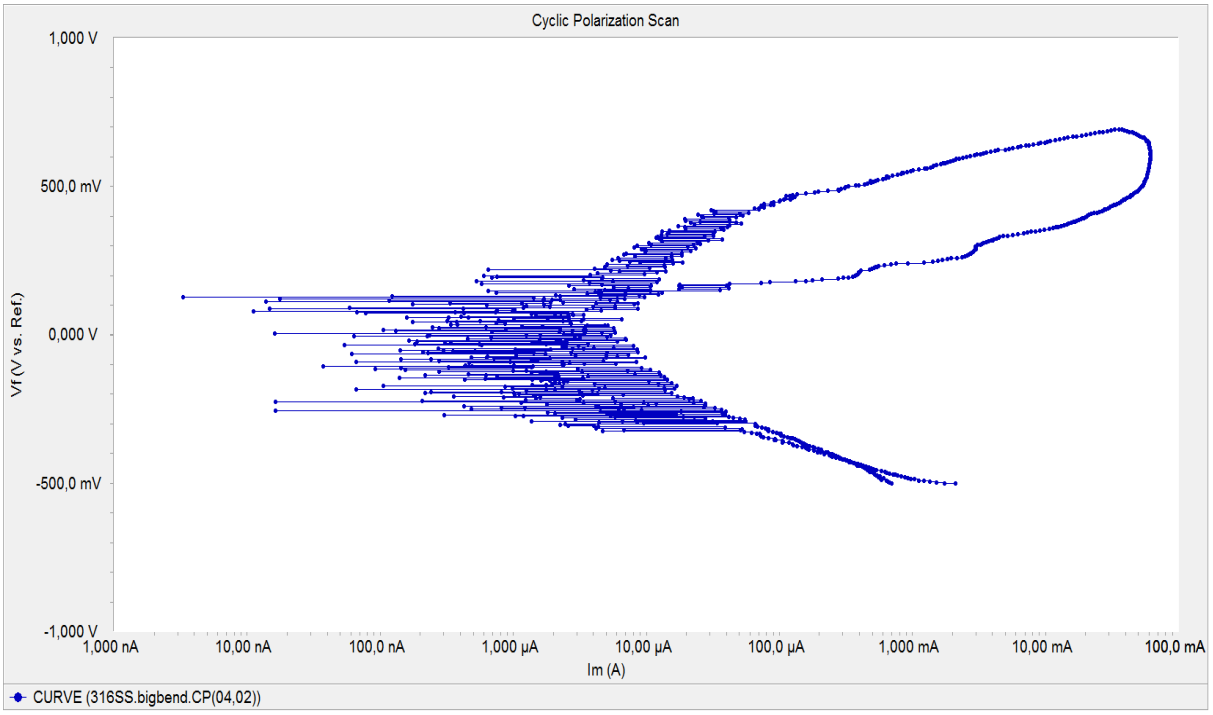

Figure 39: Cyclic Polarization for 316SS Bigger Bend

Figure 40 shows the cyclic polarization of 316SS smaller bend. The corrosion potential was observed to be about -0.1V. At the current density of 10^{-5} A/cm^2 the potential was found to be 0.5 V. The graph of potential vs current density is shown in appendix. The repassivation potential was observed to be at 0.1 V.

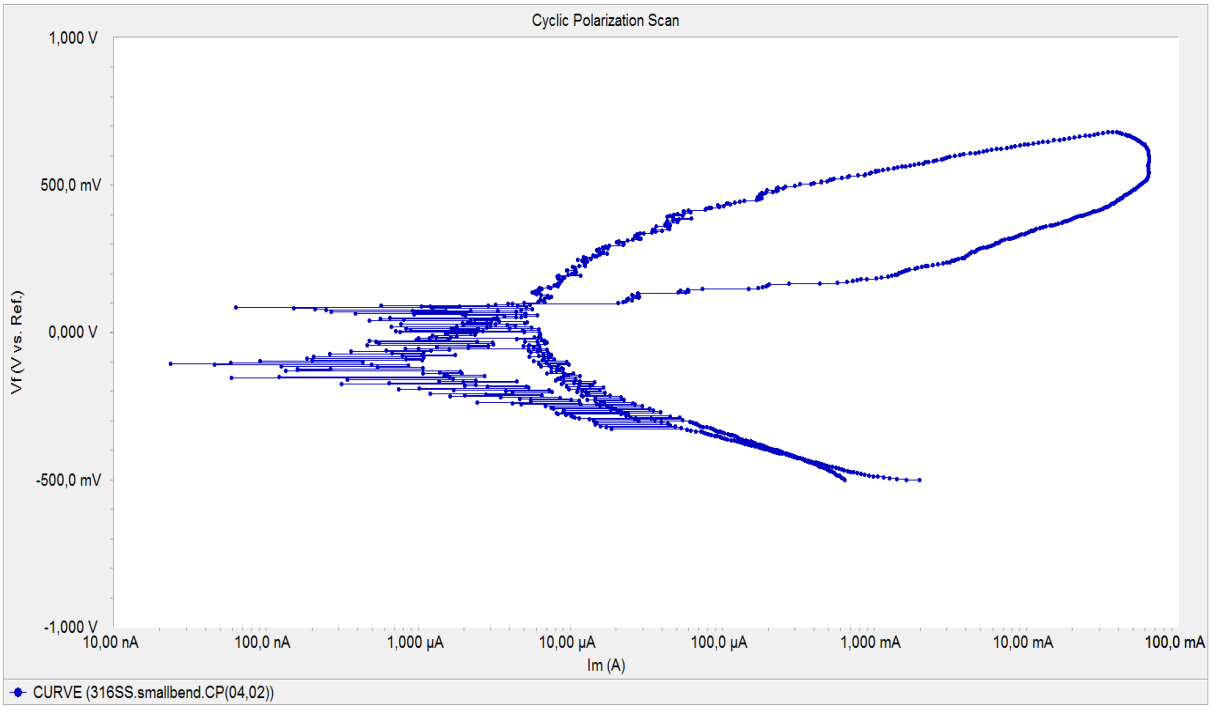

Figure 40: Cyclic Polarization for 316SS Smaller Bend

4.2.2 ASTM G61-6Mo Stainless Steel

The cyclic polarization scan for 6Mo straight part is shown in Figure 41. The pitting potential is seen at about 1 V. Repasivation potential was found at 0.9 V. There was observation of very small hysteresis as the reverse potential plot almost overlaps with the plot of potential increment. The material was found to be highly resistant to crevice corrosion. Plot of potential against current density is shown in Appendix.

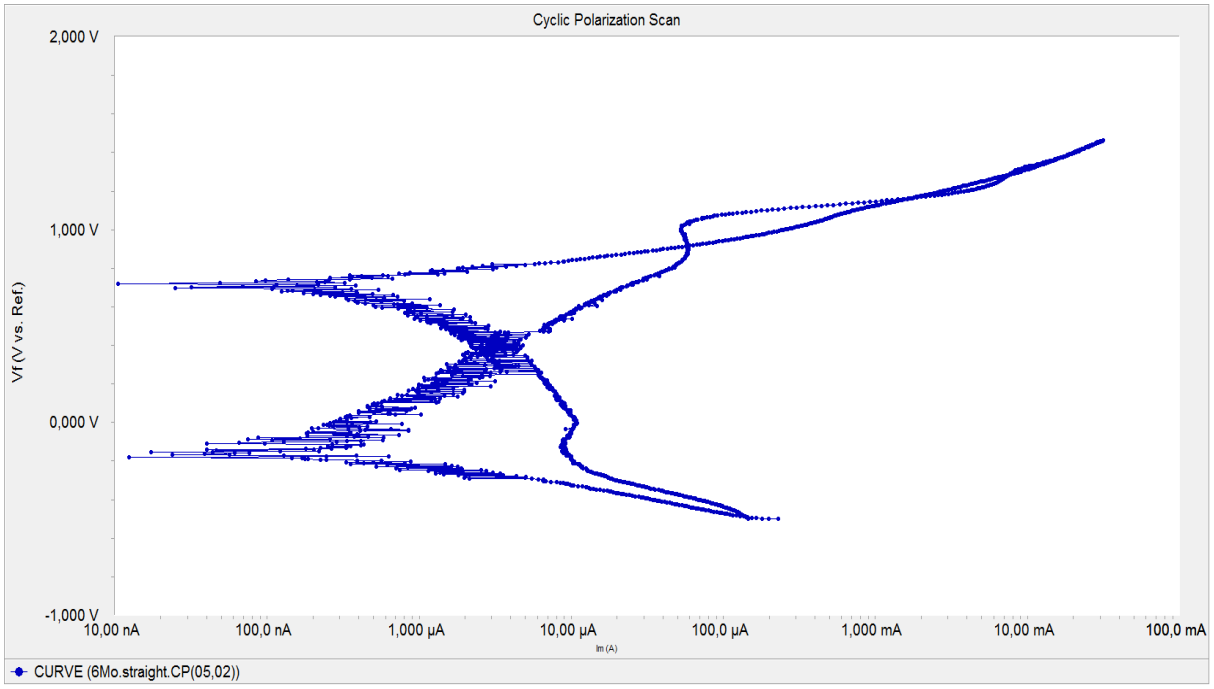

Figure 41: Cyclic Polarization Scan for 6Mo Straight Part

Figure 42 shows the cyclic polarization of 6Mo Bigger Bend. The graph shows that the pitting potential is at about 1V, with corresponding current density of 10^{-5} A/cm$^{2.}$ The hysteresis is formed, but unlike 316SS, the "negative" hysteresis was observed.

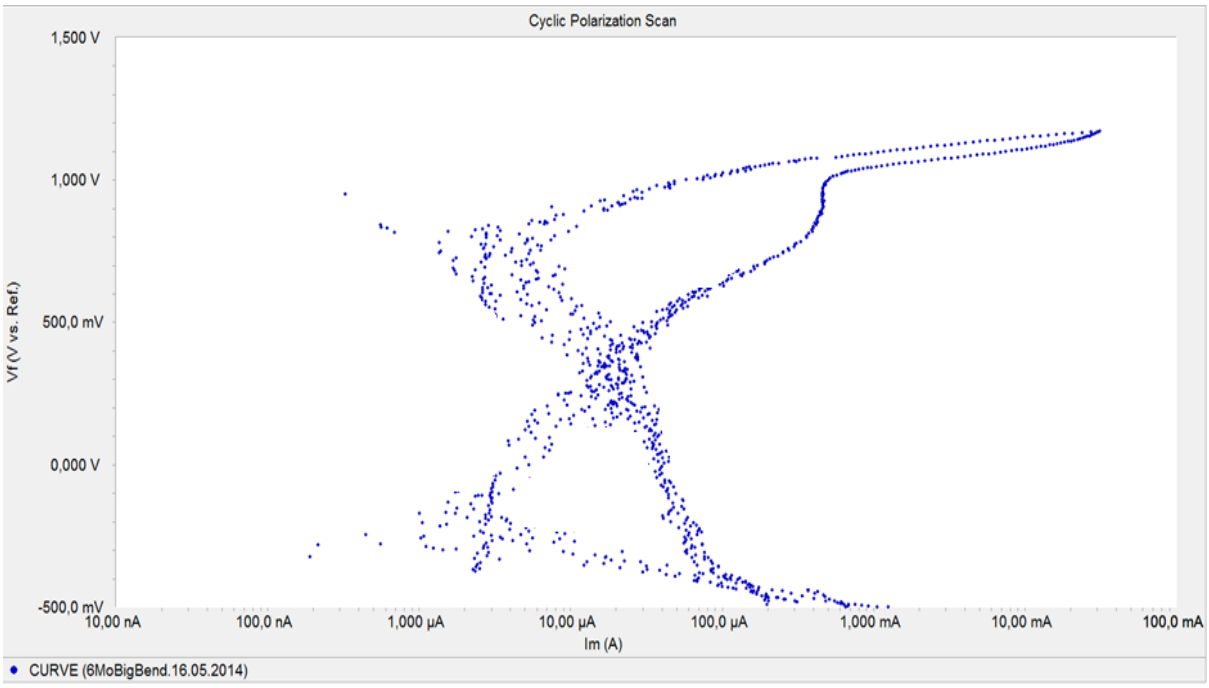

Figure 42: Cyclic Polarization Scan for 6Mo Big Bend

Figure 43 presents the cyclic polarization scan for 6Mo small bend. This plot looks smooth among other plots. The pitting potential was found to be at 1 V. The hysteresis was formed but the area was not high. The material is resistant to pitting and crevice corrosion. "Negative" hysteresis was observed.

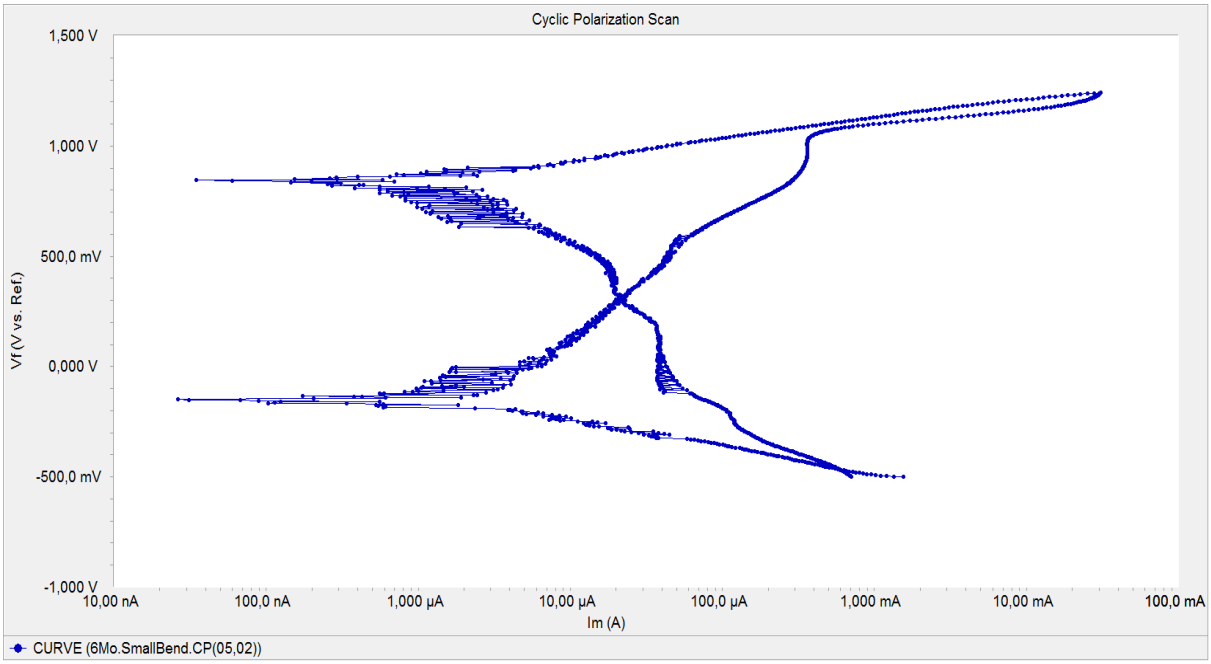

Figure 43: Cyclic Polarization Scan for 6Mo Small Bend

Table 23 shows the pitting potential and corresponding current density for the specimen tested. The pitting potential is almost similar for the bend and straight part of the same material. The 316SS straight part was found to have 0.25 V potential at 10^{-5} A/cm^2. The bended parts had similar potential but quite bigger than straight part, with 0.52 V at 10^{-5} A/cm^2 for bigger bend and 0.5 V at 10^{-5} A/cm^2 for smaller bend. The pitting potential for all 6Mo specimens was found to be about 1V. There was not significant variation between straight and bend part of 6Mo stainless steel.

Table 23: Pitting corrosion potential for the 316SS and 6MoSS specimens

SN	Material	Pitting Corrosion Potential (V)	Corresponding Current density (A/cm^2)
1	316SS Straight	0.25	10^{-5}
2	316SS Bigger Bend	0.52	10^{-5}
3	316SS Smaller Bend	0.5	10^{-5}
4	6Mo Straight	1.05	$10^{-5.1}$
5	6Mo Bend Big Bend	1.04	10^{-5}
6	6Mo Small Bend	1.04	10^{-5}

4.3 Hardness

The hardness measurements of the specimens provided are shown in Table 24. After the performance of ASTM G48 Test, the hardness was measured again. There was some variance in the hardness value obtained before and after G48 test. The bended parts of the material are found to be harder than the straight part. The hardness values of the specimens were found in the range similar to the value mentioned in the specification of material provided by company.

Table 24: Hardness Measurement for different specimens

SN	Material	Hardness (HV10)
1	316SS Straight Part	265-275
2	316SS Bend Tubes	280-295
3	6Mo Straight Part	208-223
4	6Mo Bend Tubes	240-252

Table 25 presents the hardness values of specimen after G48 Test. The hardness of 316SS was found to be more than 6Mo Stainless steel. There was slightly decrement in the surface hardness value after the exposure at acidic solution; however there was not significant decrement in hardness property of the material.

Table 25: Hardness Measurement for different specimens after G48 Test

SN	Material	Hardness (HV10)
1	316SS Straight Part	260
2	316SS Bend Tubes	280
3	6Mo Straight Part	225
4	6Mo Bend Tubes	250-280

5. DISCUSSION

All the results obtained for the project are presented in above section. ASTM G48 Test, ASTM G61 Test and the hardness measurement were the principle activities to carry out this study. The interpretations of the results are discussed below.

5.1 ASTM G48 Test

There was not much evidence in the literature on the topic of comparison of straight part and cold deformed bend part of 316 Stainless Steel and 6Mo Stainless Steel in terms of pitting corrosion resistance. It was anticipated that the bended part of the material could be more susceptible to the pitting corrosion. Results showed that there was not seen of pitting corrosion on the material until some specific high temperature, for instance pitting corrosion and crevice corrosion was evident at 30°C for 316SS. At 22°C, the pitting was observed under higher magnification i.e. 500X, but it was not observable with naked eye or at lower magnification. With the increase in temperature for test from 7°C to 30°C for 316SS, the weight loss per unit area was increasing which supports the fact that the temperature rise plays the pivotal role in the increment of corrosion of the material in the corrosive environment. Thus, the temperature is one of the important factors leading to the initiation of corrosion on the materials. This was supported with the test for 6Mo as well. The temperature rise in testing was yielding more weight loss per unit area for 6Mo specimens.

The straight and bend parts of 316SS were found to have similar impact of G48 Test. There was not any severe impact seen on the bend part compared to the straight part. The results of first approach test for 316SS showed that bended parts were losing less weight than the straight part. Similar was with the case for 6Mo specimens. In the case of second approach when the specimens were directly exposed to the designated high temperature i.e. 22°C for 316SS and 50°C for 6Mo, weight loss per unit area for straight and bend part was not uniform but rather random pattern. Conclusion was not able to be drawn upon the relationship between weight loss and deformation of pipes. 6Mo specimens (both straight and bended parts) accomplish the criteria for their usage according to Norsok Standard M-630. The pitting corrosion was not seen at 20X magnification and the weight loss per unit area was less than 4 g/m^2. The 316SS shows the similar results at lower temperature.

The weight loss pattern on the straight and bend parts were not supporting the idea of having more corrosion on bended part due to cold deformation. Furthermore, SEM images

were taken to inspect the pitting corrosion. The materials were cut wide open to observe the inner surface of the tubes. As it can be seen from Figure 32, 316 SS tubes show high pitting corrosion attack. Lot of pits were observed inside of the tube. Those pits could not be observed if tubes were not opened. It was noticed that pits and their number were higher on straight part than on bend part. Also Figure 36 shows tubes from 6Mo stainless steel show no sign of pitting corrosion inside the tubes.

Specimens of 6Mo that were tested on 60º C showed high corrosion attack. Some pits formed on the surface were not visible, but after just pressing with a finger bigger cavities were seen. It shows that material weakened after exposure at 60°C. However the corrosion effect was not distinguishable between straight and bend part. It was concluded that there is not any significant difference in the pitting corrosion resistant property due to the cold deformation of tested material 316SS and 6Mo of outer and inner diameter 0.935 cm and 0.5 cm with R=2.5ND and R=5ND bended tubes.

The microstructures of the tubes were not studied as the subject matter doesn't lie on the periphery of our relevant subjects studied. However, the study of the change in the microstructure and their corresponding effect on the material can be studied to generate a conclusive corrosion effect due to cold deformation.

5.2 ASTM G61 Test

Cyclic polarization measurement were performed in order to support result test obtained from ASTM G48, and to determine the tendency of different material to undergo pitting corrosion. Measuring and comparing the pitting potential, repassivation potential and hysteresis loop for straight and bend part of the tubes was of great importance for understanding the influence of cold bending of pipes on their corrosion behaviour. Corrosion potential (or open circuit potential) was also measured. This measure is important because can give ranking of the material in terms of their corrosion resistance. Noble materials have higher potential which means that those materials are more corrosion resistant, and more negative reading for corrosion potential indicates material more prone to corrosion. Although, this method is not very reliable, it is used as a starting point of cyclic polarisation measurement which is a method to determine the real corrosion behaviour of the material. Open circuit potential scans were ran for one hour from immersion time for each specimen. Graphs from this measurement can be found in Appendix.

From graphs it can be seen results contrary of what was expected. Corrosion potentials are shown in Table 22, and can be seen that big bend of 6Mo did not exhibit more noble stable potential when compared with big bend of 316 SS. Big bend of 6Mo was in this case most active in this environment with corrosion potential of –110 mV. Small bend of 6Mo shows slightly noble potential when compared with the same part of 316SS material. For the straight part 316 SS show more noble corrosion potential, but the difference is not that significant. The reason for this behaviour could be time given for stabilizing the corrosion potential during open circuit potential measurement. Some material need more time to come to the steady state. In this case time of one hour was given for every specimen tested, which might not be enough for material like 6Mo. Also very unstable curve for 316 SS straight part was observed. This may be result of the complexity of processes involving the immersion of stainless steel into electrolyte solution. It can be related to oxygen in the electrolyte, but it can be also related to the preparation of the specimen prior testing[43]

Results from cyclic polarisation measurement are presented in the Figure 38 to 43. Two important points were determined: pitting potential (E_{pitt}) and repasivation or protective potential (E_{re}). E_{pitt} is the potential above which pits initiate and propagate. This potential is defined in forward scan. When performing reverse scan repasivation potential can be found. E_{re} is defined at the point where reverse scan intersect the forward scan. When reaching the repasivation potential, pitting corrosion stops and decrease of the current density can be seen. The more noble potential for E_{pitt} will indicate material not prone to pitting corrosion, and also if more positive values are obtained for E_{re} potentials it will show material more resistant to localized corrosion. For high resistant to pitting corrosion materials, differences between E_{pitt} and E_{re} is very small [44].

In general, result from cyclic polarization measurement in this case showed expected results with respect to material tested. Pitting corrosion potential found for 316 SS were more negative than pitting corrosion potential found for 6Mo for the same current density. Within 316SS tested specimens, it can be seen that the straight part has a lower pitting potential than bended parts (small bend and big bend showed nearly same pitting potential). These findings support results obtained from G 48 test, where straight parts lost more weight compared with bend parts of pipes. For 6Mo stainless steel all tested specimen showed same pitting potential. Analysing repasivation potential in this project can be done only for 6Mo straight part as shown in Figure 41. In that graph, it can be clearly seen repasivation potential of 0.9 V. Difference between pitting corrosion and

repasivation corrosion values is very small, that shows that this specimen is very resistant to pitting corrosion. For 316 SS specimen tested there is no use of finding difference between pitting and repasivation potential since the clear start of pitting potential (breakout potential) was not seen. For other graphs, analyzes of hysteresis loop should be done for better understanding of corrosion behaviour of the tested specimens.

When performing forward and reverse scan during cyclic polarisation scan, hysteresis loop are formed. With their analysis information about pitting resistance of the material can be found. Hysteresis loop can be "positive" and "negative". Hysteresis loop is "positive" if the current densities in the passive region during the reverse scan are higher than for the forward scan, and hysteresis loop is "negative" if current densities in the passive region during the reverse scan are less than for the forward scan. No hysteresis or "negative" hysteresis will indicate material with high resistance of pitting corrosion [10].

Investigation of cyclic polarisation curve for 316SS straight part, big bend and small bend showed the existence of big hysteresis loop. It is a clear indicator that these specimens are prone to pitting corrosion. It can be seen that repasivation potential found in reverse scan is not far from corrosion potential of the specimen. That is the cause of these big hysteresis loops.

Figure 41 to 43 present cyclic polarization curves for straight part, big bend and small bend made of 6Mo material. Polarisation curve for straight part of 6Mo show very small hysteresis loop. As commented before, it can be seen that pitting potential and repasivation potential are very close. E_{pitt} is 1V and E_{rp} is 0.9 V. That result in formation of very small hysteresis loop and very resistant to localized corrosion material. Curves in Figure 42 and Figure 43 are showing typical "negative" hysteresis curves typical for material highly resistant to pitting corrosion. As expected cyclic polarisation test confirmed information gathered from ASTM G48. Here, as well, not any significant difference can be seen in pitting potential between bend and straight part of same material. Differences are only observed between different materials.

The hardness of the bended and straight parts was measured. It was observed that the hardness of the bended part R=5ND was higher than the straight part. Due to the limitation of the number of specimens, hardness of R=2.5ND was not able to be measured. However, the results obtained from the hardness measurement were supporting the fact that the hardness increases after the cold deformation of tubes. The hardness of some specimen

was found to increase after G48 Test. This strange behaviour could be explained as the different spot were taken for the hardness measurement that would yield different hardness values. There was not any relation found between the hardness alteration of tested material before and after G48 test.

6. CONCLUSION AND RECOMMENDATIONS

Based upon the tests performed for these three materials, the following conclusions were drawn:

1. For the materials that were tested namely 316 SS (UNS S31603) and 6Mo (UNS S31254) outer diameter 9.35 mm and inner diameter 5 mm, there was no significant difference between the straight and cold deformation of R=2.5 ND and R=5 ND in the result obtained for pitting corrosion test (ASTM G48).

2. The pitting corrosion potential of the straight and cold deformed parts were also found to be in the same range, that indicates that the cold deformation of R=2.5 ND and R=5 ND on the tubes having outer diameter 9.35 mm and inner diameter 5 mm does not have any significant impact on the pitting corrosion potential. For 316SS, the potential were compared for three materials (Straight, Smaller and Bigger bend) at the current density of 10^{-5}mA/cm^2, the bigger and smaller bend were found to have higher critical pitting potential then straight part. This shows the cold deformation of R=2.5 ND and R=5 ND for a tube size (OD=9.35 mm and ID=5 mm) of 316SS material could help in rising the value of critical pitting potential as observed in the result obtained.

3. The hysteresis area of 316SS is larger that indicates that it is highly susceptible to pitting and crevice corrosion. 6Mo is highly resistant to pitting and crevice corrosion as the area hysteresis did not have significant area as compared to 316SS, or there was existence of "negative" hysteresis.

5. The hardness of material was found to be on the range as provided on the specification of materials. The bends were observed to be harder on bended parts than straight parts.

Some recommendation and suggestion regarding this topic has been presented below:

1. The comparative study between the pitting corrosion was made in this study. However, it is suggested to carry out study on the micro structure and its effect on property changes that incur due to cold deformation.

2. It is recommended to perform these tests with different and many number of specimen, so that the results obtained could possibly help in undertaking the serious decision regarding the usage of cold deformed tubes in oil and gas industry.

3. The study regarding the hardness variation according to the material possibly could bring the light on variation of hardness property due to cold bend on different material.

4. The R&D in this sector is crucial in order to consider the cold deformation of tubes to be used for harsh environmental condition. Besides pitting corrosion potential and critical pitting temperature, it is suggested to make comparison of straight and bend tubes on several other different mechanical properties of materials.

REFERENCES

1. Statoil, *Statoil Technical Standard for Design Cold Bending Specification (English edition)*. 1994.
2. Marcus, P., *Preface*, in *Corrosion Mechanisms in Theory and Practice*, P. Marcus, Editor. 2002, Marcel Dekker, Inc.
3. Trethewey, K.R. and J. Chaamberlain, *Corrosion for Science and Engineering*. 1995: Addison Wesley Longman. 30.
4. Devis, J.R., *Corrosion: Understanding the Basics*. 2000: ASM International.
5. Revie, R.W. and H.H. Uhlig, *Corrosion and Corrosion Control*. Fourth ed. 2008: John Wiley and Sons, Inc.
6. Cicek, V. and B. Al-Numan, *Corrosion Chemistry*. 2012, Hoboken, NJ, USA: Wiley.
7. *Corrosion engineering handbook*, P.A. Schweitzer, Editor. 1996, Marcel Dekker: New York. p. X, 736 s. : ill.
8. K.Trethewey, J.C., *Corrosion for Science and Engineering*. 1995: Addison Wesley Longman
9. Schweitzer, P.A., *Encyclopedia of Corrosion Technology*. 1998, New York: Marcel Dekker, INC.
10. Robert G. Kelly, J.R.S., David W. Shoesmith, Rudolph G. Buchheit *Electrochemical Techiques in Corrosion Science and Engineering* 2003: Marcel Dekker, Inc
11. Chamberlain, K.R.T.a.J., *Corrosion for Science and Engineering* 1995: Addison Wesley Longman.
12. Schweitzer, P.A., *Fundamentals of metalic corrosion: atmospheric and media corrosion of metals*.
13. Stanbury, E.E. and R.A. Buchanan, *Fundamentals of Electrochemical Corrosion*. 2000, Materials Park, OH, USA: ASM International.
14. Wessel, J.K., *Handbook of Advanced Materials : Enabling New Designs*. 2004, Hoboken, NJ, USA: Wiley.
15. Pohlman, S.L., *General Corrosion*, in *ASM Handbook Corrosion*.
16. Perez, N., *Electrochemistry and Corrosion Science*. 2004, Hingham, MA, USA: Kluwer Academic Publishers.
17. *Pitting Corrosion*. 10.30.2013]; Available from: http://www.nace.org/Pitting-Corrosion/.
18. Uhlig, H.H., *Corrosion Handbook*. John Wiley & Sons.
19. Dexter, S.C., *Localized Corrosion*, in *ASM Handbook Corrosion*. ASM International.
20. Kopeliovich, D.D. *Pitting corrosion*. [cited 2014 15.04]; Available from: http://www.substech.com/dokuwiki/doku.php?id=pitting_corrosion.
21. Kain, R.M., *Crevice Corossion*, in *ASM Handbook , Corrosion*. ASM International.
22. Kopeliovich, D.D. *Crevce Corrosion*. 11.05.2014]; Available from: http://www.substech.com/dokuwiki/doku.php?id=crevice_corrosion&DokuWiki=0a2034ee86178cb43b5723ea59784880.
23. Dereu, B., *Raw and Finished Materials : A Concise Guide to Properties and Applications*. 2011, New York, NY, USA: Momentum Press.
24. Verhoeven, J.D., *Steel Metallurgy for the Non-Metallurgist*. 2007, Materials Park, OH, USA: ASM International.
25. Schweitzer, P.A., *What every engeneer should know about corrosion*. Vol. 21. Marcel Dekker, INC.
26. Lai, J.K.L.S., Chan Hung Lo, Kin Ho, *Stainless Steels : An Introduction and Their Recent Developments*. 2012, SAIF Zone, Sharjah, UAE: Bentham Science Publishers.
27. Davis, J.R., *Corrosion of Weldments*. 2006, Materials Park, OH, USA: ASM International.
28. McGuire, M.F., *Stainless Steels for Design Engineers*. 2008, Materials Park, OH, USA: ASM International.
29. Farrar, J.C.M., *The alloy tree: A guide to low-alloy steel, stainless steel and nickel-base alloys*. 2004: Woodenhead Publishing Limited.

30. *Heat Treater's Guide practices and procedure for Iron and Steel* 2nd Edition ed.: ASM International.
31. Penn Stainless Products, I. *316/316L Stainless Steel*. 2014 [cited 2014 15 March]; Available from: http://www.pennstainless.com/stainless-grades/300-series-stainless-steel/316l-stainless-steel/
32. Ltd, L.A. *254 SMO*. 2011 [cited 2014 20 April]; Available from: http://www.langleyalloys.com/ALLOY254.php.
33. *ASM Handbook Corrosion*. Vol. 13.
34. G48, A., *Standard Test Method for Pitting and Crevise Corrosion Resistance of Stainless Steels and Related Alloys by Use of Ferric Chloride Solution*. ASTM International.
35. Sprowls, D.O., *Evaluation of pitting corrosion*, in *ASM Handbook Corrosion*. AMS International.
36. *Handbook for analytical methods for materials*. Electrochemical Corrosion Testing 2009 [cited 2014 05.04]; Available from: http://mee-inc.com/esca.html.
37. Schweitzer, P.A., *Corrosion Mechanism, Causes and Preventive Methods*. 2010: Taylor & Francis Group.
38. Andrew C. Palmer, R.A.K., *Subsea Pipeline Engineering*. 2008: PennWell Corporation.
39. *Bending Stainless Steel Tubes-Design Benefits in Engineering and Architecture*. Material and Applications Series. **15**.
40. Reza Javaherdashti, C.I., Henry Tan, *Corrosion and Materials in the Oil and Gas Industries* 2013: Taylor & Francis Group.
41. Herrman, K., *Hardness Testing Principle and Aplicatins* ASM International.
42. Norway, S., *Norsok M630 , Material data sheets and element data sheets for piping*. 2010.
43. ALONSO -FALLEIROS, N.a.W., Stephan *Correlation between Corrosion Potential and Pitting Potential for AISI 304L Austenitic Stainless Steel in 3.5 % NaCl Aqueous Solution*. 2002.
44. Z. Szklarska- Smialowska, M.J.-C., *The Analysis of Electrochemical Methods for the Determination of Characteristic Potential of Pitting Corrosion*, in *Corrosion Science*. 1971.

APPENDICES

Appendix 1: Images from SEM

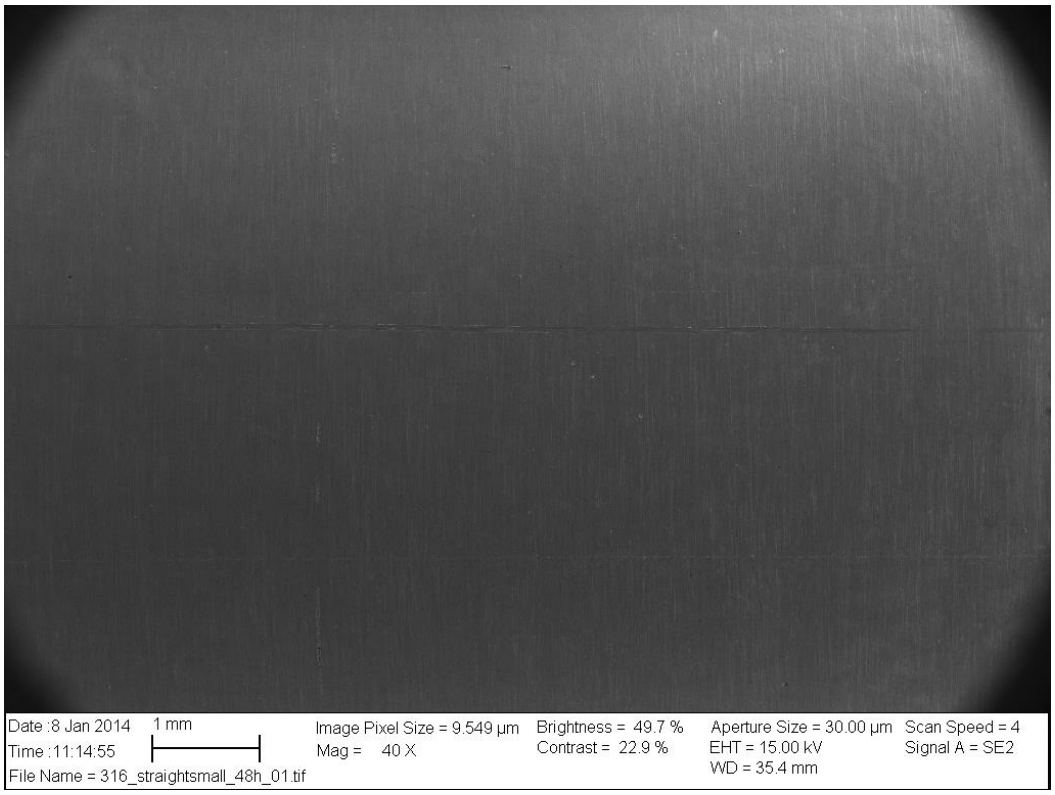

Image: 316SS straight small specimen after exposure at 15°C

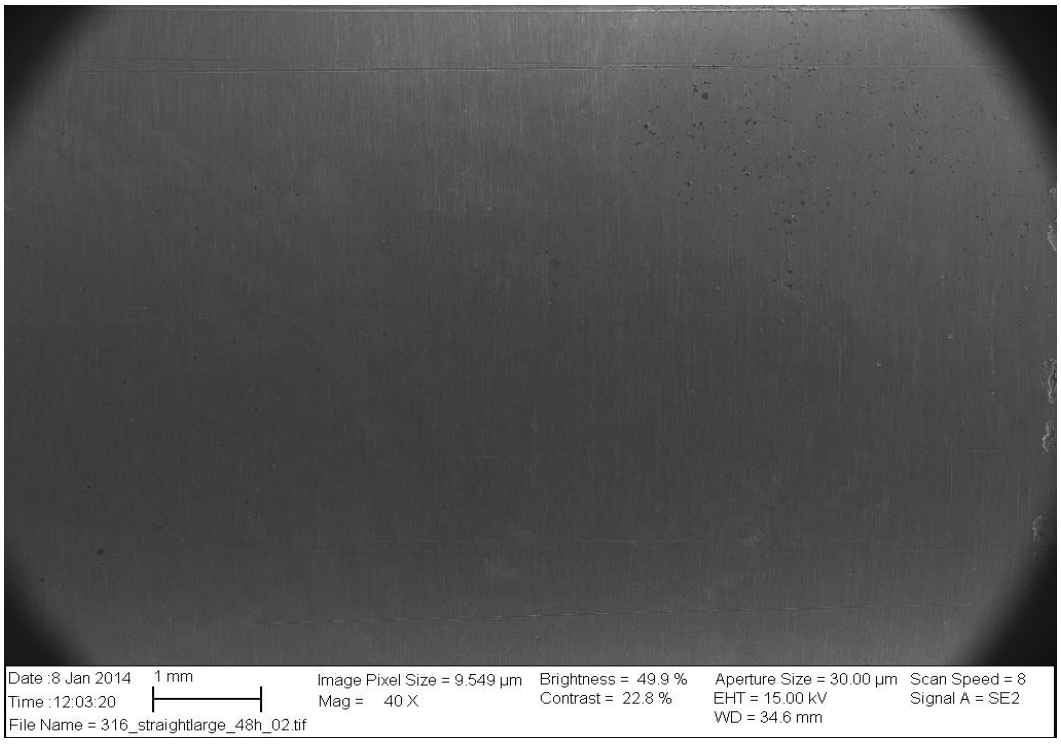

Image: 316SS straight large specimen after exposure at 15°C

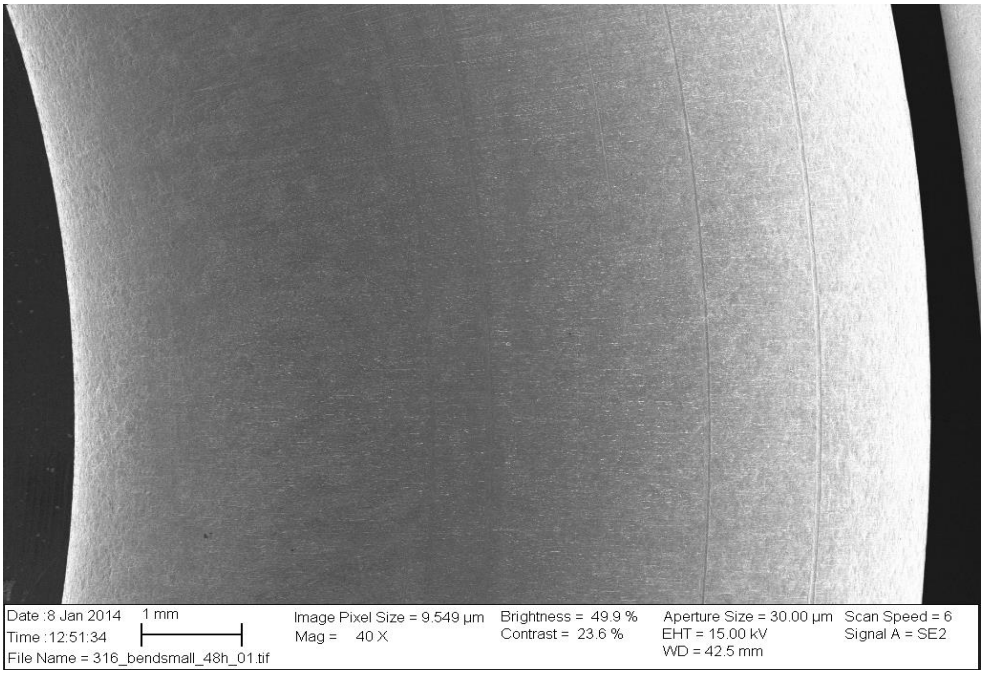

Image: 316SS bigger bend specimen after exposure at 15°C

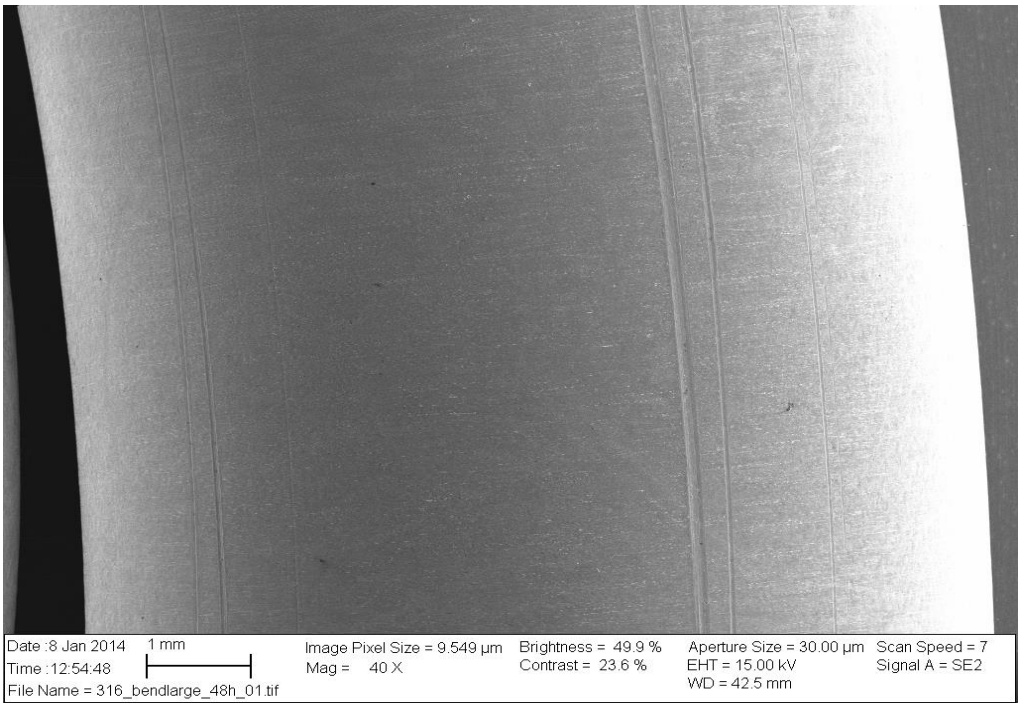

Image: 316SS smaller bend specimen after exposure at 15°C

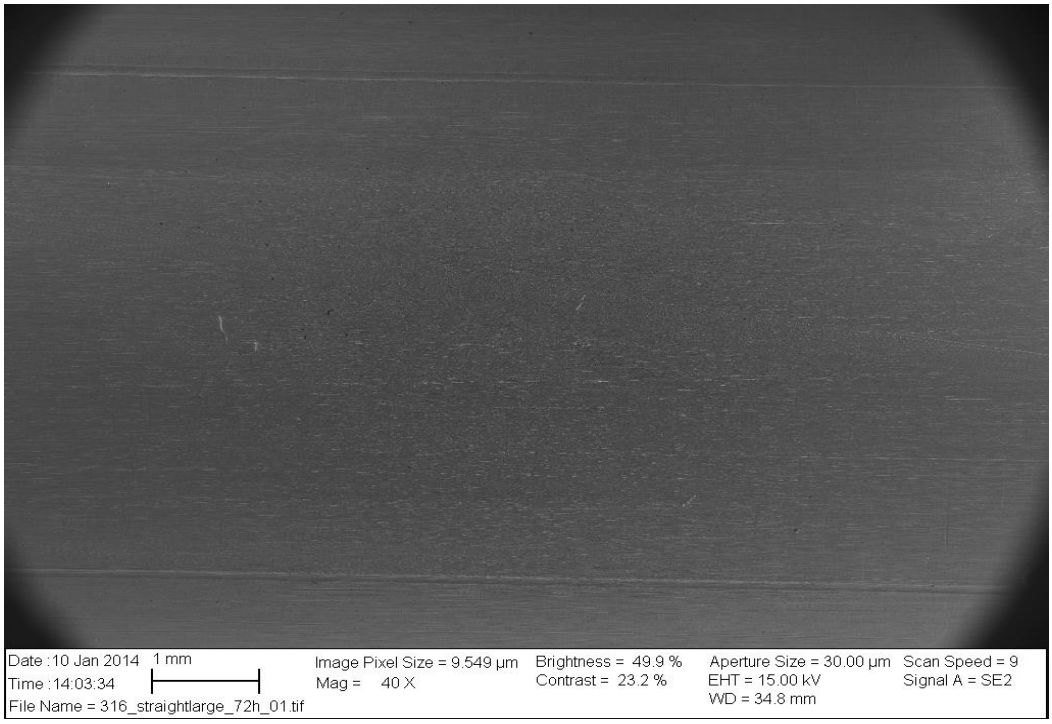

Image: 316SS straight large specimen after exposure at 22°C

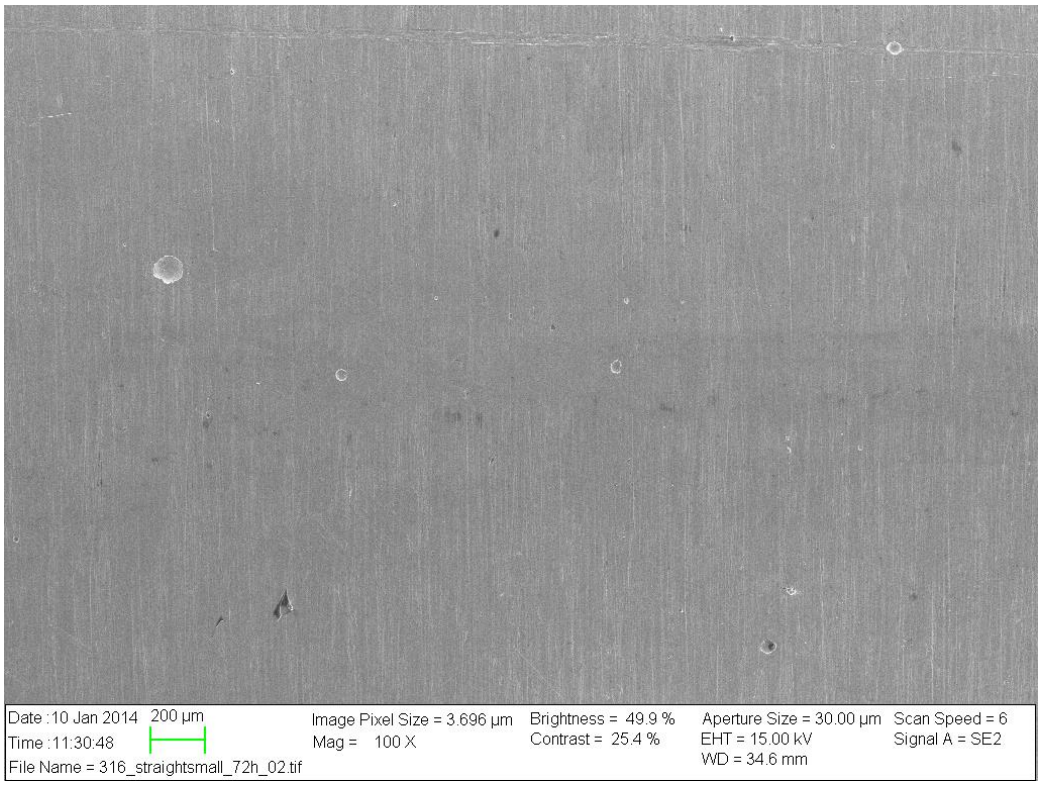

Image: 316SS straight small specimen after exposure at 22°C

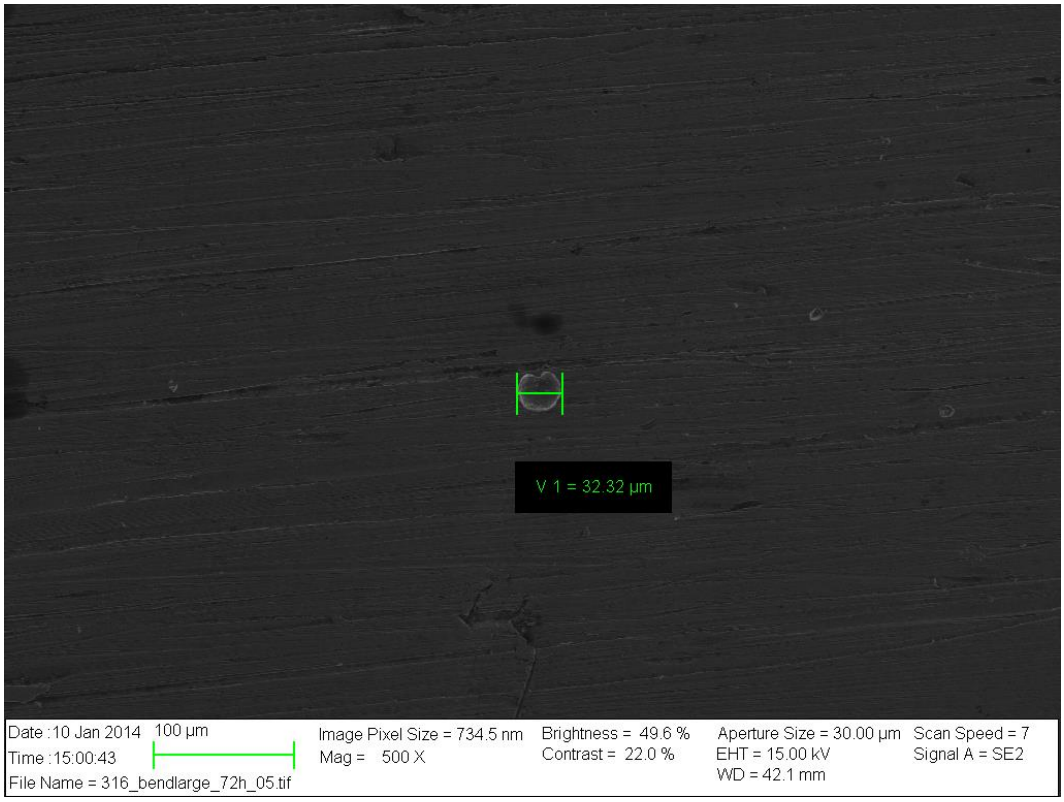

Image: Pits on 316SS bigger bend specimen after exposure at 22°C

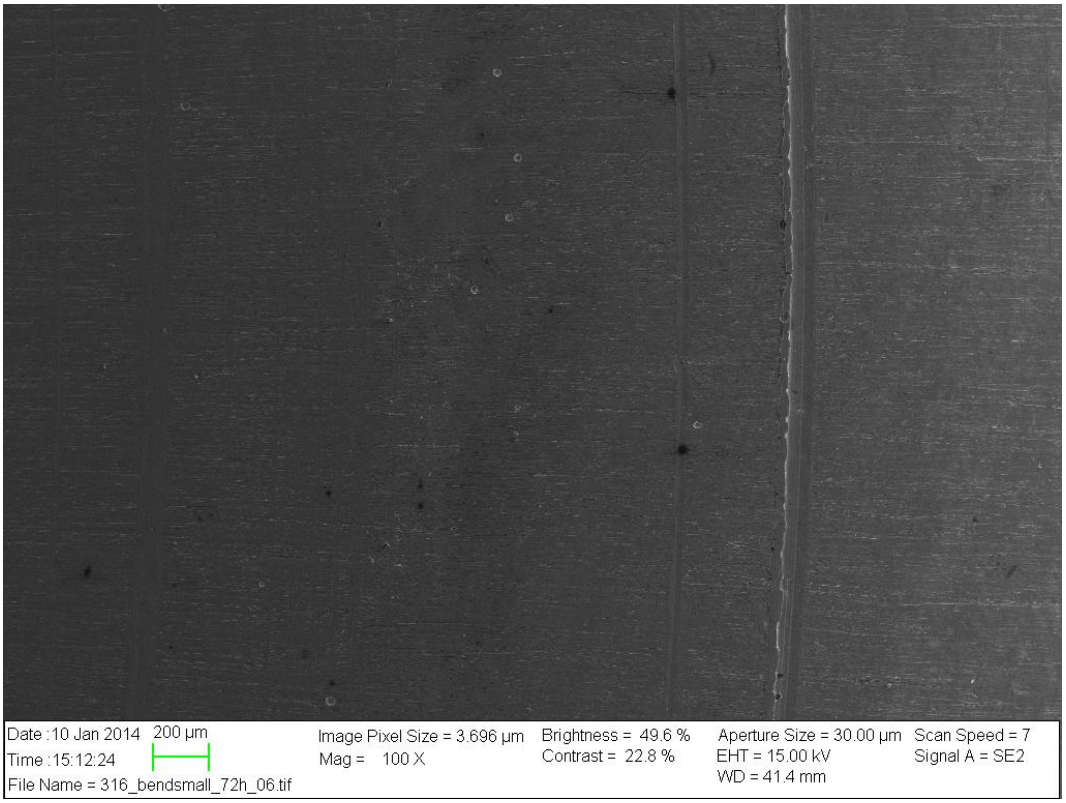

Image: 316SS small bend specimen after exposure at 22°C

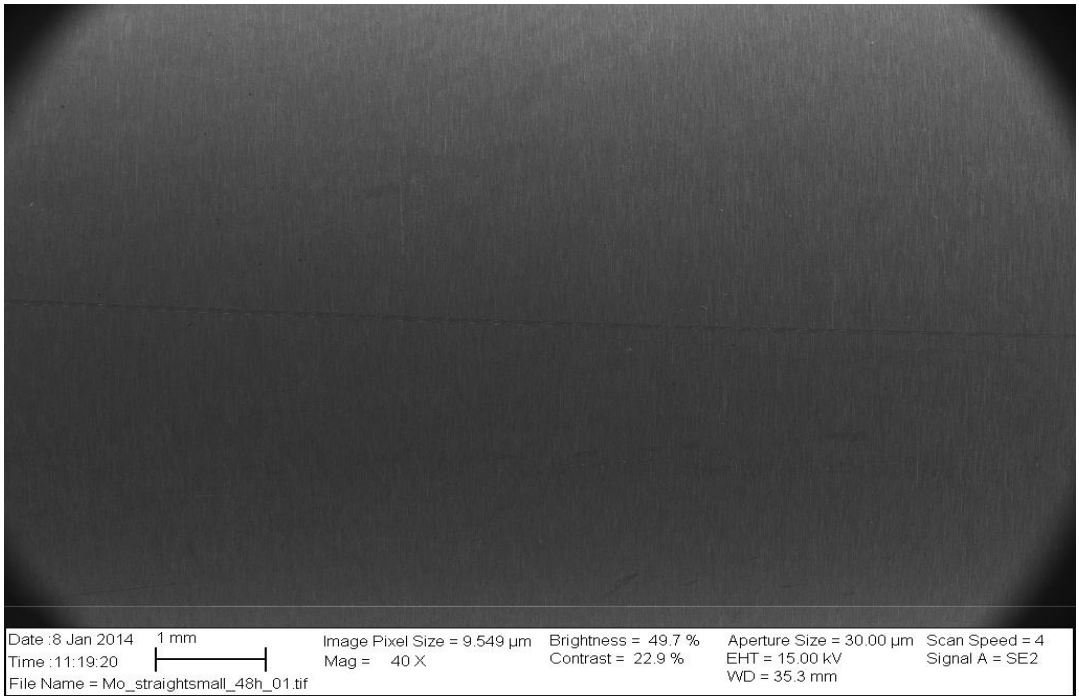

Image: 6Mo small straight specimen after exposure at 30°C

Image: 6Mo large straight specimen after exposure at 30°C

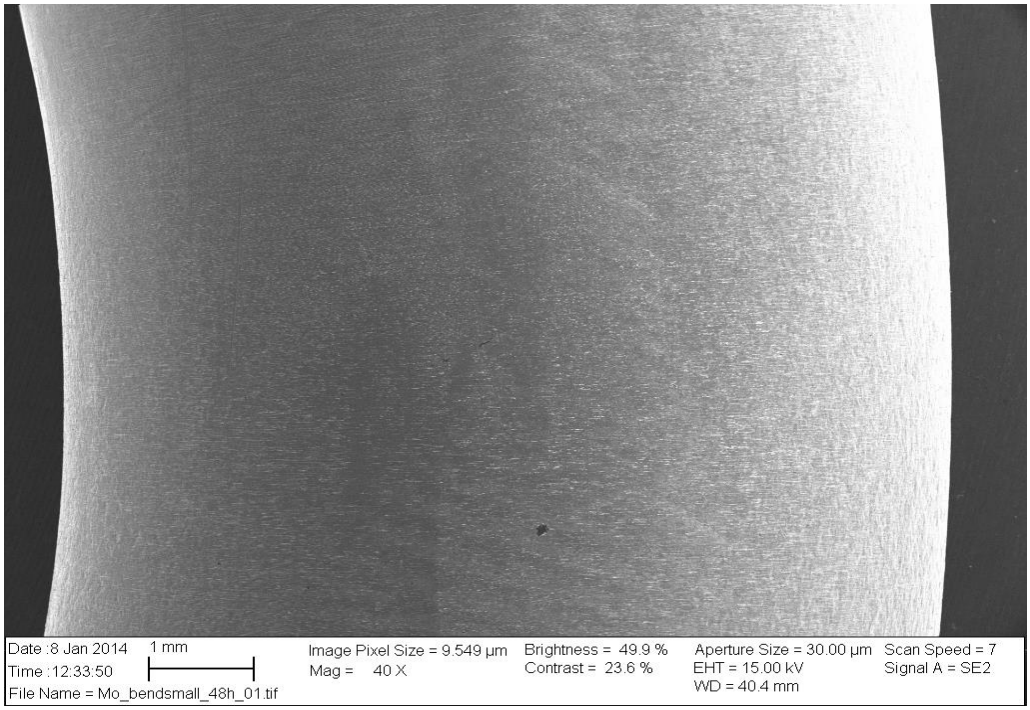

Image: 6Mo smaller bend specimen after exposure at 30°C

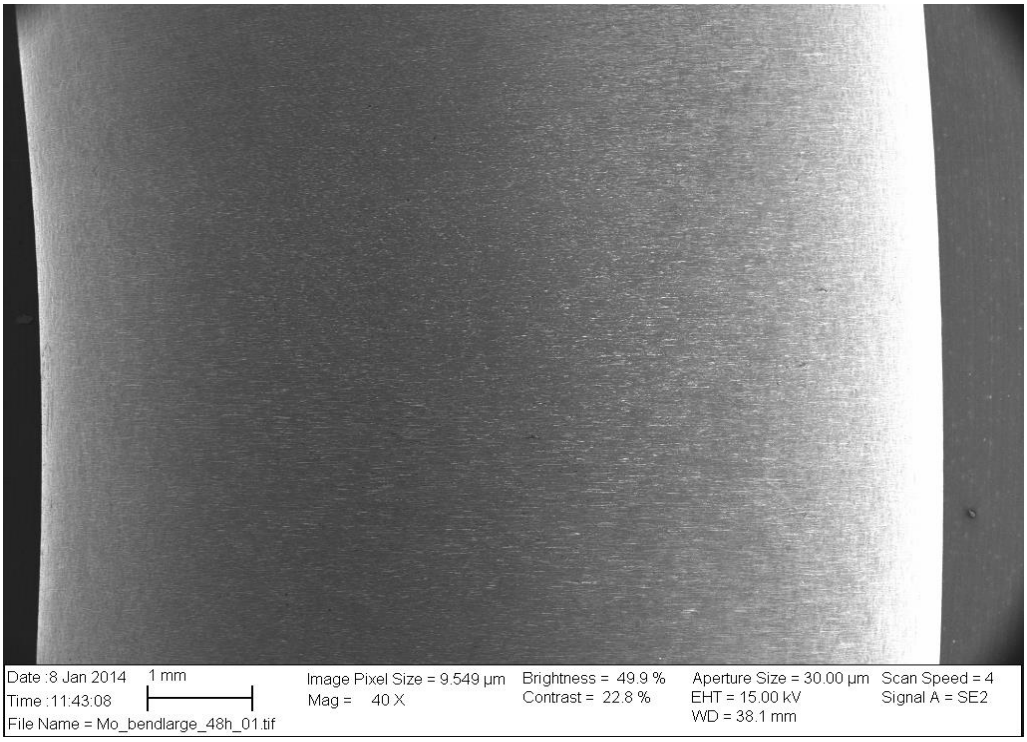

Image: 6Mo bigger bend specimen after exposure at 30°C

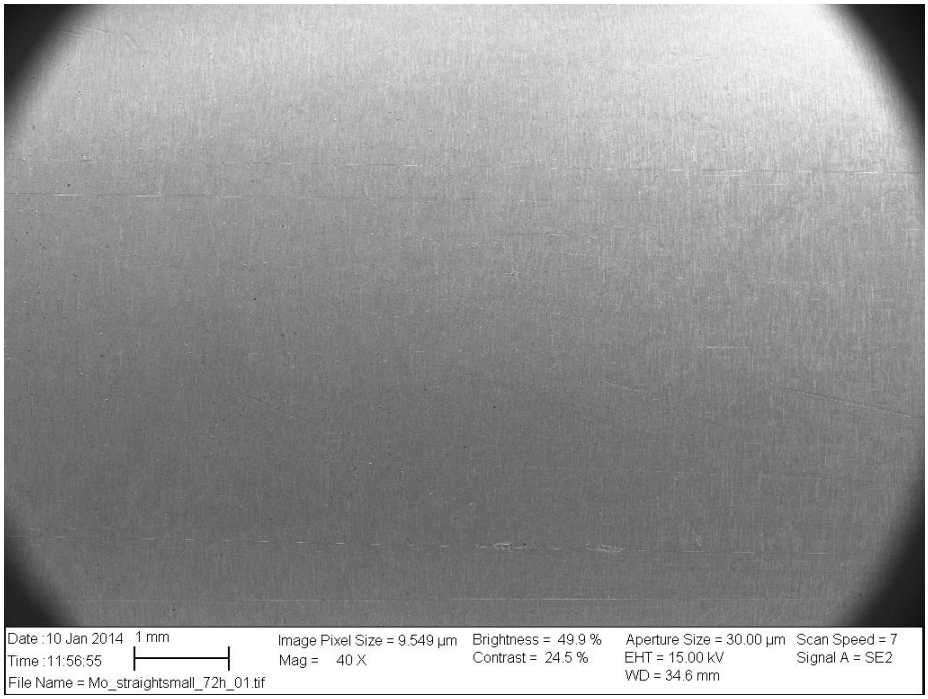

Image: 6Mo straight small specimen after exposure at 40°C

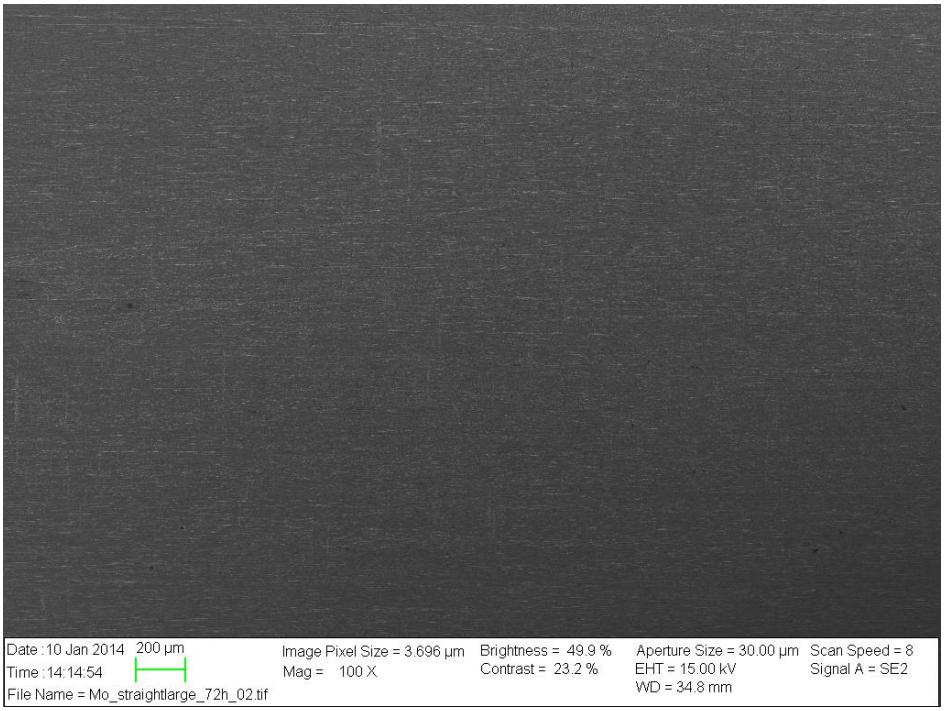

Image: 6Mo straight large specimen after exposure at 40°C

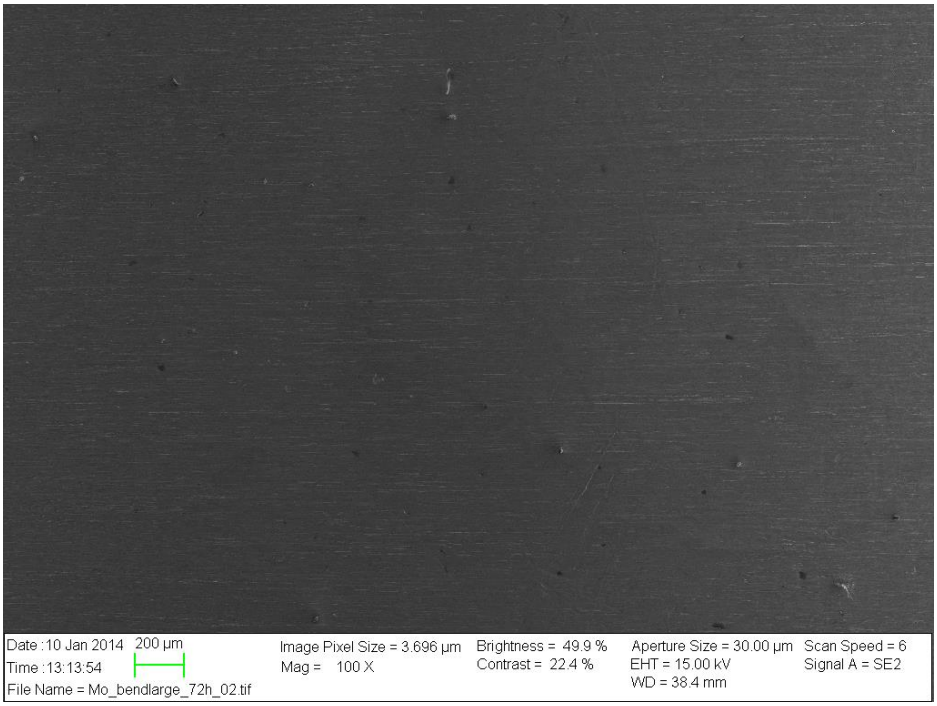

Image: 6Mo bigger bend specimen after exposure at 40°C

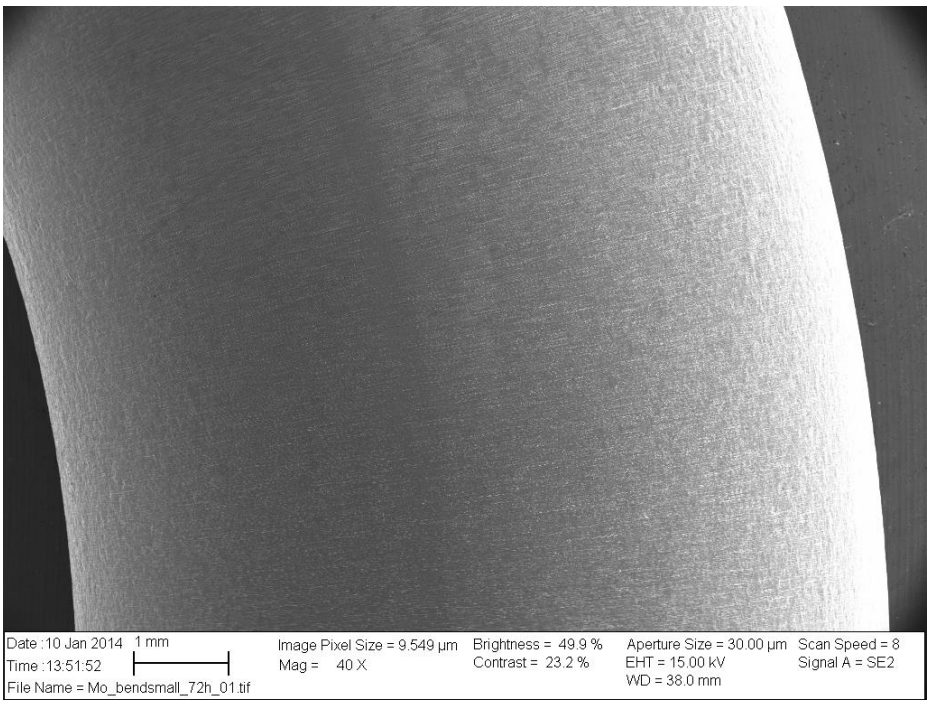

Image: 6Mo small bend specimen after exposure at 40°C

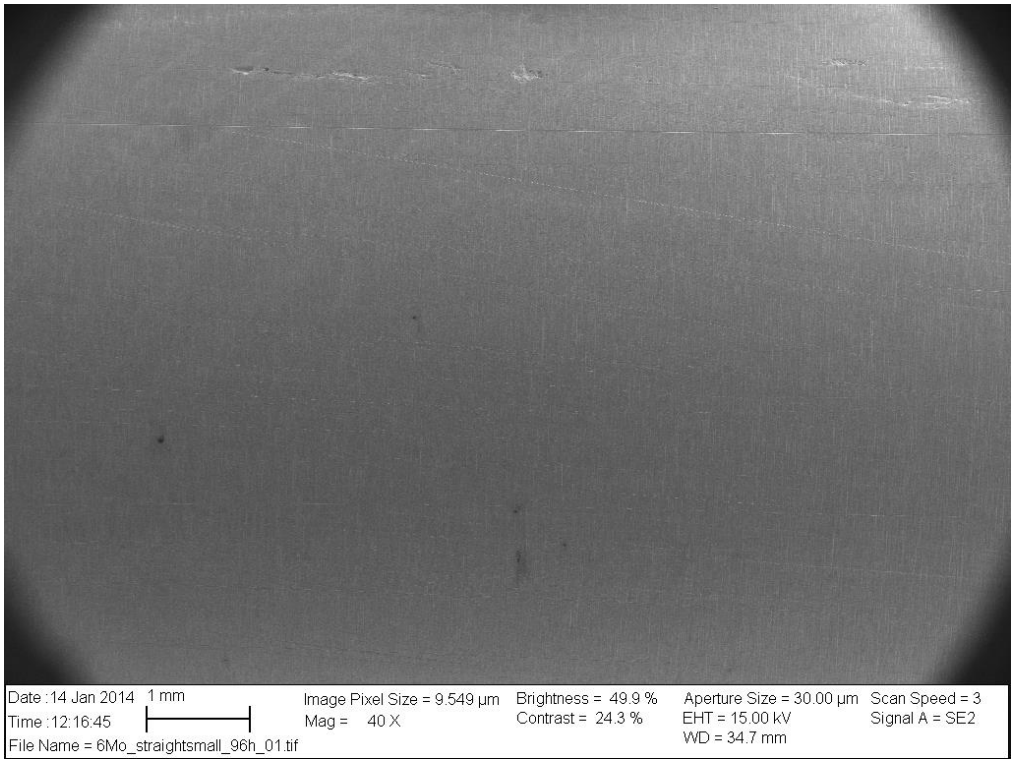

Image: 6Mo straight small specimen after exposure at 50°C

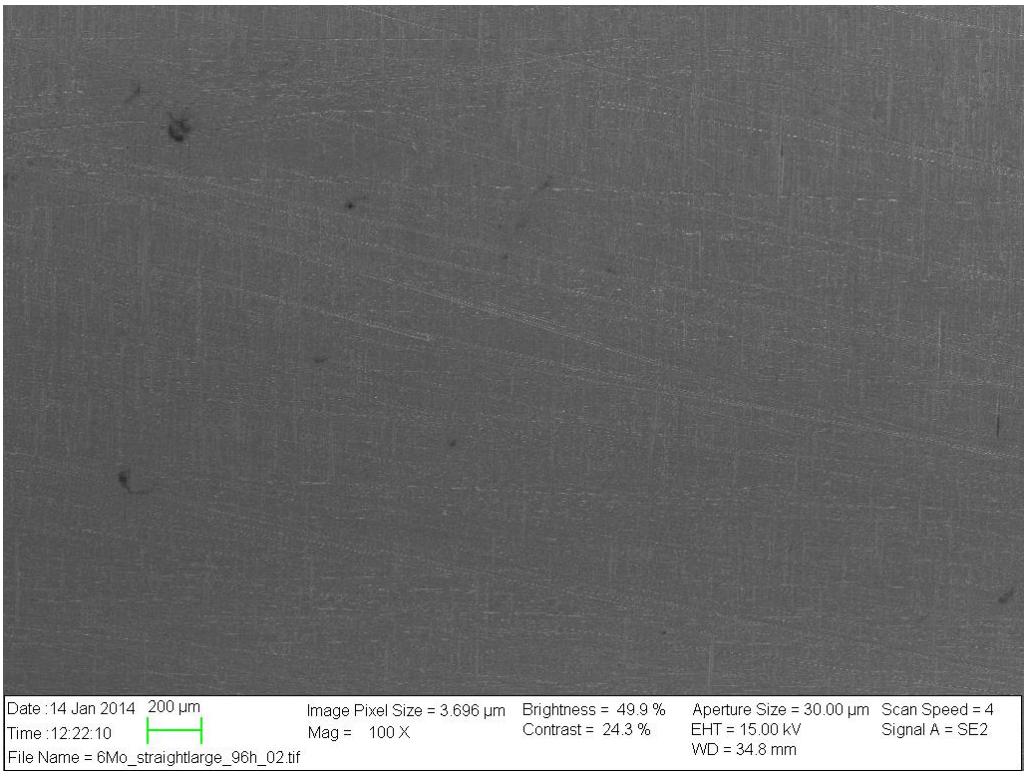

Image: 6Mo straight large specimen after exposure at 50°C

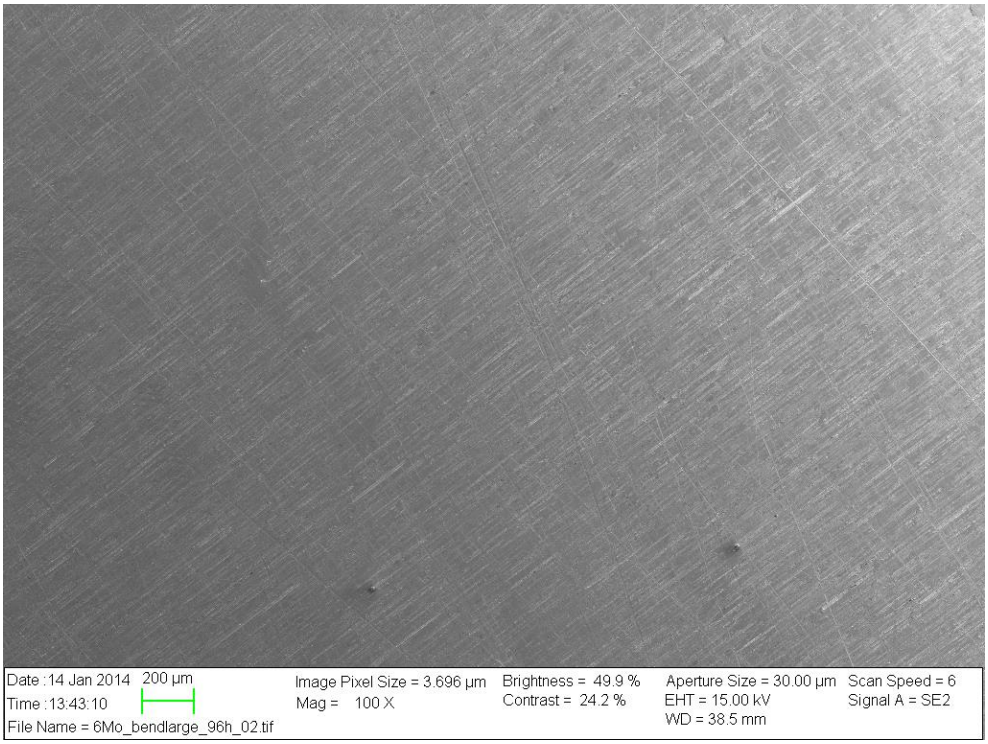

Image: 6Mo bigger bend specimen after exposure at 50°C

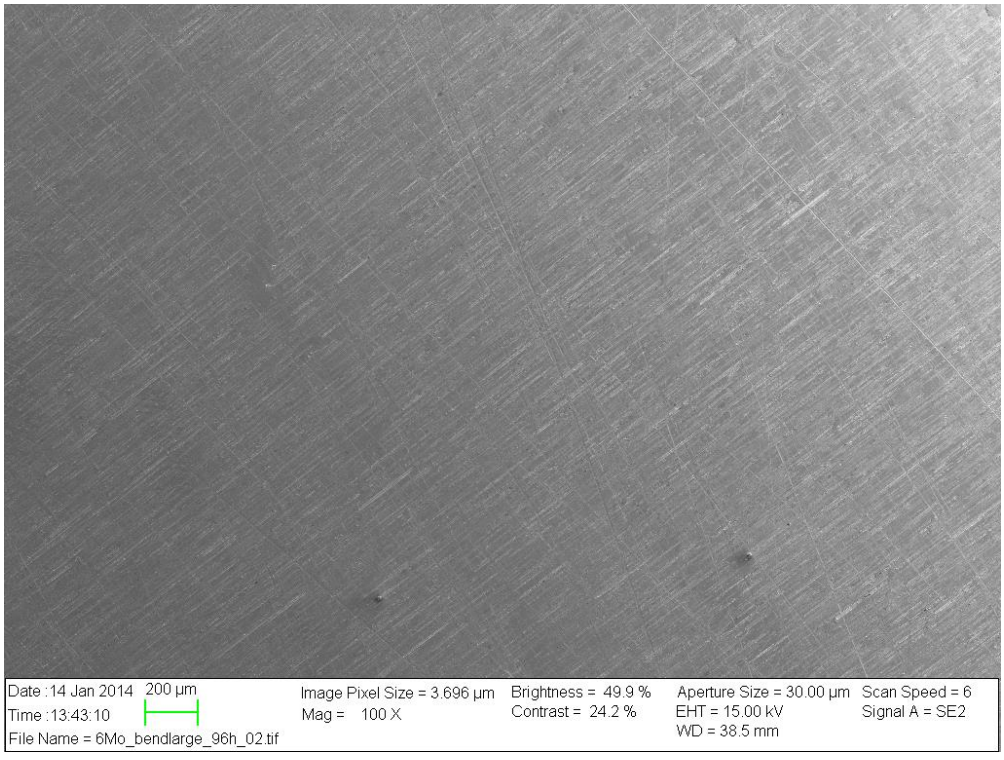

Image: 6Mo smaller bend specimen after exposure at 50°C

Appendix 2: Open Circuit Potential

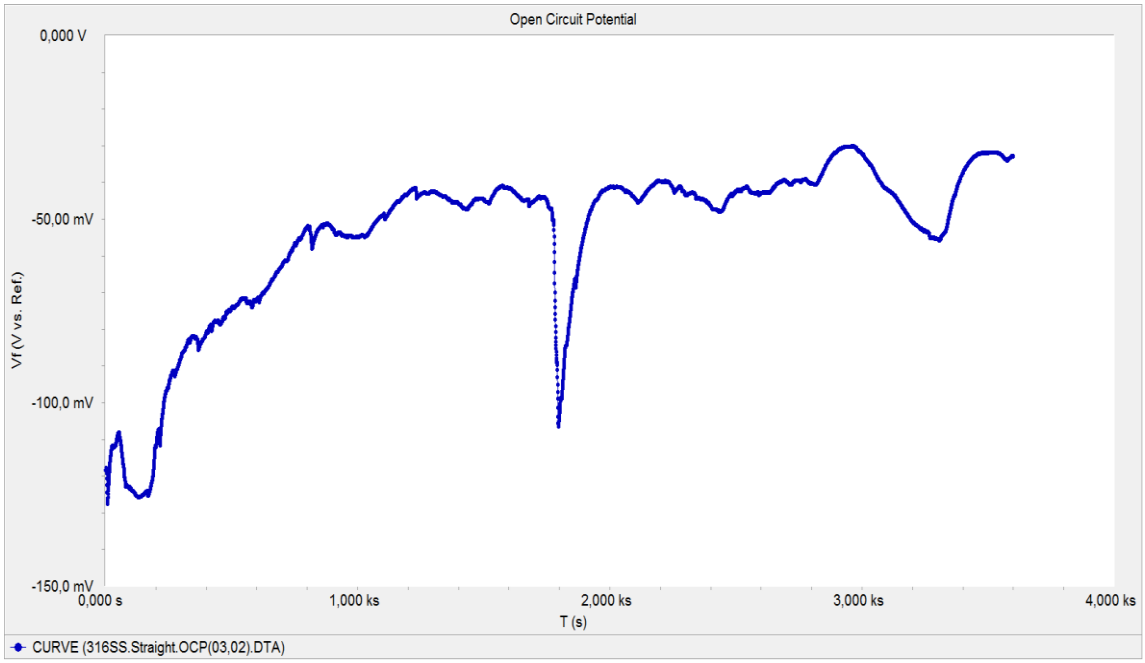

Graph: OCP for 316SS straight tube

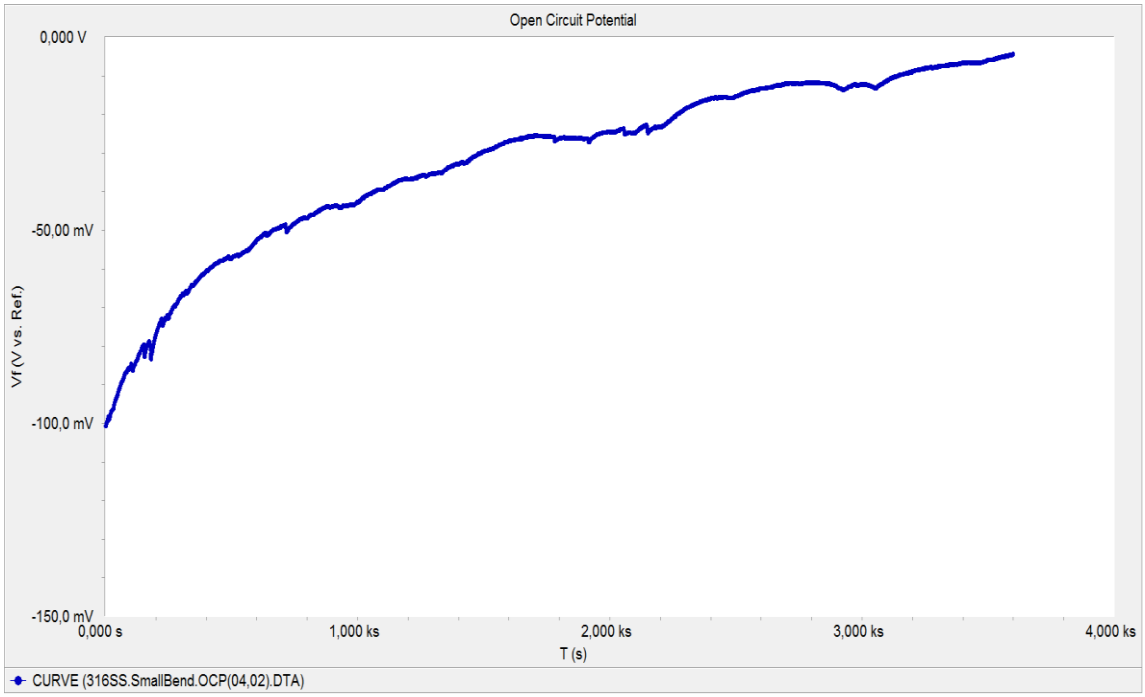

Graph: OCP for 316SS smaller bend tube

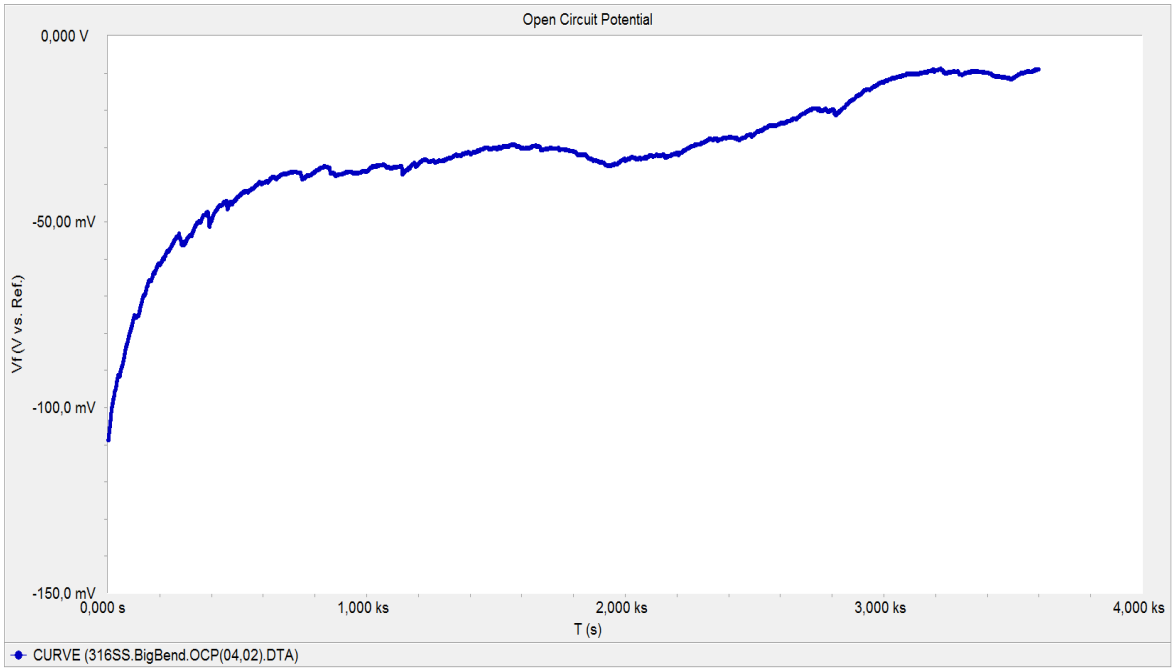

Graph: OCP for 316SS bigger bend tube

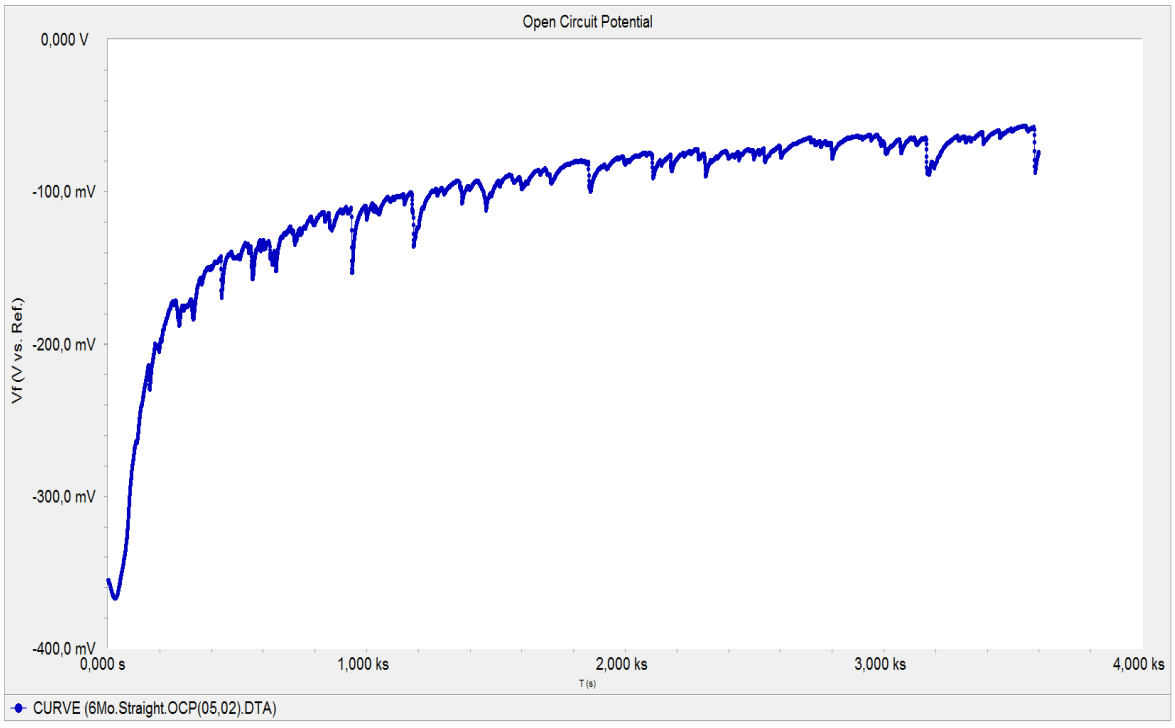

Graph: OCP for 6Mo straight tube

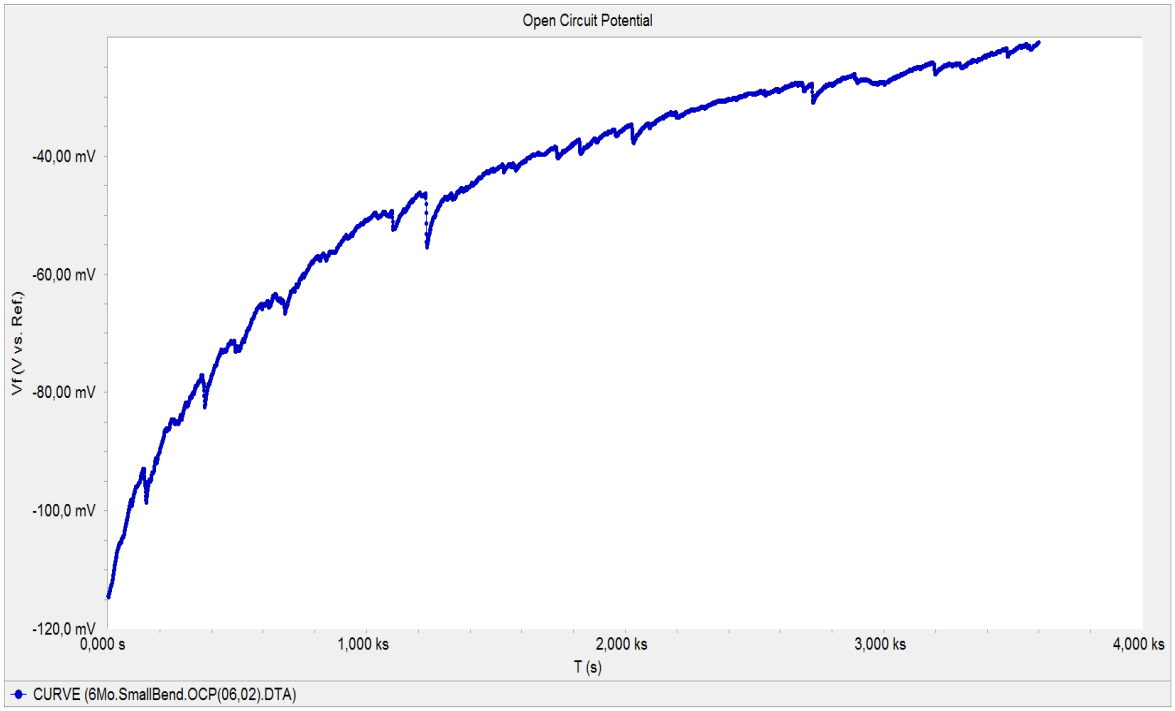

Graph: OCP for 6Mo smaller bend tube

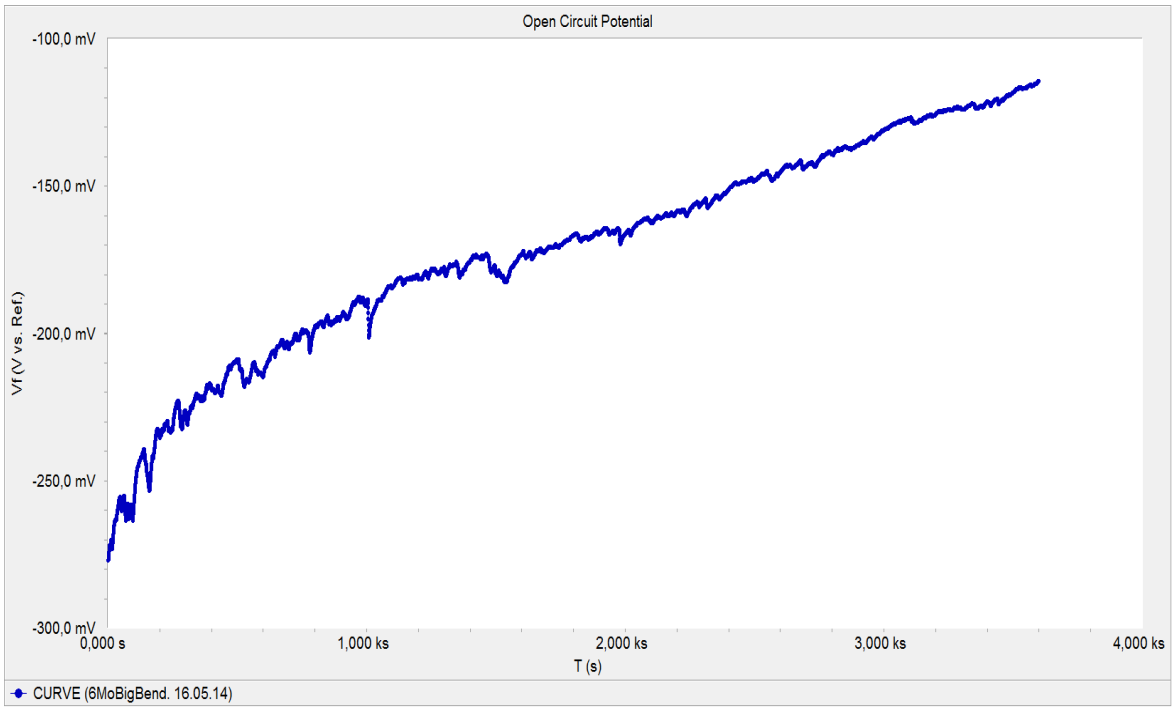

Graph: OCP for 6Mo bigger bend tube

Appendix 3: Cyclic polarization curve

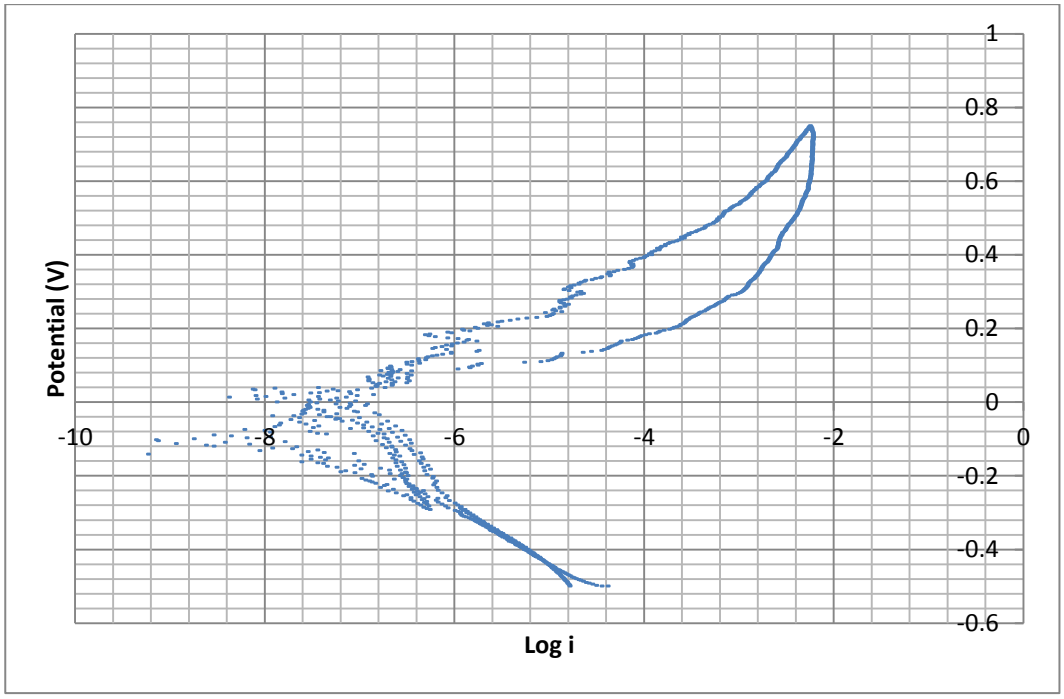

Graph: Cyclic polarization curve for 316SS Straight tube

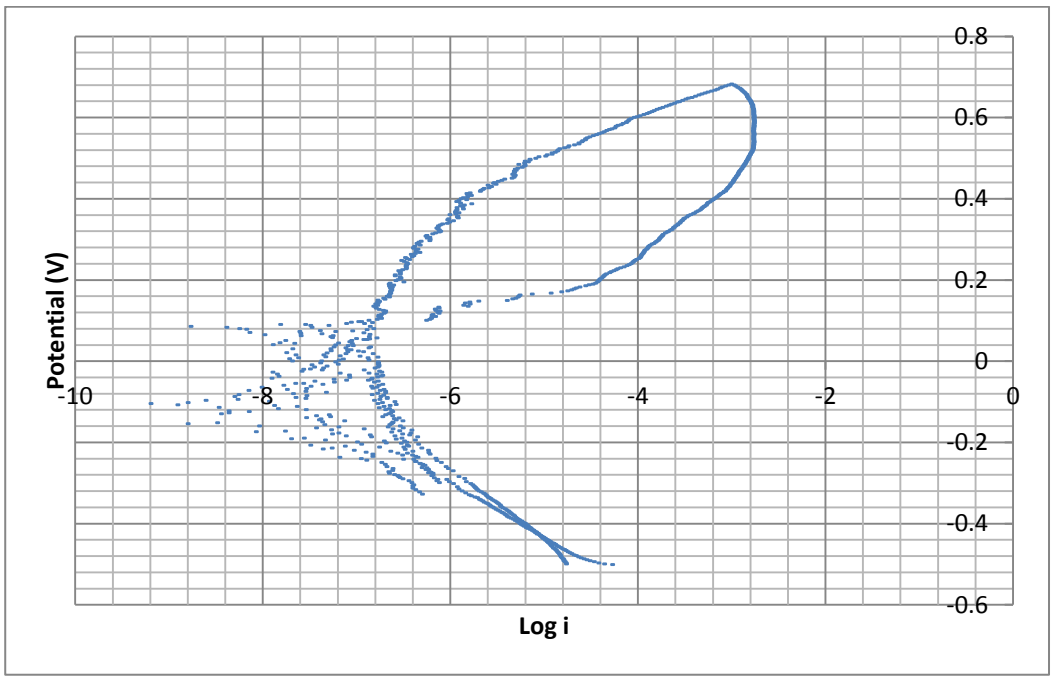

Graph: Cyclic polarization curve for 316SS smaller bend tube

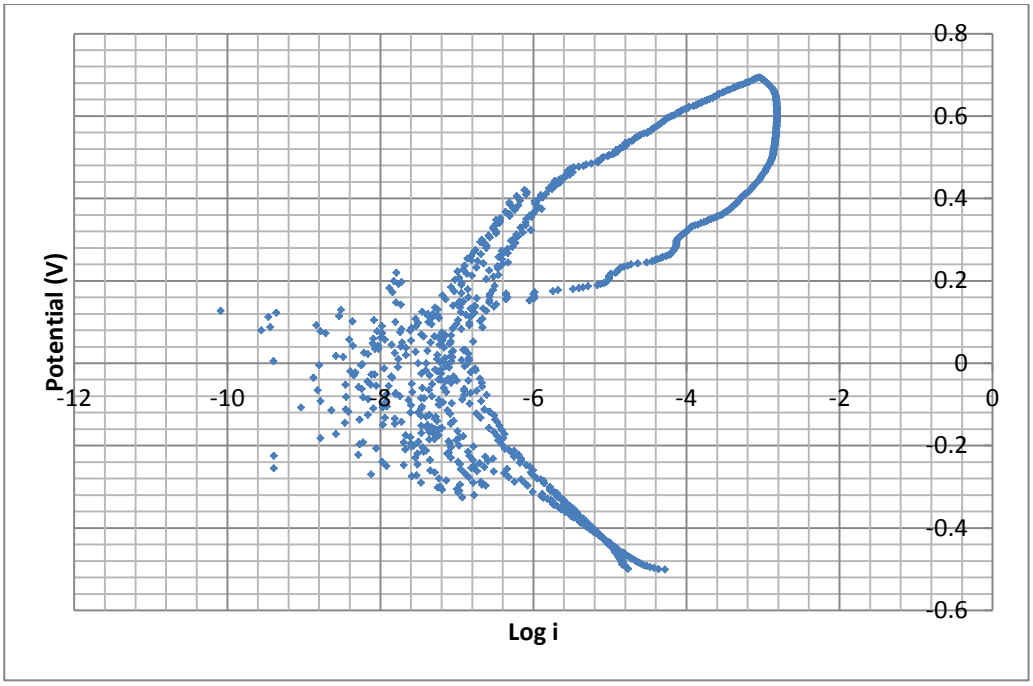

Graph: Cyclic polarization curve for 316SS bigger bend tube

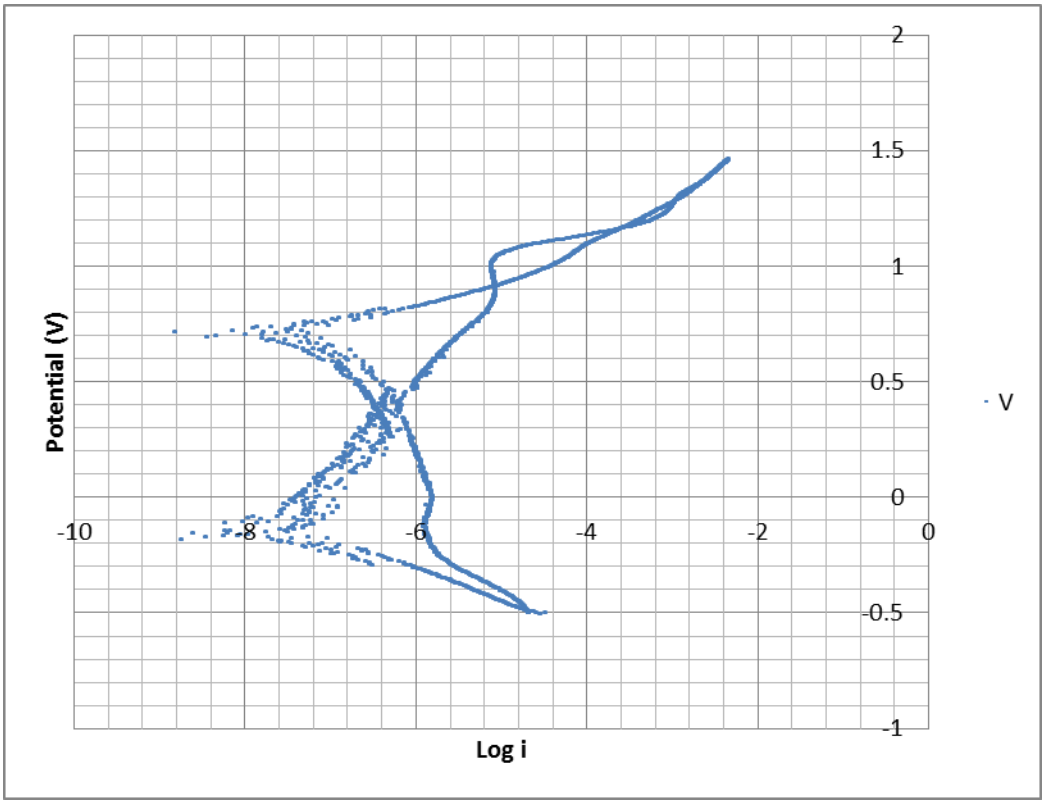

Graph: Cyclic polarization curve for 6Mo straight tube

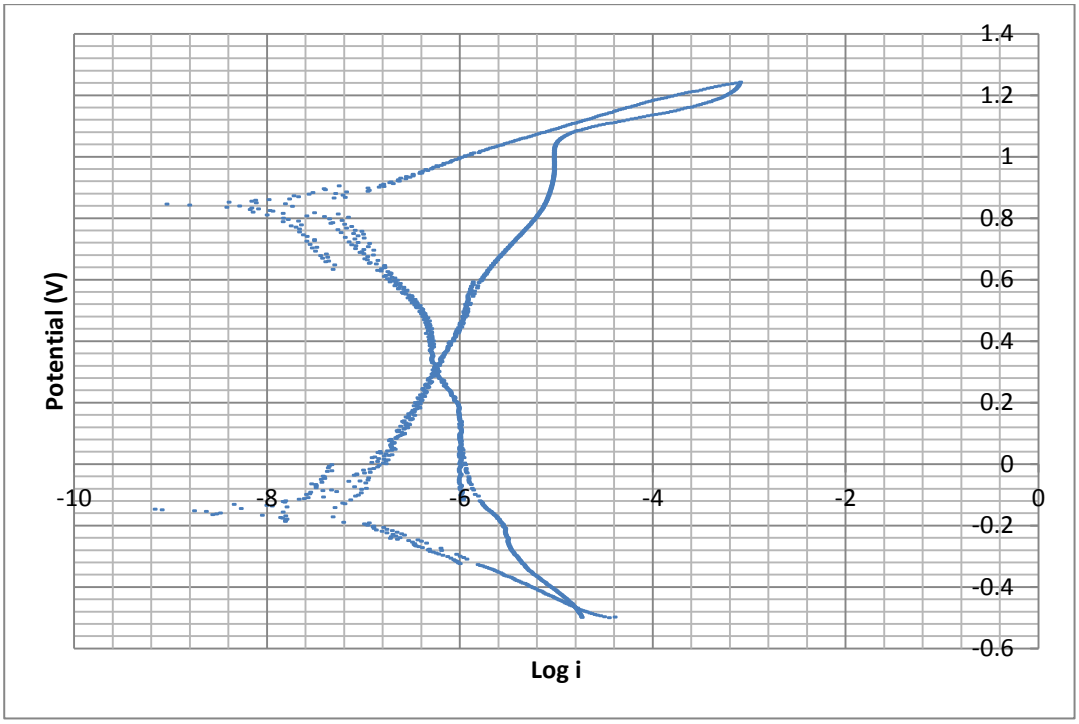

Graph: Cyclic polarization curve for 6Mo smaller bend tube

Appendix 4: Photos

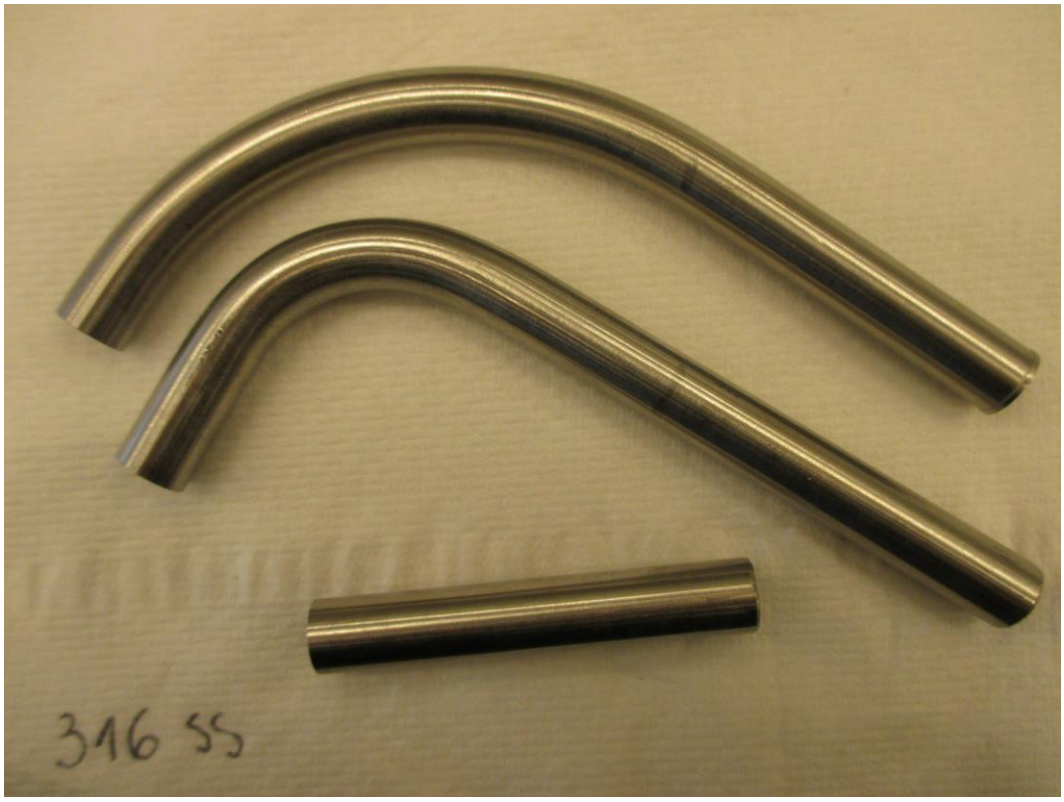

316SS specimens after G61 Test

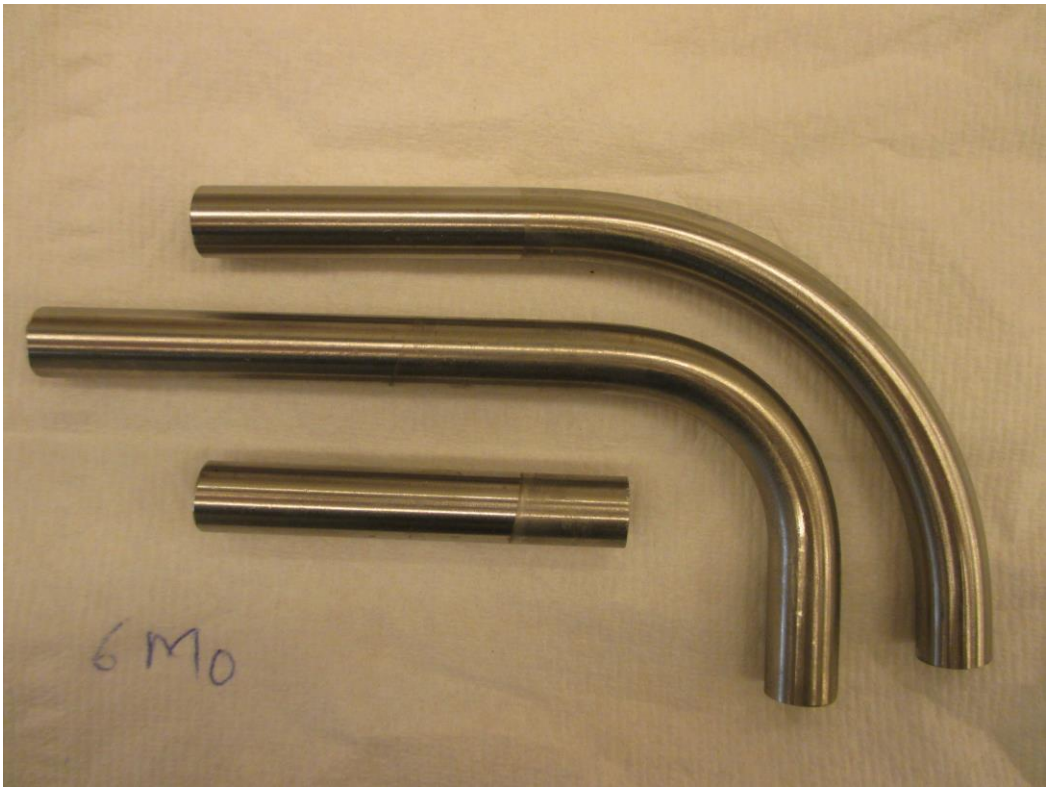

6Mo specimens after G61 Test

Mechanical saw for cutting the specimen laterally

Inner surface of 316SS straight tubes after G48 test

Inner surface of 316SS bended tubes after G48 test

Inner surface of 6Mo bended and straight tubes after G48 test

Outer surface of 6Mo bended and straight tubes after G48 test

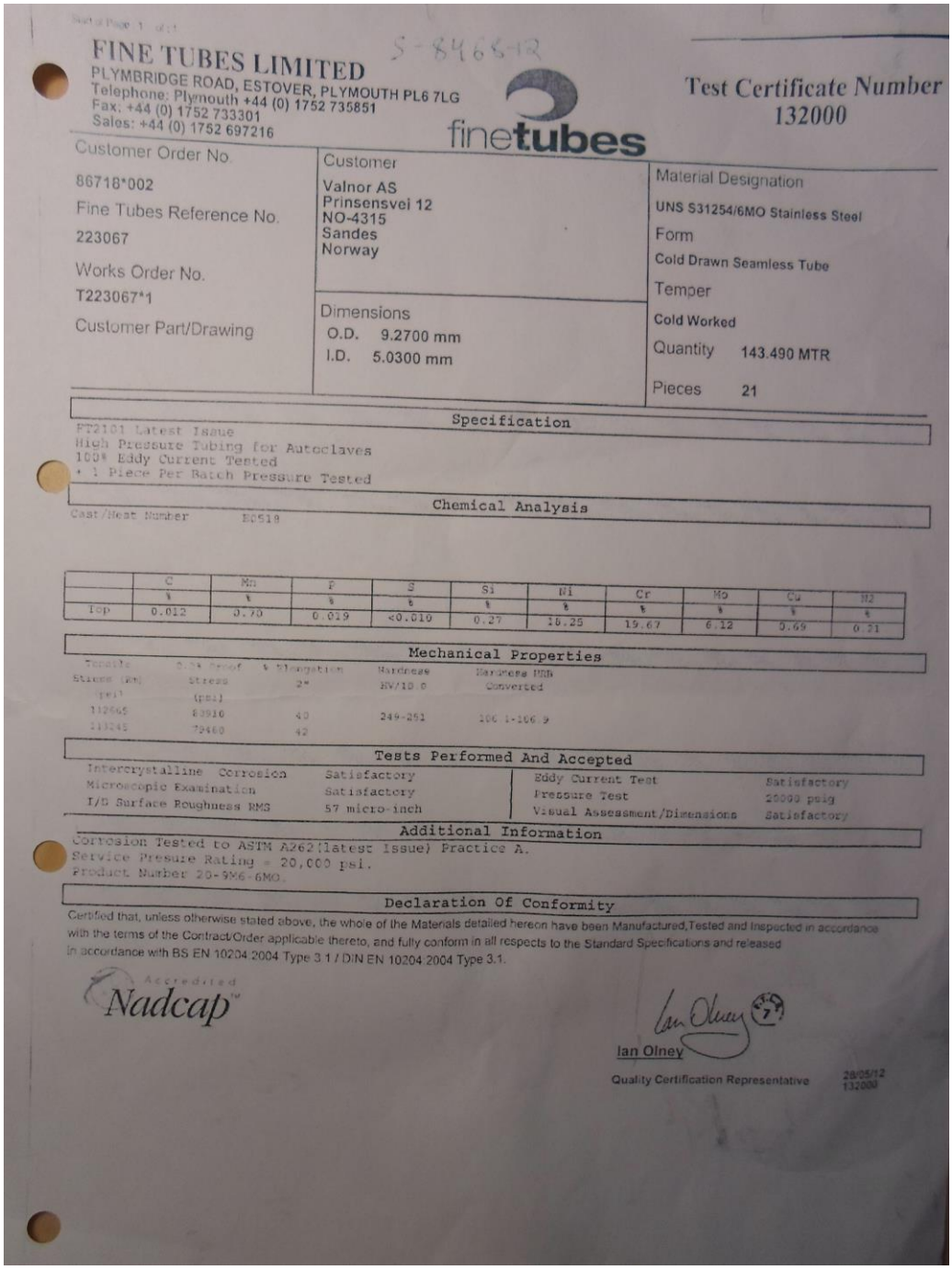

FINE TUBES LIMITED
PLYMBRIDGE ROAD, ESTOVER, PLYMOUTH PL6 7LG
Telephone: Plymouth +44 (0) 1752 735851
Fax: +44 (0) 1752 733301
Sales: +44 (0) 1752 697216

finetubes

Test Certificate Number 132000

Customer Order No.	Customer	Material Designation
86718*002	Valnor AS Prinsensvei 12 NO-4315 Sandes Norway	UNS S31254/6MO Stainless Steel
Fine Tubes Reference No. 223067		Form: Cold Drawn Seamless Tube
Works Order No. T223067*1	Dimensions O.D. 9.2700 mm I.D. 5.0300 mm	Temper: Cold Worked
Customer Part/Drawing		Quantity 143.490 MTR
		Pieces 21

Specification

FT2101 Latest Issue
High Pressure Tubing for Autoclaves
100% Eddy Current Tested
+ 1 Piece Per Batch Pressure Tested

Chemical Analysis

Cast/Heat Number E0519

	C	Mn	P	S	Si	Ni	Cr	Mo	Cu	N2
	%	%	%	%	%	%	%	%	%	%
Top	0.012	0.70	0.019	<0.010	0.27	18.25	19.67	6.12	0.69	0.21

Mechanical Properties

Tensile Stress (Rm) (psi)	0.2% Proof Stress (psi)	% Elongation 2"	Hardness HV/10.0	Hardness HRB Converted
112645	83910	48	249-251	100.1-100.9
113245	79460	42		

Tests Performed And Accepted

Intercrystalline Corrosion	Satisfactory	Eddy Current Test	Satisfactory
Microscopic Examination	Satisfactory	Pressure Test	20000 psig
I/D Surface Roughness RMS	57 micro-inch	Visual Assessment/Dimensions	Satisfactory

Additional Information

Corrosion Tested to ASTM A262(latest Issue) Practice A.
Service Presure Rating = 20,000 psi.
Product Number 20-9M6-6MO.

Declaration Of Conformity

Certified that, unless otherwise stated above, the whole of the Materials detailed hereon have been Manufactured,Tested and Inspected in accordance with the terms of the Contract/Order applicable thereto, and fully conform in all respects to the Standard Specifications and released in accordance with BS EN 10204:2004 Type 3.1 / DIN EN 10204:2004 Type 3.1.

Accredited Nadcap

Ian Olney
Quality Certification Representative
24/05/12
132000

6Mo material specification provided by a company

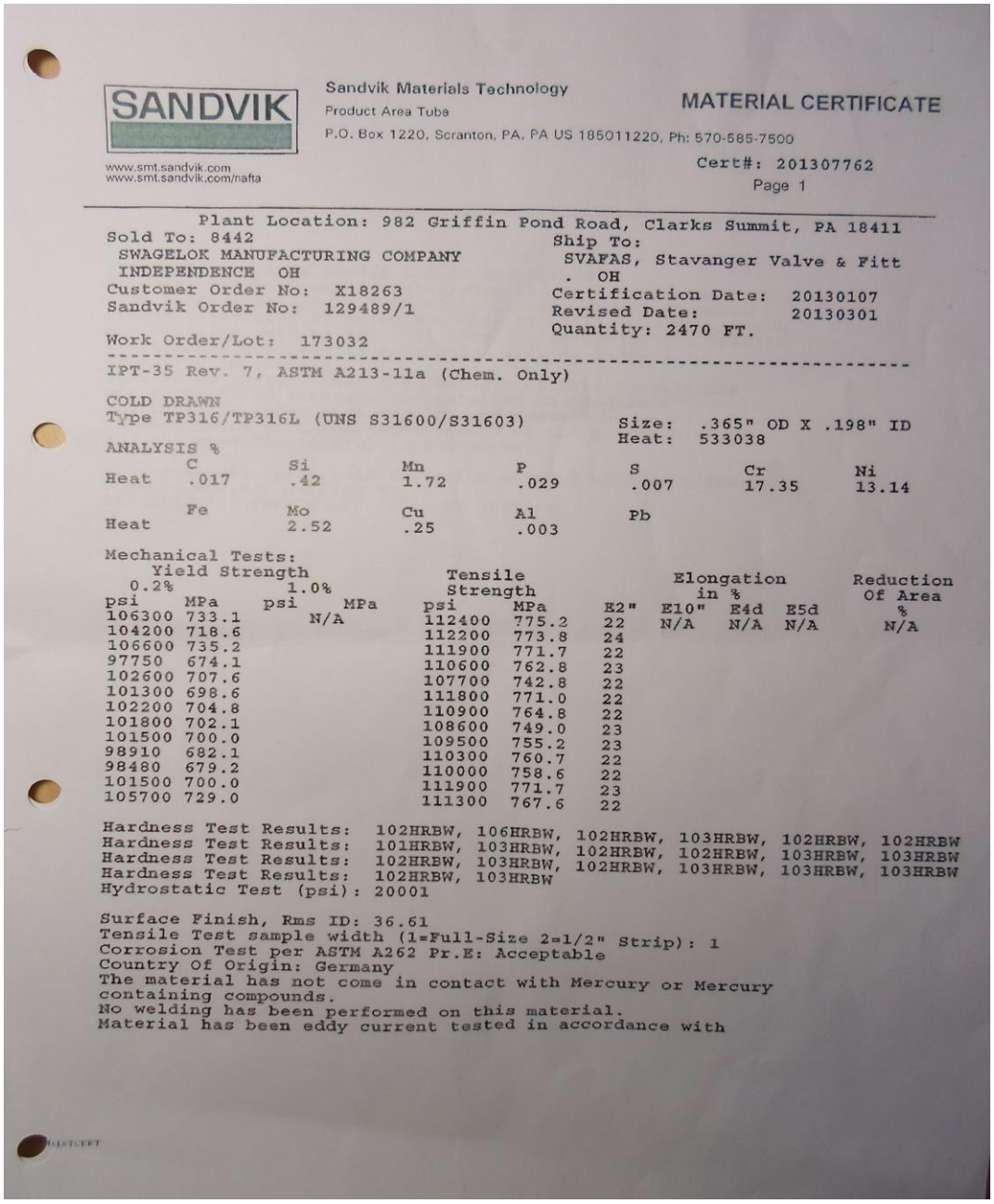

SANDVIK

Sandvik Materials Technology
Product Area Tube
P.O. Box 1220, Scranton, PA, PA US 185011220, Ph: 570-585-7500

www.smt.sandvik.com
www.smt.sandvik.com/nafta

MATERIAL CERTIFICATE

Cert#: 201307762
Page 1

Plant Location: 982 Griffin Pond Road, Clarks Summit, PA 18411

Sold To: 8442
SWAGELOK MANUFACTURING COMPANY
INDEPENDENCE OH
Customer Order No: X18263
Sandvik Order No: 129489/1

Ship To:
SVAFAS, Stavanger Valve & Fitt
. OH
Certification Date: 20130107
Revised Date: 20130301
Quantity: 2470 FT.

Work Order/Lot: 173032

IPT-35 Rev. 7, ASTM A213-11a (Chem. Only)

COLD DRAWN
Type TP316/TP316L (UNS S31600/S31603)

Size: .365" OD X .198" ID
Heat: 533038

ANALYSIS %

	C	Si	Mn	P	S	Cr	Ni
Heat	.017	.42	1.72	.029	.007	17.35	13.14

	Fe	Mo	Cu	Al	Pb
Heat		2.52	.25	.003	

Mechanical Tests:

Yield Strength 0.2%		Yield Strength 1.0%		Tensile Strength		Elongation in %				Reduction Of Area
psi	MPa	psi	MPa	psi	MPa	E2"	E10"	E4d	E5d	%
106300	733.1		N/A	112400	775.2	22	N/A	N/A	N/A	N/A
104200	718.6			112200	773.8	24				
106600	735.2			111900	771.7	22				
97750	674.1			110600	762.8	23				
102600	707.6			107700	742.8	22				
101300	698.6			111800	771.0	22				
102200	704.8			110900	764.8	22				
101800	702.1			108600	749.0	23				
101500	700.0			109500	755.2	23				
98910	682.1			110300	760.7	22				
98480	679.2			110000	758.6	22				
101500	700.0			111900	771.7	23				
105700	729.0			111300	767.6	22				

Hardness Test Results: 102HRBW, 106HRBW, 102HRBW, 103HRBW, 102HRBW, 102HRBW
Hardness Test Results: 101HRBW, 103HRBW, 102HRBW, 102HRBW, 103HRBW, 103HRBW
Hardness Test Results: 102HRBW, 103HRBW, 102HRBW, 103HRBW, 103HRBW, 103HRBW
Hardness Test Results: 102HRBW, 103HRBW
Hydrostatic Test (psi): 20001

Surface Finish, Rms ID: 36.61
Tensile Test sample width (1=Full-Size 2=1/2" Strip): 1
Corrosion Test per ASTM A262 Pr.E: Acceptable
Country Of Origin: Germany
The material has not come in contact with Mercury or Mercury containing compounds.
No welding has been performed on this material.
Material has been eddy current tested in accordance with

316SS specification provided by company